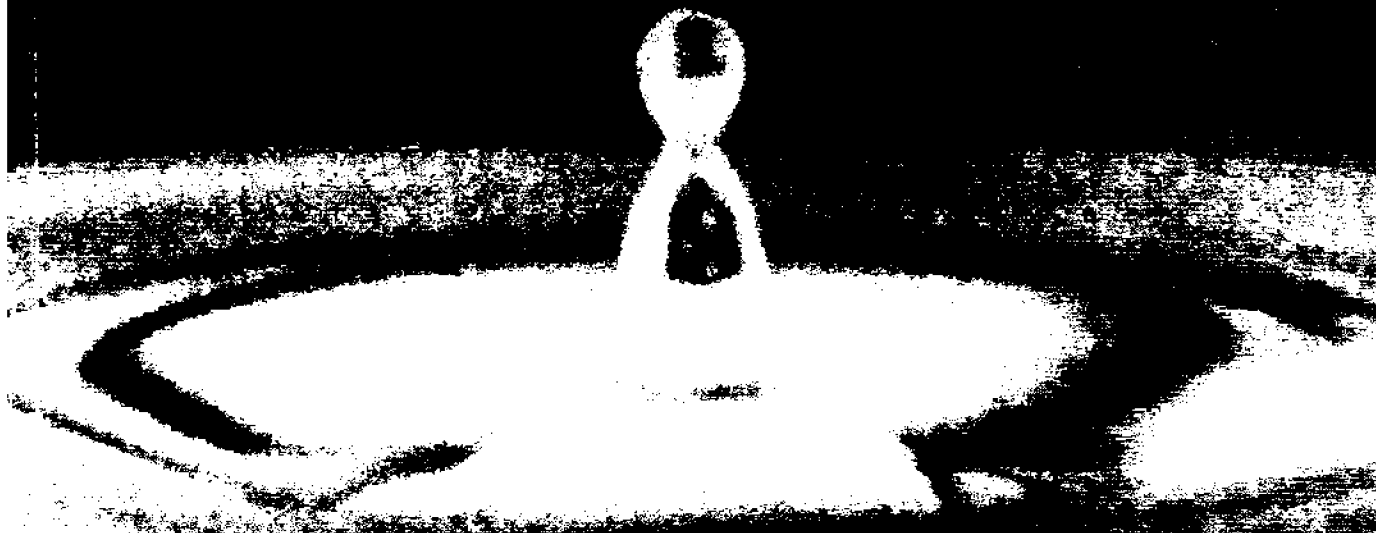


Climate and Heat Implications of Bubble-Mediated Sea-Air Exchange

CHICAGO
Sea Air

Edward C. Monahan
and
Margaret A. Van Patten

Editors



The Climate and Health Implications of Bubble-Mediated Sea-Air Exchange

Edward C. Monahan
and
Margaret A. Van Patten

Editors

Proceedings of an international symposium by the same title held at the University of Connecticut at Avery Point, Groton, Connecticut, on October 7-9, 1988, sponsored by the Connecticut Sea Grant College Program.

A publication of the Connecticut
Sea Grant College Program
CT-SG-89-06



Library of Congress Catalog Card Number: 89-08110
ISBN: 1-878301-00-4

Copyright © 1989 by the Connecticut Sea Grant College Program

All rights reserved. Printed in the United States of America. No part of this book may be used or reproduced in any form or by any means, or stored in a database or retrieval system, without prior written permission of the publisher, except in the case of brief quotations embodied in critical articles and reviews.

Publication of this book is supported by the National Oceanic and Atmospheric Administration via Sea Grant No. NA85AA-D-SG101.

Production Editor: Margaret A. Van Patten
Editorial Assistant: Patricia A. Beetham
Book Design: Margaret A. Van Patten
Cover Design: Betsy J. Suprenant

Distributed by the Connecticut Sea Grant College Program, Marine Sciences Institute, University of Connecticut at Avery Point, Groton, CT 06340

\$12.50

Contents

Preface	<i>iv</i>
Chapter 1	
Bacteria and Other Materials in Drops From Bursting Bubbles <i>Duncan C. Blanchard</i>	1
Chapter 2	
The Aerosolization of Mycobacteria <i>Joseph O. Falkinham, III</i>	17
Chapter 3	
Marine Toxins in Bubble-Generated Aerosol <i>Richard H. Pierce et al.</i>	27
Chapter 4	
From the Laboratory Tank to the Global Ocean <i>Edward C. Monahan</i>	43
Chapter 5	
The Occurrence of Large Salt Water Droplets at Low Elevations Over the Open Ocean <i>Gerrit de Leeuw</i>	65
Chapter 6	
Relationships Between Marine Aerosols, Oceanic Whitecaps, and Low-Elevation Winds Observed During the HEXMAX Experiment in the North Sea <i>Roman Marks and Edward C. Monahan</i>	83
Chapter 7	
Enhancement of Sea-to-Air Moisture Flux by Spray Droplets Associated With Breaking Waves and Bubble Entrainment: Simulations in IMST Wind Tunnel <i>Patrice Mestayer</i>	101
Chapter 8	
Modeling the Droplet Contribution to the Sea-to-Air Moisture Flux <i>C.W. Fairall and J.B. Edson</i>	121
Chapter 9	
Abstracts From Poster Presentations <i>E.L. Andreas; D. K. Woolf; T. Torgersen et al.; R. Cipriano and D.K. Woolf</i>	147
Chapter 10	
Panel Discussion: Identification of Critical Research Topics <i>S. E. Larsen</i>	165

Preface

The papers included in this volume were all presented during the Sea Grant Symposium on "Climate and Health Implications of Bubble Mediated Sea-Air Exchange" held at the University of Connecticut, Avery Point, on 6 and 7 October 1988. This symposium was one of several events scheduled to celebrate the designation, by the U. S. Secretary of Commerce, of the University of Connecticut as a full-fledged Sea Grant College.

The topic of this symposium was felt to be particularly appropriate at this time, when an improved understanding of climate, and of those factors which influence global climate change, is the goal of the National Oceanic and Atmospheric Administration, the federal agency which sponsors the several dozen Sea Grant programs located in the various coastal and Great Lakes states.

This scientific meeting also coincided with the formal dedication, on this same campus, of the Laboratory for the Study of the Physics and Chemistry of the Sea Surface, and of the new whitecap simulation tank housed in this facility. The research into a variety of bubble-mediated sea surface processes carried out in this laboratory, whose outfitting was made possible by a grant from the University of Connecticut Research Foundation, is supported by such funding agencies as the Office of Naval Research and the National Science Foundation. In the six months that have elapsed since its dedication, scientists from France, the Netherlands, Denmark, and the United Kingdom, and from states as distant as California, have traveled to the Marine Sciences Institute at Avery Point and participated in a series of co-operative experiments

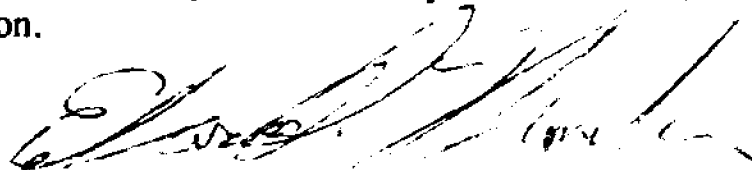
centered on the new whitecap simulation tank. Involved in the work in this laboratory during this same interval have been Graduate Students and Post-Doctoral Scholars from Ireland, Poland, the People's Republic of China, and the United Kingdom, as well as from the United States. This bringing together of scientists from all over, to pool their insights, talents, and equipment in pursuit of the answers to pressing questions relevant to our marine environment, is, we believe, an ideal, and at the same time and efficient, way to conduct research. Certainly this practical approach to the scientific endeavor is one fully consonant with the responsibility of each Sea Grant College to foster research, education, and advisory services, in the fields of applied marine science.

We are particularly pleased to be able to include in this volume a number of papers which are truly multi-disciplinary in nature, spanning within a single paper the range of disciplines from microbiology/medicine to physics/meteorology. We trust that the reading of these contributions may encourage others to engage in these sorts of fruitful, cross-disciplinary, studies.

This symposium, and the associated poster session, benefited immeasurably from the dedicated efforts of all of the staff of the Connecticut Sea Grant Office.

This volume was brought to its final form thanks in large measure to the work and perserverance of my co-editor, Ms. Peg Van Patten, who was assisted in this effort by Ms. Patricia Beetham.

Neither the symposium nor this volume would have been possible without the funding provided to the Connecticut Sea Grant College Program by the National Sea Grant Office, National Oceanic and Atmospheric Administration, U. S. Department of Commerce, via Grant NA85AA-D-SG101. Additional support for the symposium was provided by the University of Connecticut Research Foundation.



Edward C. Monahan
Avery Point, April 1989



The new Whitecap Simulation Tank IV on its podium in the Laboratory for the Study of the Physics and Chemistry of the Sea Surface at the University of Connecticut Marine Sciences Institute. Visible near the bottom of the tank is an array of frits used to produce a continuous plume of bubbles as required in the series of Petit-CLUSE experiments, carried out with the support of N.S.F. and C.N.R.S. (France), to assess the contribution of bubble-generated droplets to the sea-air moisture flux. Beneath the movable gantry, the hood that serves to enclose the space above the tank can be seen.

..1..

Bacteria and Other Materials in Drops from Bursting Bubbles

Duncan C. Blanchard
Atmospheric Sciences Research Center
State University of New York at Albany
Albany, NY 12222

Abstract

The ubiquitous breaking waves on lakes, rivers, and at sea are probably the most important source of air bubbles, but on a local scale the falling of precipitation into the water may also be important. Bubbles can collect bacteria as they rise through the water, and when they burst at the surface many of the bacteria are skimmed off the bubble and into the jet drops. Depending upon a number of factors, including drop size and the distance the bubbles move through the water, the bacterial concentration in the jet drops can be several hundred times that in the water where the bubbles burst. Film drops enriched in bacteria have also been found. Under certain conditions, the enrichment of jet and film drops with bacteria, viruses, and toxins may be a health hazard to people living along the shore.

1. Introduction

Over 2,300 years ago, Hippocrates wrote about the influence of weather and the environment on human health. His ideas, and those of others down through the centuries, have been discussed by Sargent (1982). Much of our environment consists of the lakes,

rivers, and oceans that cover over 70% of the surface of the earth. From these waters an aerosol is produced and carried by the winds to great distances and heights.

Since all natural waters contain bacteria, it would only be common sense to believe that the concentrations of bacteria in the droplets rising from these waters are unchanged in their journey from the water into the atmosphere. Common sense, however, in this case can be wrong. Numerous laboratory experiments have shown that the concentration of some species of bacteria in the droplets is hundreds of times that in the water from whence they came. Many of us are exposed to these droplets, since our cities and towns are usually located near rivers, lakes, or the sea. We must understand how bacteria are enriched in the droplets, for they may occasionally pose a hazard to human health.

This paper, a review of the work on the problem, begins with a short account of the experiments that showed the importance of bursting bubbles in producing an aerosol from natural bodies of water. Much of this review, especially that dealing with the bacteria, draws heavily from one of my earlier papers (Blanchard, 1983).

2. The Production of Jet and Film Drops

Over 30 years ago, marine meteorologists studying the formation of rain-drops in marine clouds (Woodcock and Blanchard, 1955) began to investigate the mechanism by which giant condensation nuclei are produced at the surface of the sea (Moore and Mason, 1954; Blanchard and Woodcock, 1957). This work still goes on and, consequently, most of what we know about aerosol production from natural waters is only for seawater. Relatively little work has been done with freshwater (Monahan and Zietlow, 1969; Monahan, 1969).

Most of the aerosol generated from natural waters is in the form of jet and film drops from the bursting of air bubbles. The bubbles can be produced by a variety of ways: by rain and snow falling into the water (Fig. 1), by waterfalls and rapids, and by the breaking of wind-induced waves (Blanchard and Woodcock, 1957). The coverage of the sea by breaking waves or whitecaps

increases with more than the third power of the wind speed (Monahan and O'Muircheartaigh, 1980), and on average the world ocean whitecap coverage is about 1 per cent. Bubble spectra within whitecaps at sea have not been obtained, but in a laboratory model breaking wave, Cipriano and Blanchard (1981) found bubbles from <1 mm to about 10 mm diameter. The bubble flux to the surface was about $2 \times 10^6 \text{ m}^{-2} \text{ s}^{-1}$.

When a bubble bursts at the surface of the water (Fig. 2), some of its surface free energy is converted into kinetic energy of a jet of water that rises rapidly from the bubble cavity (Blanchard, 1963; MacIntyre, 1972). The jet, first postulated by Stuhlman (1932) and experimentally confirmed by Woodcock *et al.* (1953), breaks up into 1 to 10 drops, the more the smaller the bubble. The first jet drop, usually called the top drop, is about one-tenth the bubble diameter, but the lower drops can be larger or smaller. Most are larger. The maximum in the ejection height of the top drop is nearly 20 cm for drops from bubbles of 2 mm diameter. No jet drops are produced from bubbles >7 or 8 mm.

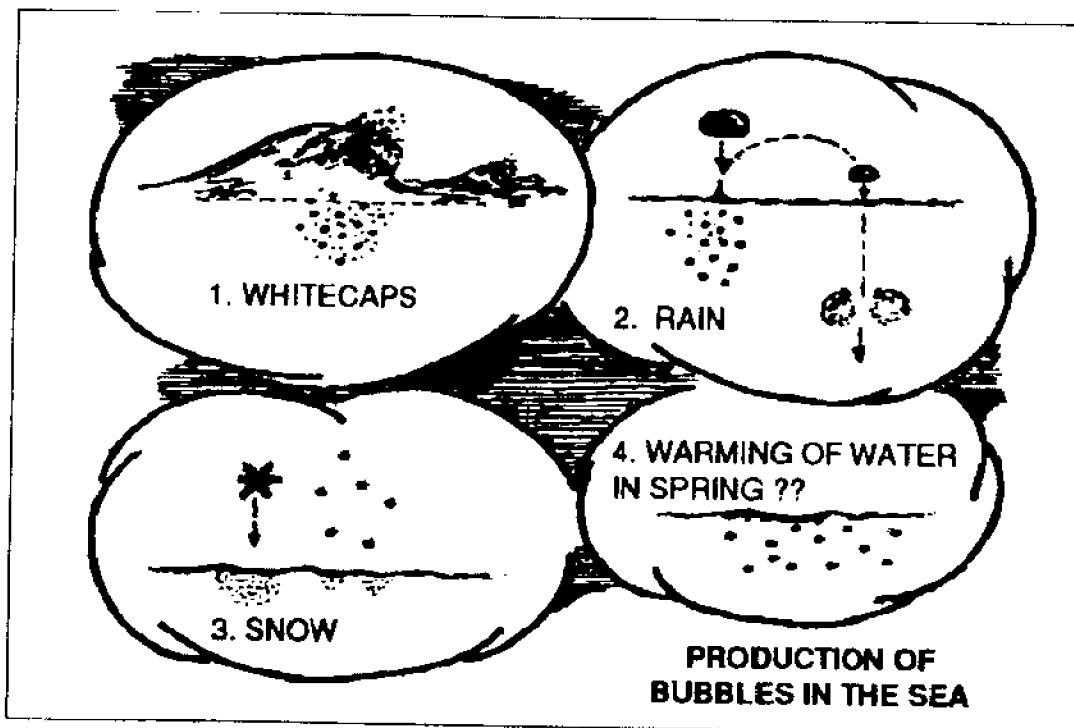


Fig. 1. Four ways to produce bubbles in the sea. The first three have been experimentally proven, but the fourth is still only conjecture.

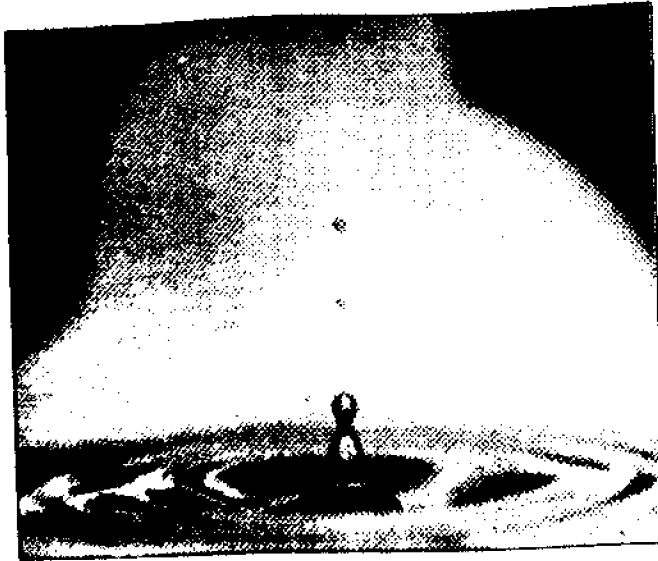


Fig. 2. Jet drops moving rapidly upward from the jet of a collapsing 1-mm diameter bubble. Some of the drops may have escaped from the field of view.

Bursting bubbles also produce film drops that arise from the disintegration of the thin film of water that separates the air in the bubble from the atmosphere (Fig. 3). Unlike jet drops, film drops are hard to measure, most being $<4 \mu\text{m}$ diameter (Cipriano *et al.*, 1987), but some are $>100 \mu\text{m}$ (Resch *et al.*, 1986). It has long been thought that film drop production increased steadily with bubble size, but Blanchard and Syzdek (1988) recently reported a maximum of about 75 film drops from bubbles of 2 to 2.5 mm diameter.

3. The Enrichment of Bacteria in Jet and Film Drops

Horrocks (1907) appears to have been the first to show that bacteria could be ejected into the atmosphere by bubbles bursting at the surface of bacterial-laden waters. Nearly half a century passed before Woodcock (1955), unaware of the earlier work, suggested that jet drops could carry bacteria. In 1970, Blanchard and Syzdek found that the concentration of the bacterium, *S. marcescens*, in jet drops could far exceed that in the water where the bubbles burst. A measure of the bacterial enrichment is given by the enrichment factor EF, the ratio of the concentration of bacteria in the drop at the moment of production (before evaporation occurs) to the concentration in the water from which the drop was produced. High EFs depend on 1) a bubble arriving at the surface with many bacteria attached to it, and 2) by having these bacteria skimmed off the surface of the bubble and into the jet drops.

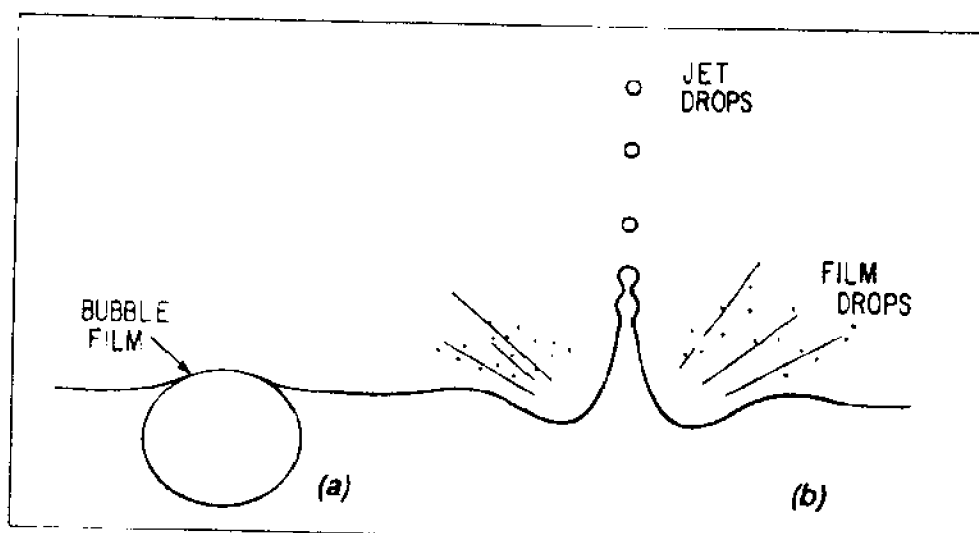


Fig. 3. (a) An air bubble at rest at the surface of the water; (b) The production of jet and film drops from a bursting bubble. (From Blanchard and Syzdek, 1982)

The simple apparatus shown in Fig. 4 has been used to determine jet drop EF, especially that of the top jet drop. An inverted agar plate is lowered to a height over the water just sufficient for the top jet drop from a bursting bubble to strike and stick to it. Details of the preparation of the bacterial suspensions, the determination of the number of bacteria carried by the drop, the measurement of drop size, the construction of bubble-producing capillary tips, and other things required to calculate EF can be found elsewhere (Blanchard and Syzdek, 1975, 1977, 1978).

The bacterial EF in jet drops is controlled by 1) bubble scavenging, 2) drop size, 3) drop position in the jet set, and 4) the hydrophobicity of the bacteria. Each is discussed below.

Bubble scavenging.

The number of bacteria collected by a bubble depends on the distance the bubble moves through the water. This is often referred to as the bubble rise distance, BRD. Since some, perhaps all, of the bubble bacteria are transferred to the jet drops, the EF of the drops should be a function of BRD.

Figure 5, from Blanchard *et al.* (1981), shows how the EF increased with BRD for a bubble of 380 μm diameter rising through a bacterial suspension of *S. marcescens* in pond water. The cell concentration in the water was about 10^6 ml^{-1} . The EF increased

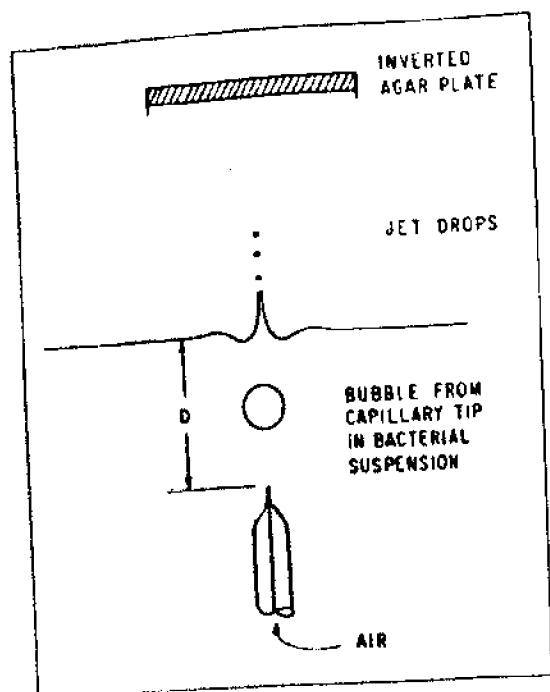


Fig. 4. Schematic outline of an experiment to obtain the number of bacteria carried by the top jet drop (or the top two or more) as a function of the distance the bubble has risen through the bacterial suspension.

dramatically from near-negligible values to about 400 as the BRD increased to only 3 cm, but then increased more slowly to 600 at a BRD of 10 cm. The marked decrease in the rate of increase of EF at about 3 cm appears to be because the bubble changes from a fluid to a solid sphere. During the first few centimeters of rise, a bubble of this size moves as a fluid sphere (clean bubble) with a clean surface (Tedesco and Blanchard, 1979). In addition to bacteria, it collects surface-active material during its ascent. The mobility of the bubble surface, therefore, decreases until enough surfactant has accumulated to render the surface immobile (Clift *et al.*, 1978). From then on it rises as a solid sphere (dirty bubble). The rate of collection of bacteria by a bubble in the early period of rise, when its surface is clean, is much higher than the rate later on, when its surface is dirty (Weber *et al.*, 1983).

Very few bacteria make contact with the bubble by diffusion or inertial forces. Most do so by interception, a collection mechanism that depends on the finite size of the bacteria (Weber, 1981). Since inertial effects are negligible, bacteria follow the fluid streamlines around the bubble. Due to their finite size, however, those bacteria following streamlines very close to the bubble make contact and are scavenged.

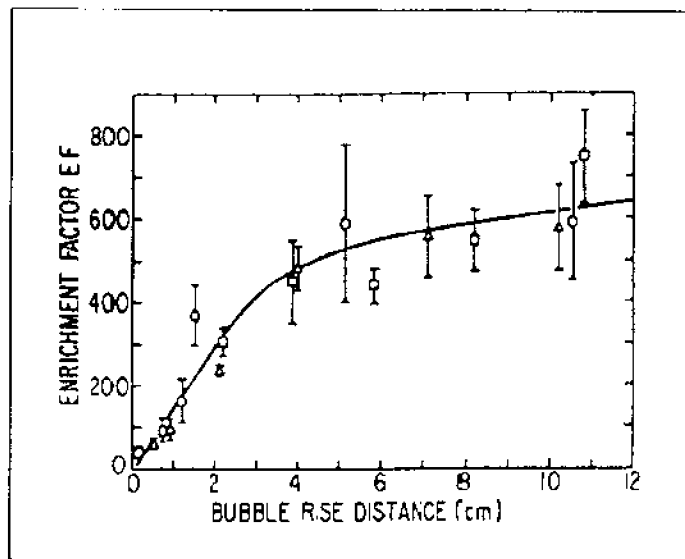


Fig. 5. The enrichment factor (EF) for bacteria in the top jet drop as a function of the distance the bubble rises through a bacterial suspension of *S. marcescens* in pond water. Three different experiments are shown. (From Blanchard *et al.* 1981)

Drop size.

Having seen how the EF increases with BRD for a given bubble size, we'll now look at what happens when the BRD is held constant and bubble size is varied. This is how Blanchard and Syzdek (1970) did their first bacterial experiments. Their results, presented in a graph of the top drop EF as a function of drop size (or, if multiplied by 10, the bubble size, since the top drop is about one tenth the bubble size), showed that the EF reached a maximum for drops of about 50 μm diameter. The maximum was also found by Bezdek and Carlucci (1972) with seawater suspensions of *S. marinorubra*, by Blanchard and Syzdek (1972), again using distilled water suspensions of *S. marcescens*, and by Hejkal *et al.* (1980) with suspensions of a number of species of marine bacteria in NaCl solutions.

In the center of Fig. 6 is a graph showing a composite of all the data. The surrounding sketches suggest a possible explanation for the EF maximum. Let us assume, following MacIntyre (1972), that the microlayer thickness, kR , skimmed off the surface of the bursting bubble to produce the jet drops, is proportional to the bubble radius R . For the smallest bubbles it is probable that kR is less than the size of the bacteria attached to the bubble. Most of these bacteria, therefore, will be left behind when the microlayer is transformed into jet drops. In fact, the EF might be <1 for drops $< 20 \mu\text{m}$ (from bubbles less than about 200 μm diameter).

As bubble size increases from small to intermediate, an optimal

thickness kR is reached where only the highly enriched layer of bacteria attached to the bubble is skimmed off into the jet drops. This produces a maximum EF. With increasing bubble size, kR extends deeper into the bulk suspension. The jet drop EF decreases and approaches unity when the layer kR is so thick that its bacterial concentration approaches that of the bulk suspension. The decrease of the EF to unity in Fig. 6 is more rapid than we would expect. This suggests that either the thickness of the microlayer is increasing with bubble size faster than we have assumed, or that the experimental results are in error. Clearly, further experiments are needed.

The maximum EF is attained when the thickness of the bubble microlayer is about $0.5 \mu\text{m}$, the width of a bacterial cell (we assume that the cells attach to the bubble as shown in Fig. 6). Since the bubble diameter is about $500 \mu\text{m}$, the microlayer thickness is 0.1 percent of the bubble diameter. This is in reasonable agreement with the estimate of 0.05 percent calculated by MacIntyre (1972) on the basis of a mass balance between the microlayer and the jet drops.

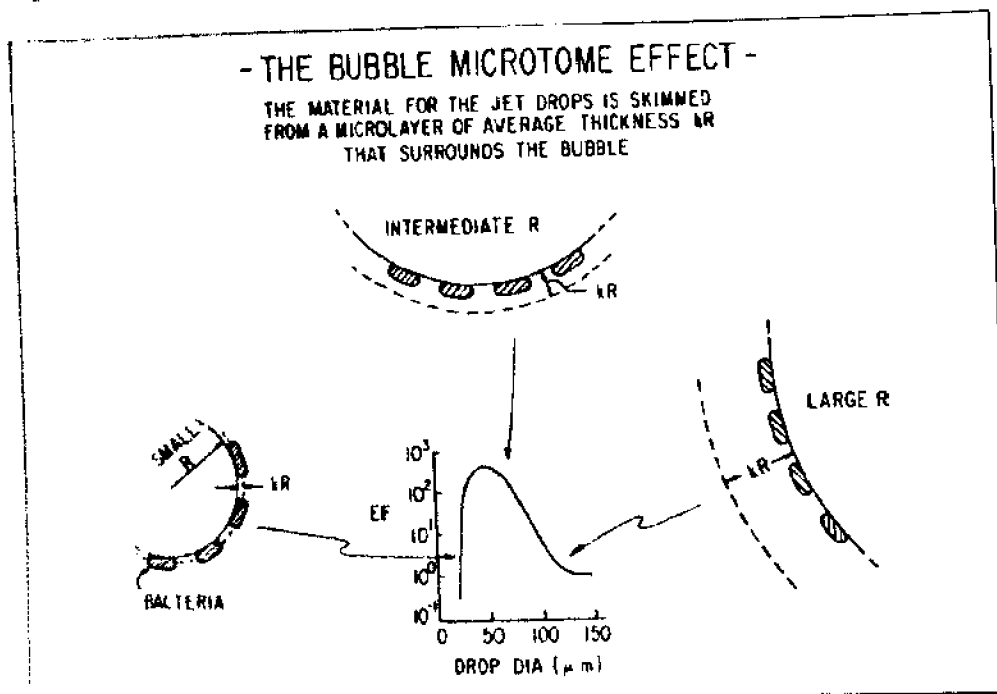


Fig. 6. Schematic diagram of a hypothesis to explain the occurrence of the maximum bacterial enrichment factor (EF) shown in the lower center graph. (From Blanchard, 1983)

Drop position in the jet set.

The jet set is the entire set of drops produced from the jet of a bursting bubble. How might the bacterial EF vary in drops other than the top drop of the jet set? MacIntyre (1968, 1972) hypothesized that the liquid for the top drop comes from the surface layer of the bubble, while that for the lower drops is from progressively deeper layers. If true, we should find the EF decreasing from the top to the bottom drop of the jet set. This appears to happen. In experiments with *S. marcescens*, Blanchard and Syzdek (1975) found an EF of about 1200 for the top drop that decreased with drop position to 8 for the fifth or lowest drop in the jet set.

Hydrophobicity of the bacteria.

Bacterial cells do not necessarily stick to a bubble upon collision. This is a function of its sticking or attachment efficiency which, in turn, is a function of the hydrophobicity of the cell wall (Dahlbäck *et al.*, 1981). For normal *S. marcescens* cells the sticking efficiency is estimated to be about unity, since the calculated collision efficiency, about 10^{-3} , is nearly the same as the observed collection efficiency (Weber *et al.*, 1983). Sometimes, however, large differences in bubble collection efficiency and jet drop EF are found. Normally, *S. marcescens* cells generate prodigiosin, a pigment that produces bright red colonies. But a number of environmental stresses can alter prodigiosin production to produce colonies ranging in color from the normal red to pink, orange, and white (Williams, 1973).

Blanchard and Syzdek (1978) let bubbles rise through a suspension of both red and white *S. marcescens* cells. They found the EF for the top jet drops to be several hundred for the red cells but only unity for the white cells. This strongly suggests that the production of prodigiosin by a cell is correlated with its hydrophobicity. This work has been extended by Syzdek (1985), and Burger and Bennett (1985) have suggested a possible selective function for prodigiosin in the ejection of *S. marcescens* into the atmosphere.

Film drop enrichment.

Although Smith (1968) appears to have been the first to show that film drops can carry bacteria, he was not able to determine the EF. Cipriano (1979) found EFs of 50-100 on drops $<10 \mu\text{m}$ in the aerosol produced from the bubbling of seawater suspensions of *S. marinorubra*. He concluded that these drops were film drops, primarily because jet drops of this size show little bacterial enrichment (Fig. 6). Film drops, unlike jet drops, have a wide size range and unpredictable trajectories (Fig. 3). They are not as easy to collect and analyze for bacteria as are jet drops. Blanchard and Syzdek (1975), however, have used electrostatic induction to charge and pull film drops upward to impact randomly on inverted agar plates. With this method of drop collection, they were able to show unequivocally that film drops from 1.7 mm diameter bubbles rising <2 cm through an *S. marcescens* suspension have EFs between 10 and 20 (Blanchard and Syzdek, 1982).

4. Potential Health Hazards

High concentrations of bacteria can be found in estuaries (Ferguson and Palumbo, 1979), and even higher concentrations have been found at the surface of the water (Crow *et al.*, 1975). Although this may be a health hazard, it has been hard to show an adverse effect on the health of swimmers and others along the shore who breathe the bacterial-laden aerosol (Cabelli *et al.*, 1976). There is, however, one health hazard attributed to the aerosol produced by bursting bubbles. This is the burning sensation in the eyes and respiratory tract and the coughing experienced by people living along the shore in Florida and the Gulf of Mexico when on-shore winds pass over coastal waters that contain high concentrations of the red tide organism, *Pyrodiscus brevis*. Woodcock (1948) showed that the toxic agent was not a gas but an aerosol produced by bursting bubbles. Asai *et al.* (1982) have found evidence that asthma attacks are induced in susceptible people who breathe this aerosol. As yet, there is no evidence that the toxins produced by *P. brevis* are enriched on the bubble-produced aero-

sol, but Pierce (1986) believes they might be and has experiments underway to detect it.

Legionella pneumophila, the cause of the respiratory disease legionellosis, commonly known as the Legionnaires' disease, is a pathogen that can cause disease after being ejected into the atmosphere by bubbling and splashing processes. Although it has been isolated from many lakes (Fliermans *et al.*, 1979), the outbreak of the disease appears to be singularly associated with the aerosol generated by air conditioning cooling towers (Dondero *et al.*, 1980; Friedman *et al.*, 1987). *L. pneumophila* has been found enriched in the foam in cooling towers (Colbourne *et al.*, 1987) and in jet drops from bursting bubbles (Parker *et al.*, 1983).

Gruft *et al.* (1975), aware that *Mycobacterium intracellulare* infections in humans occur more frequently along the southeastern shores of the United States, suggested that the source of the bacterium was in estuaries and other coastal waters. Since their experiments showed that the bacterium could be enriched in jet drops, they postulated that the infectious aerosol was produced by the sea and carried inland by onshore winds. Later, Parker *et al.* (1983) indicated that the source of infection might also be an aerosol produced by fresh and brackish waters.

Viruses deliberately mixed with seawater in the surf zone (Baylor *et al.*, 1977) were found to be highly enriched in the bubble-produced aerosol that passed over the shore. This could have public health implications since viruses exist in the sewage that is often dumped into the coastal regions of the sea.

Some pollutants produced on land are carried to the sea by rivers, where a portion of them are ejected into the atmosphere in jet and film drops to be carried by onshore winds back to the land again. Fraizier *et al.* (1977) have used this scenario to explain the sharp falloff of radioactivity in plants with distance inland from the shore along sections of the French coast.

In certain regions along the shore in Italy, pine trees have been affected by a bubble-produced aerosol. Gellini *et al.* (1985) believe that surfactants carried to the sea by rivers become airborne aboard jet and film drops. During onshore winds the drops stick to the pine needles where a synergistic reaction between the sodium

chloride and the surfactant kills the needles and eventually the tree. Little damage is done by either salt or surfactant alone.

It is only the interference of humans in the ecosystem that causes the destruction of trees and vegetation along the shores of estuaries and other coastal regions of the world. Left alone, these trees and plants have evolved to take advantage of nutrients carried ashore on the jet and film drops produced by bursting bubbles in the sea (Art *et al.*, 1974).

5. Summary

Raindrops and snowflakes produce bubbles as they fall into the water, but whitecaps or breaking waves appear to be the primary bubble producers. On average about 1 percent of the sea is covered with whitecaps. Bubble sizes in whitecaps extend from <0.1 mm to at least 10 mm diameter.

Both jet and film drops are ejected into the atmosphere when bubbles burst at the surface of the water. Jet drops are about one-tenth the bubble diameter, while the more numerous film drops can range in size from <1 μm to >100 μm . The concentrations of these drops can be high. In the lowest kilometer of the atmosphere over the sea, for example, they can exceed 10^6 m^{-3} (Woodcock, 1972).

Air bubbles rising to the surface of the water collect any material, dissolved or particulate, that is surface-active. When the bubbles burst, the material is skimmed off the bubble to become highly enriched in the jet and film drops. The enrichment factors for some bacteria in jet drops can exceed several hundred for bubbles that have risen only a few centimeters through a bacterial suspension. The magnitude of the enrichment factor depends not only on the number of bacteria scavenged by the bubble but on other factors, including bubble size.

Health hazards may exist for those who live along the shore and inhale a bacterial-enriched aerosol, although a cause-and-effect relationship has not been clearly and convincingly shown. The only bubble-produced aerosol that has been definitely linked to human infections is that produced in air-conditioning cooling

towers containing the bacterium responsible for Legionnaires' disease. Under some conditions, trees and other vegetation along the shore can be damaged by pollutants that are scavenged from the water by bubbles and then ejected into the air on an aerosol that is carried inland by the wind.

Acknowledgments

I am grateful to my colleague, Lawrence Syzdek, whose expertise and persistence over the years has made much of this work possible. The present work was supported by the National Science Foundation under ATM-8514211.

References

- Art, H. W., F. H. Bormann, G. K. Voigt, and G. M. Woodwell, 1974: Barrier island forest ecosystem: role of meteorologic inputs. *Science*. 184:60-62.
- Asai, S., J. J. Krzanowski, W. H. Anderson, D. F. Martin, J. B. Polson, R. F. Lockey, S. C. Bukantz, and A. Szentivanyi, 1982: Effects of the toxin of red tide, *Ptychodiscus brevis*, on canine tracheal smooth muscle: a possible new asthma-triggering mechanism. *J. Allergy Clin. Immunol.* 69:418-428.
- Baylor, E. R., M. B. Baylor, D. C. Blanchard, L. D. Syzdek, and C. Appel, 1977: Virus transfer from surf to wind. *Science*. 198:575-580.
- Bezdek, H. F., and A. F. Carlucci, 1972: Surface concentration of marine bacteria. *Limnol. Oceanogr.* 17:566-569.
- Blanchard, D. C., 1963: The electrification of the atmosphere by particles from bubbles in the sea. *Prog. Oceanogr.* 1:71-202.
- Blanchard, D. C., 1983: The production, distribution, and bacterial enrichment of the sea-salt aerosol. 1983: pp. 407-454. In P. S. Liss and W. G. N. Slinn (eds.), *The Air-Sea Exchange of Gases and Particles*. Reidel Pub. Co.
- Blanchard, D. C. and L. D. Syzdek, 1970: Mechanism for the water-to-air transfer and concentration of bacteria. *Science*. 170:626-628.
- Blanchard, D. C. and L. D. Syzdek, 1972: Concentration of bacteria in jet drops from bursting bubbles. *J. Geophys. Res.* 77:5087-5099.
- Blanchard, D. C. and L. D. Syzdek, 1975: Electrostatic collection of jet and film drops. *Limnol. Oceanogr.* 20:762-774.
- Blanchard, D. C., and L. D. Syzdek, 1977: Production of air bubbles of a specified size. *Chem. Engr. Sci.* 32:1109-1112.
- Blanchard, D. C., and L. D. Syzdek, 1978: Seven problems in bubble and jet drop researches. *Limnol. Oceanogr.* 23:389-400.
- Blanchard, D. C., and L. D. Syzdek, 1982: Water-to-air transfer and enrichment of bacteria in drops from bursting bubbles. *Appld. Environ.*

- Microbiol.* 43:1001-1005.
- Blanchard, D. C., and L. D. Syzdek, 1988: Film-drop production as a function of bubble size. *J. Geophys. Res.* 93:3649-3654.
- Blanchard, D. C., L. D. Syzdek, and M. E. Weber, 1981: Bubble scavenging of bacteria in freshwater quickly produces bacterial enrichment in airborne drops. *Limnol. Oceanogr.* 26:961-964.
- Blanchard, D. C., and A. H. Woodcock. 1957: Bubble formation and modification in the sea and its meteorological significance. *Tellus.* 9:145-158.
- Burger, S. R., and J. W. Bennett, 1985: Droplet enrichment factors of pigmented and nonpigmented *Serratia marcescens*: possible selective function for prodigiosin. *Appl. Environ. Microbiol.* 50:487-490.
- Cabelli, V. J., H. Kennedy, and M. A. Levin, 1976: *Pseudomonas aeruginosa*-fecal coliform relationships in estuarine and fresh recreational waters. *J. Water Poll. Control Fed.* 48:367-376.
- Cipriano, R. J., 1979: Bubble and aerosol spectra produced by a laboratory 'breaking wave.' Ph.D. thesis. State University of New York at Albany.
- Cipriano, R. J. and D. C. Blanchard, 1981: Bubble and aerosol spectra produced by a laboratory 'breaking wave.' *J. Geophys. Res.* 86:8085-8092.
- Cipriano, R. J., E. C. Monahan, P. A. Bowyer, and D. K. Woolf, 1987: Marine condensation nucleus generation inferred from whitecap simulation tank results. *J. Geophys. Res.* 92:6569-6576.
- Clift, R., J. R. Grace, and M. E. Weber, 1978: *Bubbles, Drops, and Particles.* Academic Press. 380 pp.
- Colbourne, J. S., P. J. Dennis, J. V. Lee, and M. R. Bailey, 1987: Legionnaires' disease: reduction in risks associated with foaming in evaporative cooling towers. *Lancet.* 1(#8534):684.
- Crow, S. A., D. G. Ahearn, W. L. Cook, and A. W. Bourquin, 1975: Densities of bacteria and fungi in coastal surface films as determined by a membrane-adsorption procedure. *Limnol. Oceanogr.* 20:644-646.
- Dahlbäck, B., M. Hermansson, S. Kjelleberg, and B. Norkrans, 1981: The hydrophobicity of bacteria - an important factor in their initial adhesion at the air-water interface. *Arch. Microbiol.* 128:267-270.
- Dondero, T. J., Jr., R. C. Rendtorff, G. F. Mallison, R. M. Weeks, J. S. Levy, E. W. Wong, and W. Schaffner, 1980: An outbreak of Legionnaires' Disease associated with a contaminated air-conditioning cooling tower. *N. Engl. J. Med.* 302:365-370.
- Ferguson, R. L., and A. V. Palumbo, 1979: Distribution of suspended bacteria in neritic waters south of Long Island during stratified conditions. *Limnol. Oceanogr.* 24:697-705.
- Fliermans, C. B., W. B. Cherry, L. H. Orrison and L. Thacker, 1979: Isolation of *Legionella pneumophila* from nonepidemic-related aquatic habitats. *Appl. Envir. Microb.* 37:1239-1242.
- Fraizier, A., M. Masson, J. C. Guary, 1977: Recherches preliminaires sur le role des aerosols dans le transfert de certains radioelements du milieu marin au milieu terrestre. *J. Rech. Atmos.* 11:49-60.

- Friedman, S., K. Spitalny, J. Barbaree, Y. Faur, and R. McKinney, 1987: Pontiac fever outbreak associated with a cooling tower. *Amer. J. Public Health*. 77:568-572.
- Gellini, R., F. Pantani, P. Grossoni, F. Bussotti, E. Barbolani, and C. Rinallo. 1985: Further investigation on the causes of disorder of the coastal vegetation in the part of San Rossore (central Italy). *Eur. J. For. Path.* 15:145-157.
- Gruft, H., J. Katz, and D. C. Blanchard, 1975: Postulated source of *Mycobacterium intracellulare* (Battey) infection. *Amer. J. Epidemiology*. 102:311-318.
- Hejkal, T. W., P. A. LaRock, and J. W. Winchester, 1980: Water-to-air fractionation of bacteria. *Appl. Envir. Microbiology*. 39:335-338.
- Horrocks, W.H., 1907: Experiments made to determine the conditions under which "specific" bacteria derived from sewage may be present in the air of ventilating pipes, drains, inspection chambers and sewers. *Proc. Roy. Soc. London* 79B:255-266.
- MacIntyre, F., 1968: Bubbles: a boundary-layer "microtome" for micron-thick samples of a liquid surface. *J. Phys. Chem.* 72:589-592.
- MacIntyre, F., 1972: Flow patterns in breaking bubbles. *J. Geophys. Res.* 77:5211-5228.
- Monahan, E. C., 1969: Fresh water whitecaps. *J. Atmos. Sci.* 26:1026-1029.
- Monahan, E. C., and I. O' Muirheartaigh, 1980: Optimal power-law description of oceanic whitecap coverage dependence on wind speed. *J. Phys. Oceanogr.* 10:2094-2099.
- Monahan, E. C., and C. R. Zietlow, 1969: Laboratory comparisons of fresh-water and salt-water whitecaps. *J. Geophys. Res.* 74:6961-6966.
- Moore, D. J., and B. J. Mason, 1954: The concentration, size distribution and production rate of large salt nuclei over the oceans. *Q. J. Roy. Met. Soc.* 80:583-590.
- Parker, B. C., M. A. Ford, H. Gruft, and J. O. Falkinham III., 1983: Epidemiology of infection by nontuberculous mycobacteria. *Am. Rev. Respir. Dis.* 128:652-656.
- Pierce, R. H., 1986: Red tide (*Ptychodiscus brevis*) toxin aerosols: a review. *Toxicon*. 24:955-965.
- Resch, F. J., J. S. Darrozes, and G. M. Afeti, 1986: Marine liquid aerosol production from bursting of air bubbles. *J. Geophys. Res.* 91:1019-1029.
- Sargent, F.S. II, 1982: *Hippocratic Heritage: A History of Ideas about Weather and Human Health*. Pergamon Press. 581 pp.
- Smith, B. J., 1968: A study of the mechanism by which bioaerosols are generated when liquids containing microorganisms are aerated. Ph.D. thesis, Georgia Institute of Technology.
- Stuhlman, O., 1932: The mechanics of effervescence. *Physics* 2:457-466.
- Syzdek, L. D., 1985: Influence of *Serratia marcescens* pigmentation on cell concentrations in aerosols produced by bursting bubbles. *Appl. Environ. Microbiol.* 49:173-178.

- Tedesco, R., and D. C. Blanchard, 1979: Dynamics of small bubble motion and bursting in freshwater. *J. Rech. Atmos.* 13: 215-226.
- Weber, M. E., 1981: Collision efficiencies for small particles with a spherical collector at intermediate Reynolds numbers. *J. Separation Process Technology.* 2: 29-33.
- Weber, M. E., D. C. Blanchard, and L. D. Syzdek, 1983: The mechanism of scavenging of water-borne bacteria by a rising bubble. *Limnol. Oceanogr.* 28: 101-105.
- Williams, R. P. 1973. Biosynthesis of prodigiosin, a secondary metabolite of *Serratia marcescens*. *Appld. Microb.* 25: 396-402.
- Woodcock, A. H., 1948: Note concerning human respiratory irritation associated with high concentrations of plankton and mass mortality of marine organisms. *J. Marine Res.* 7: 56-62.
- Woodcock, A. H., 1955: Bursting bubbles and air pollution. *Sewage and Industrial Wastes.* 27: 1189-1192.
- Woodcock, A. H., 1972: Smaller salt particles in oceanic air and bubble behavior in the sea. *J. Geophys. Res.* 77: 5316-5321.
- Woodcock, A. H., and D. C. Blanchard, 1955: Tests of the salt-nuclei hypothesis of rain formation. *Tellus.* 7: 437-448.
- Woodcock, A.H., C.F. Kientzler, A.B. Arons, and D.C. Blanchard, 1953: Giant condensation nuclei from bursting bubbles. *Nature* 172: 1144.

Factors Influencing the Aerosolization of Mycobacteria

Joseph O. Falkinham, III
Department of Biology
Virginia Polytechnic Institute
Blacksburg, VA 24061

Abstract

Strains of the *Mycobacterium avium*, *M. intracellulare* and *M. scrofulaceum* (MAIS) group are highly concentrated in droplets ejected from the surfaces of natural waters and suspensions of cells in the laboratory. However, values reflecting the *in vitro* concentration of these mycobacteria in the ejected droplets are quite variable. The observed variation is due to both methodologic and biologic factors. Methodologic factors include differences in the growth medium composition, the formation of cell aggregates, the age of the culture and the concentration of salt in the suspending medium. Biologic factors include species and strain differences which remain after methodologic factors are taken into account. Surface charge of cells does not appear to be a major factor influencing differences in aerosolization.

Introduction

Representatives of the *Mycobacterium avium*, *M. intracellulare* and *M. scrofulaceum* (MAIS) group are human pathogens which are found in high numbers in southeastern United States waters (Falkinham, *et al.*, 1980). Because *M. avium* and *M. intracellulare* cause pulmonary infections (Wolinsky, 1979), the possibility that MAIS organisms were aerosolized from natural waters was

investigated. Not only were MAIS organisms shown to be aerosolized and associated with particles able to penetrate human lung alveoli (Wendt, *et al.*, 1980), but those aerosolized were identical to those recovered from patients with pulmonary infections (Fry, *et al.*, 1986; Meissner and Falkinham, 1986).

Because of the evident importance of this pathway for human infection by these environmental human pathogens, the aerosolization of MAIS strains was studied in the laboratory. Ejected droplets produced by bubbles rising through a suspension of bacteria can be collected on medium suitable for growth and the number of cells in each droplet directly determined (Blanchard and Syzdek, 1970). Studies of the *in vitro* aerosolization of strains of *M. avium*, *M. intracellulare* and *M. scrofulaceum* demonstrated that representatives of the former two species were highly concentrated in ejected droplets with respect to their concentration in the bulk suspension (Parker, *et al.*, 1983). That observation was consistent with the fact that *M. scrofulaceum* is rarely found as a pulmonary pathogen (Wolinsky, 1979). However, that conclusion was weakened by the fact that values for the relative concentration of mycobacteria in ejected droplets varied widely (Parker, *et al.*, 1983). In addition to such methodologic factors as uniform bubble diameter (Blanchard and Syzdek, 1977) and bubble rise distance through the bacterial suspension (Blanchard, *et al.*, 1981; Weber, *et al.*, 1983), we sought to identify biologic and other methodologic factors capable of influencing the measurement of mycobacterial enrichment in aerosolized droplets.

Materials and Methods

Mycobacterial Strains.

The *Mycobacterium avium* and *M. scrofulaceum* strains used in this study are listed in Table 1 along with their origin of isolation and enrichment in ejected droplets. *M. intracellulare* strains were not included because they behave as do those of *M. avium*.

Growth of Mycobacteria.

Stock cultures were maintained in Middlebrook 7H9 broth base (BBL Microbiology Systems, Cockeysville, MD) containing 0.5%

(vol/vol) glycerol and 10% (vol/vol) OADC enrichment (BBL Microbiology Systems, Cockeysville, MD). For aerosolization experiments, strains were grown in either Middlebrook 7H9 broth base containing 0.5% (vol/vol) glycerol, Middlebrook 7H9 broth base containing 0.5% (vol/vol) glycerol and 10% (vol/vol) OADC enrichment, or in autoclaved natural water (George, *et al.*, 1980) collected from the James River in Richmond, Virginia. All strains were grown to late log phase at 30°C for each experiment. For some experiments cultures were vortexed vigorously for 3 minutes before suspension at low density for aerosolization.

Measurement of Aerosolization.

Enrichment of the strains in droplets ejected from suspensions in filter-sterilized James River water was measured as described by Parker, *et al.* (1983). For examination of the influence of salinity on aerosolization, artificial sea salts (Forty Fathoms Bio-crystals Marine Mix, Marine Enterprises, Timonium, MD) were added to the bacterial suspension. Results are expressed as the enrichment factor (EF) obtained by dividing the colony forming units/ml (cfu/ml) of the collected ejected droplets by the cfu/ml of the bulk suspension (Parker, *et al.*, 1983).

Measurement of Cell Surface Charge.

The surface charge of cells grown and suspended in James River water was measured by micro-electrophoresis using a cytopherometer (Carl Zeiss, Oberkochen, FRG) as described by George, *et al.* (1986).

Results

Species and Strain Differences in Enrichment.

The data in Table 1 show that there were wide differences in the potential for aerosolization (i.e. expressed as enrichment factor) between species and strains of the same species. *Mycobacterium avium* strains were generally more enriched in ejected droplets than were strains of *M. scrofulaceum* (Table 1; Parker, *et al.*, 1983). Note that one strain of *M. scrofulaceum* (14S) was highly enriched in ejected droplets (Table 1). The mean values for

enrichment factors (EF) were significantly different ($P < 0.05$, Student's T-test) between some representatives of a single species (i.e. *M. avium* strains 13S and 18S and *M. scrofulaceum* strains 14S and 16S, Table 1). However, in spite of the significance of the differences, there was great variability in the enrichment factors (Table 1) and we sought to identify the sources of that variability.

Influence of Medium Composition on Aerosolization.

The enrichment factor of cells of *M. avium* strain 13S grown in Middlebrook 7H9 broth containing 1% (vol/vol) glycerol and 10% (vol/vol) OADC enrichment (EF = 230 ± 160) was significantly lower ($P < 0.05$, Student's T-test) than the value for cells grown in filter-sterilized James River water (EF = $1,100 \pm 470$). This difference was observed in spite of the fact that cells of both strains were suspended in a portion of the same sample of James River water for aerosolization.

Table 1. List of mycobacteria strains.

Species and Strain	Source of Isolation	Enrichment Factor ^a	Reference
<i>Mycobacterium avium</i>			
13S	aerosol	$5,200 \pm 3,400$	Wendt, <i>et al.</i> (1980)
18S	water	$1,060 \pm 340$	Wendt, <i>et al.</i> (1980)
W227	water	$2,200 \pm 1,300$	Falkinham, <i>et al.</i> (1980)
<i>Mycobacterium scrofulaceum</i>			
14S	aerosol	$1,600 \pm 1,300$	Wendt, <i>et al.</i> (1980)
16S	water	130 ± 99	Wendt, <i>et al.</i> (1980)
W220	water	180 ± 150	Falkinham, <i>et al.</i> (1980)
W256	water	130 ± 78	Falkinham, <i>et al.</i> (1980)

^a Mean values \pm standard deviation.

Effect of Cell Aggregation on Aerosolization.

Earlier data had suggested that cell aggregation contributed to variation in enrichment factors (Parker, *et al.*, 1983). To determine whether aggregation of cells could influence measurement of droplet enrichment, two approaches were chosen. Table 2 shows the results of the effect of spreading ejected droplets following

bubble impact on the medium. The values for enrichment factors of *M. avium* strain W227 and *M. scrofulaceum* strain 14S were significantly higher ($P < 0.05$, Student's T-test) when the droplets were spread over the surface of the medium (Table 2). Though not statistically significant, EF values for both *M. scrofulaceum* strains 16S and W220 were higher when droplets were spread (Table 2).

The second approach examined the effect of 3-minute-vortexing a culture of *M. avium* strain 13S before suspending cells in James River water for aerosolization. The EF value for an untreated suspension of *M. avium* strain 13S was $10,500 \pm 2,900$. The EF value for the same culture vortexed 3 minutes before suspension in James River water was 510 ± 130 . Vortexing, to produce a

Table 2. Effect of aggregation on mycobacterial aerosolization.		
Species and Strain	Enrichment Factor	
	Unspread	Spread
<i>Mycobacterium avium</i>		
W227	550 ± 420	2,800 ± 1,400
<i>Mycobacterium scrofulaceum</i>		
14S	170 ± 54	1,600 ± 1,300
16S	84 ± 41	130 ± 99
W220	210 ± 130	380 ± 220

less aggregated suspension, led to a significant drop in the enrichment factor ($P < 0.05$, Student's T-test).

Effect of Salinity on Aerosolization.

Because MAIS organisms are recovered (Falkinham, *et al.*, 1980) and can grow (George, *et al.*, 1980) in natural waters of moderate salinity (i.e. 1 and 2% sea salts), the possibility that salt concentration influenced aerosolization of mycobacteria was investigated. The data in Table 3 illustrate that mean enrichment factor values changed as the concentration of artificial sea salts added to James River water increased. At low sea salts concentrations (i.e. 1-3%), the EF values for *M. avium* strain 18S rose significantly ($P < .05$, Student's T-test), while at the highest

concentration (i.e. 4%) they were unchanged. In addition, sea salts decreased the volume of ejected droplets within the 60 second period of aerosol collection (Table 3).

Table 3. Effect of artificial sea salts on enrichment of *Mycobacterium avium* strain 18S in ejected droplets.

Sea Salts Concentration	Enrichment Factor	Droplet Volume*
0	110 ± 10	580
1%	2,900 ± 2,100	10
2%	1,300 ± 280	9
3%	1,300 ± 600	13
4%	170 ± 40	100

*Expressed as $10^6 \mu^3$.

Effect of Cell Surface Charge on Aerosolization.

Because of the effect of sea salts on aerosolization of mycobacteria, the possibility that differences in cell surface charge were associated with differences in EF values was investigated. Cell surface charge of mycobacteria grown and suspended in the James River water for aerosolization was measured by migration in an electric field as described in George, *et al.* (1986) and the results shown in Table 4. Though there were wide differences in EF values of both *M. avium* and *M. scrofulaceum* strains, these did not correlate with differences in either the magnitude or polarity of cell surface charge (Table 4).

Discussion

The results demonstrate that both biologic and methodologic factors influence values for mycobacterial enrichment in ejected droplets. It is likely that differences in aerosolization of both *M. avium* and *M. scrofulaceum* strains when grown in either filter-sterilized natural water or complex mycobacterial medium reflect the ability of the organisms to alter their cell surface composition.

Table 4. Cell surface charge and enrichment factors for mycobacteria.

Species and Strain	Enrichment Factor	Surface Charge
<i>Mycobacterium avium</i>		
13S	5,200 ± 3,400	-0.80
18S	1,060 ± 340	-0.36
<i>Mycobacterium scrofulaceum</i>		
14S	1,600 ± 1,300	-0.51
16S	130 ± 99	-0.80
W220	180 ± 150	-0.58
W256	130 ± 78	-0.60

Cell aggregation also affected enrichment in droplets (Table 2). Increased EF values for droplets which were spread probably reflect the fact that droplets contained aggregated mycobacterial cells and spreading disrupted the aggregates. Likewise, the fall in EF values following vortexing was probably due to the disruption of aggregates, so fewer aggregates were present in ejected droplets yielding high cell numbers when spread. Because the extent of aggregation of mycobacterial cells changes with their growth stage (i.e. late log and early stationary phase cultures are heavily aggregated; Falkinham, unpublished), the growth stage of *M. avium* and *M. scrofulaceum* cells is likely to influence enrichment in ejected droplets as well.

Although low concentrations of artificial sea salts increased the EF values for mycobacterial strains, this was accompanied by changes in the volume of ejected droplets (Table 3). Because the increases in EF values were offset by decreases in droplet volume ejected, measured within the same time period for James River water with and without 1% artificial sea salts, approximately the same number of mycobacterial cells were transferred except at the highest concentration tested (i.e. 4%, Table 3).

The data demonstrate that the differences in droplet enrichment values of *M. avium* and *M. scrofulaceum* strains are not associated

with differences in cell surface charge measured in filter-sterilized James River water (Table 4). Values for cell surface charge were negative and of similar magnitude for strains which differed widely in enrichment factors even though all strains were grown in and EF values measured in the James River water. Thus, surface charge was not a determinant of aerosolization of mycobacteria.

Acknowledgments

The author acknowledges the expert technical assistance of Karen George and Mary Ann Ford and the advice and encouragement of Drs. Bruce Parker, Duncan Blanchard, Lawrence Syzdek and Ramon Cipriano.

This research was supported by Public Health Service grant AI-13813 from the National Institute of Allergy and Infectious Disease.

References

- Blanchard, D.C. and L.D. Syzdek, 1970: Mechanisms for the water-to-air transfer and concentration of bacteria. *Science* 170:626-628.
- Blanchard, D.C. and L.D. Syzdek, 1977: Production of air bubbles of a specified size. *Chem. Engr. Sci.* 32:1109-1112.
- Blanchard, D.C., L.D. Syzdek and M.E. Weber, 1981: Bubble scavenging of bacteria in freshwater quickly produces bacterial enrichment in airborne jet drops. *Limnol. Oceanogr.* 26:961-964.
- Falkinham, J.O., III, B.C. Parker and H. Gruft, 1980: Epidemiology of infection by nontuberculous mycobacteria. I. Geographic distribution in the eastern United States. *Am. Rev. Respir. Dis.* 121:931-937.
- Fry, K.L., P.S. Meissner and J.O. Falkinham, III, 1986: Epidemiology of infection by nontuberculous mycobacteria. VI. Identification and use of epidemiologic markers for studies of *Mycobacterium avium*, *M. intracellulare* and *M. scrofulaceum*. *Am. Rev. Respir. Dis.* 134:39-43.
- George, K.L., A.T. Pringle and J.O. Falkinham, III, 1986: The cell surface of *Mycobacterium avium-intracellulare* and *M. Scrofulaceum*: effect of specific chemical modifications on cell surface charge. *Microbios* 45:199-207.
- George, K.L., B.C. Parker, H. Gruft and J.O. Falkinham, III, 1980: Epidemiology of infection by nontuberculous mycobacteria. II. Growth and survival in natural waters. *Am. Rev. Respir. Dis.* 122:89-94.
- Meissner, P.S. and J.O. Falkinham, III, 1986: Plasmid DNA profiles as

- epidemiological markers for clinical and environmental isolates of *Mycobacterium avium*, *M. intracellulare* and *M. scrofulaceum*. *J. Infect. Dis.* **153**:325-331.
- Parker, B.C., M.A. Ford, H. Gruft and J.O. Falkinham, III, 1983: Epidemiology of infection by nontuberculous mycobacteria. IV. Preferential aerosolization of *Mycobacterium intracellulare* from natural waters. *Am. Rev. Respir. Dis.* **128**:652-656.
- Weber, M.E., D.C. Blanchard and L.D. Syzdek, 1983: The mechanism of scavenging of waterborne bacteria by a rising bubble. *Limnol. Oceanogr.* **28**:101-105.
- Wendt, S.L., K.L. George, B.C. Parker, H. Gruft and J.O. Falkinham, III, 1980: Epidemiology of infection by nontuberculous mycobacteria. III. Isolation of potentially pathogenic mycobacteria from aerosols. *Am. Rev. Respir. Dis.* **122**:259-263
- Wolinsky, E., 1979: Nontuberculous mycobacteria and associated diseases. *Am. Rev. Respir. Dis.* **119**:107-159.

Marine Toxins in Bubble-Generated Aerosols

Richard Pierce, Michael Henry, Stephanie Boggess¹ and
Ann Rule²

Mote Marine Laboratory
1600 City Island Park
Sarasota, Florida 34236

¹Current Address: Chemistry Department, Univ. N.Carolina, Chapel Hill,
NC 27514

²Current Address: Chemistry Department, Emory Univ., Atlanta, GA 30322

Abstract

Red tide toxin association with marine aerosol is indicated by respiratory irritation experienced along the shore during episodes of the Florida red tide, caused by the dinoflagellate, *Ptychodiscus brevis*. Toxin analyses were performed on samples of seawater and marine aerosol collected during red tide blooms, showing the composition of aerosolized toxins to be similar to those extracted from the seawater, with an apparent enhancement of one toxin (PbTx-3) over the others in aerosol. For a more consistent comparison between the composition of toxins in aerosol and the source water, laboratory cultures of *P. brevis* were used. Toxin analyses showed that the toxins recovered from laboratory-maintained cultures were similar in composition to those extracted from red tide-containing seawater. Of the eight toxins produced by *P. brevis*, four were observed in sufficient quantity to monitor bubble-mediated transport. The results showed that air bubbles passing through *P. brevis* culture concentrated toxins from the bulk solution, producing toxin-enriched surface foam, jet drops and aerosol. Toxin

concentration in foam was enriched 3 to 5 times the original solution whereas jet drops and aerosol were enriched 20 to 50 times. The apparent enhancement of PbTx-3 over other toxins in aerosol was due to conversion of PbTx-2 to PbTx-3, rather than selective adsorption of PbTx-3 to the air bubble surfaces.

Introduction

This study was undertaken to investigate the incorporation of red tide toxins into marine aerosol. The hypothesis is that bubbles entrained in seawater from breaking waves scavenge marine toxins from the water, effecting transport to the sea-air interface. Toxin-enriched jet- and film-drops ejected from bubbles bursting at the sea surface result in toxin-enriched marine aerosol.

Marine toxins are present in many coastal regions throughout the world. About thirty species of dinoflagellates have been documented to produce toxins which, during "red tide" blooms may cause fish kills and contaminate seafood through bioaccumulation (Shimizu, 1978; Baden, 1983; Steidinger, 1983). Marine bacteria also have been implicated in toxin production (Narita *et al.*, 1986; Simidu *et al.*, 1987), and some of these species (*Vibrio alginoliticus*, *V. parahaemolyticus*) have been isolated from red tide blooms of the Florida Gulf coast (Buck and Pierce, 1989).

Red tides, caused by the toxic dinoflagellate, *Ptychodiscus brevis* (formerly *Gymnodinium breve*) occur periodically in the Gulf of Mexico, most prevalently along the Southwest Florida coasts. During periods of on-shore winds, severe respiratory irritation is experienced near the shore, indicating the presence of toxins in association with the marine aerosol. Human health hazards are apparent through the effects of *P. brevis* red tide toxin aerosol on humans which include burning and watering of the eyes, severe irritation of the nose and throat with a dry, choking cough and breathing difficulty. Although acute symptoms generally subside when exposure is eliminated, many individuals complain of lingering respiratory problems including asthmatic attacks and allergic reactions.

While investigating a red tide episode at Venice, Florida, in 1947, Woodcock (1948) surmised the relationship between respiratory irritation and aerosolized dinoflagellate products. At that time he suggested that the irritant-containing aerosols were probably formed by bursting bubbles from breaking waves within the dinoflagellate bloom area.

Since this early insight, very little new information about biosynthesized marine toxin aerosols has been provided (Steidinger and Joyce, 1973; Baden *et al.*, 1982; Pierce, 1986). Recent advances in knowledge about red tide toxins and improved analytical methods have allowed a more in-depth investigation of this phenomenon. The chemical structures of two of the primary neurotoxins biosynthesized by *P. brevis* were elucidated by Lin *et al.* (1981) and Shimizu (1982). These compounds consist of a heterocyclic oxygenated fused ring system, with a terminal aldehyde or alcohol, designated brevetoxin-B (BTX-B) and GB-3, respectively. To date, as many as eight chemical toxins have been reported under various nomenclatures (Padilla *et al.*, 1975; Baden and Mende, 1982; Chou *et al.*, 1985; Nakanishi, 1985; Pierce *et al.*, 1985; Shimizu *et al.*, 1986). Poli *et al.*, 1986, proposed a revised nomenclature to help eliminate confusion from the various systems in use. The chemical structure of six of these toxins identified in our samples is given in Figure 1.

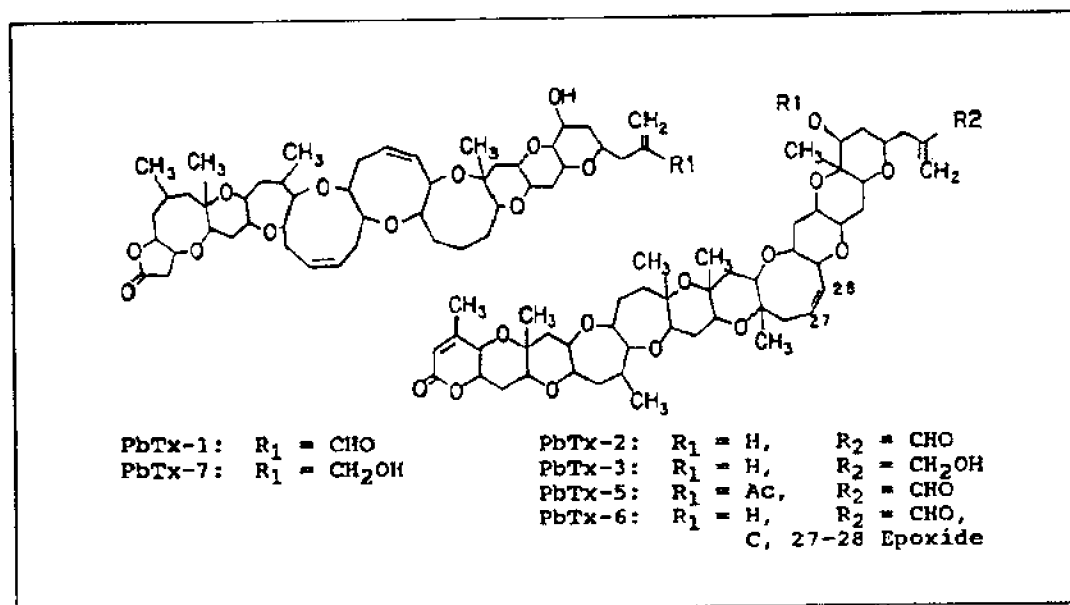


Figure 1. Chemical structures for *P. brevis* toxins.

The process by which these toxins become airborne is probably through the production of marine aerosols by bursting bubbles at the sea-air interface, which in turn jettisons minute droplets of water with contained salts and other substances into the air as shown in Figure 2 (Blanchard, 1975, 1983; Duce, 1983; Gershey, 1983; Woolf *et al.*, 1987).

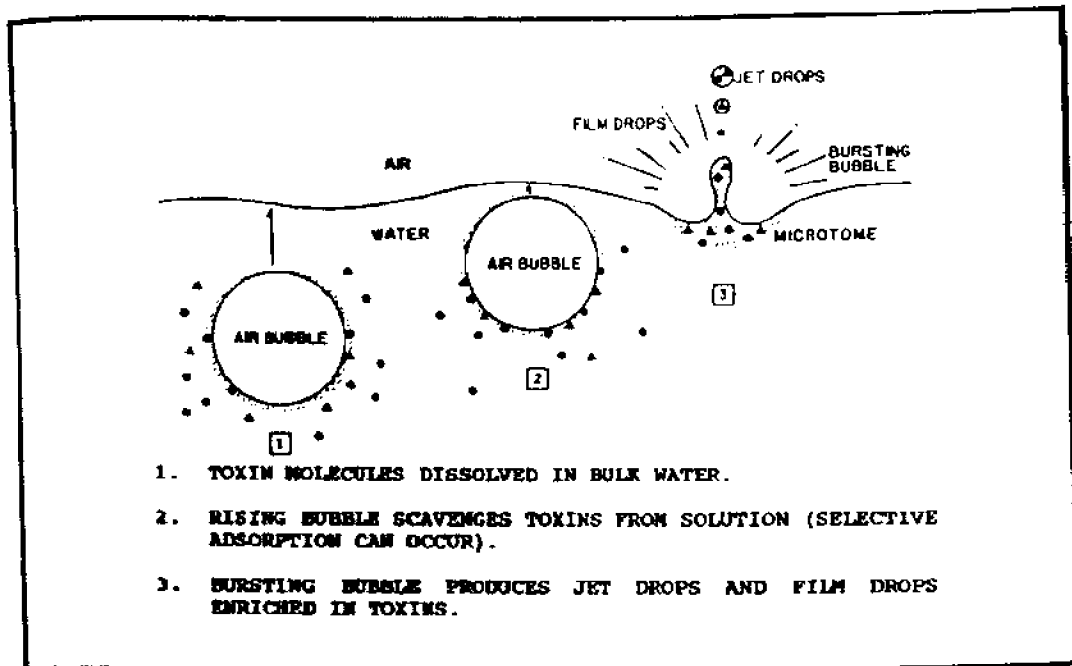


Figure 2. Toxin aerosol production scenario for dissolved toxins.

This bubble-jet explanation for aerosol formation was verified by high speed photography (Woodcock *et al.*, 1953; Kientzler *et al.*, 1954; Blanchard and Woodcock, 1957), showing a wide range of sea-salt nuclei produced from bubbles bursting at the sea-air interface, many of which are in the $<10 \mu\text{m}$ size range, which could be deposited within the human respiratory system (MacIntyre, 1974; Blanchard, 1983; Blanchard and Syzdek, 1988).

This investigation encompassed the analysis of red tide toxins in water and marine aerosol during natural blooms, followed by observations of toxin composition in water, foam, jet drops and aerosol under carefully controlled laboratory conditions. The latter experiments were conducted with laboratory cultures of *P. brevis* using air bubbles to mediate toxin transport.

Experimental Methods

Field Collection

Toxin composition was investigated in field samples of water and aerosol during natural red tide blooms along the Florida Gulf Coast in May, 1987 (Pierce *et al.*, 1987), and along the North Carolina coast in November, 1987 (Pierce, 1987; Tester *et al.*, 1989). Although all six toxins depicted in Figure 1 were observed among the samples, only three of the toxins (PbTx-2, -3 and -5) were recovered from field samples in sufficient quantities and with consistent frequency to provide quantitative as well as qualitative results.

Water samples were collected in 20-l glass carboys and extracted into dichloromethane (CH_2Cl_2) according to the procedure of Pierce *et al.* (1985) outlined below under Toxin Analysis. Aerosol samples were collected by drawing air through 0.45 μ glass fiber filters, 20 cm x 25 cm, using a Model GMWI-2000 High Volume Air Sampler with Model FH-2100 Filter Holder (General Metal Works, Inc., Cleves, OH). Air samplers were secured in wooden stands and placed on the beach at the dune line about 100m from the surf. The samples pulled 40 to 50 cfm for a duration of 3 to 6 hours. Filters were folded collection-side in, placed in 1 pt glass jars with 100-ml CH_2Cl_2 added for immediate extraction. Samples were stored in the dark for transport to the lab for immediate processing.

Toxin Degradation in Seawater

The rate of toxin decomposition and/or conversion was observed by monitoring the toxin content of seawater samples collected from an intensive red tide bloom off Sarasota, FL. Duplicate, 10-l samples were sonicated with a Model CV-500 ultrasonic cell disrupter (Sonics & Materials, Danbury, CT) to release all toxins simultaneously. The sonicated samples were then placed in 20-l carboys with slight aeration to maintain aerobic conditions. Temperature, salinity and dissolved oxygen also were monitored.

Toxins were analyzed in the original culture and in 2-l aliquots collected from each carboy at designated time intervals of 0, 1, 3, 9 and 21 days.

Toxin Enrichment in Bubbled-Mediated Foam and Jet Drops

The enrichment of toxins in surface foam and jet drops relative to bulk solution was investigated by passing air bubbles through 10 cm of ultra-sonicated *P. brevis* culture (2 l of culture in a 4-l glass beaker, 25×10^6 cells/l), collecting separately the foam and jet drops produced during a 30-minute sampling period. Foam was collected in a side-arm flask by aspiration through a tygon tube. Jet drops were collected by impact on a glass-fiber filter placed 5-cm above the surface of the culture, with replacement of the filter when saturation was approached. Room and culture temperature was 24°C and relative humidity was 50%. A complete mass balance of toxin composition was obtained in duplicate studies by analyzing toxins in the original culture, post-bubbled culture, foam and filters.

Toxin Enrichment in Bubble-Mediated Aerosol

The production of toxin aerosol by bursting bubbles was investigated in a specially designed aerosol production and collection chamber. The chamber (Figure 3) was designed such that air traveling at a pre-determined velocity impacts bubble-produced jet and film drops carrying the droplets as aerosol particles a minimum of 40 cm before impacting the glass-fiber filter of the high volume air sampler. A foam overflow and water recirculation system was built into the bubble chamber to maintain a constant water level and reduce foam build-up which would inhibit the formation of jet drops as observed by Garrett (1968). Air bubbles averaging 1 mm diameter were produced by passing air through a fritted glass aerator.

Duplicate sets of analyses were performed on a *P. brevis* culture consisting of 40×10^6 cells/l. The cells were lysed by ultrasound prior to aerosol production. Experimental conditions included 3.6 l of culture originally in the chamber, 4-hr duration aerosol production-collection, resulting in 3.4 l of residual culture remaining after aerosolization. Toxin mass balance was provided by analyzing toxins in the original culture, bubbled culture, glass-fiber filter (aerosol), and material deposited on the sides of the chamber from dried foam, jet and film drops impacting the chamber. Room temperature was 24°C, relative humidity 75%, air

velocity over the bubble chamber was 10 knots and the high volume air sampler was pulling approximately 38 cfm.

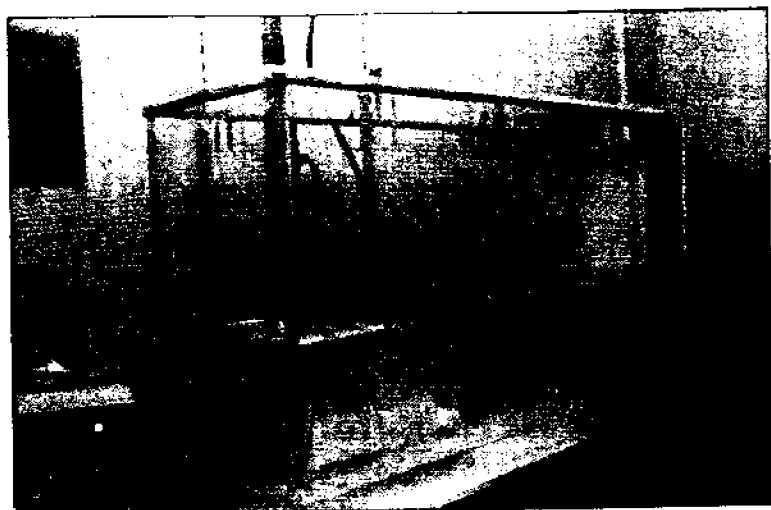


Figure 3. Toxin aerosol production and collection chamber.

Toxin Analysis

Toxins were extracted from water or filters into CH_2Cl_2 . The CH_2Cl_2 was evaporated and the residue dissolved in methanol (CH_3OH). Ten percent water was added to the CH_3OH and the solution was washed with petroleum ether to remove pigments. Additional water was added and the toxins were recovered in CH_2Cl_2 . Further purification was obtained with silica column and thin layer chromatography. Final quantitative and qualitative analysis was obtained by high performance liquid chromatography (HPLC) (Pierce *et al.*, 1985).

Toxin analysis was performed using a Varian Model 5020 HPLC with a Varian UV-50, uv/vis spectrophotometer at 215 nm (Varian Instruments, Palo Alto, CA). The column was B&J OD-5 (ODS-C18, reverse phase), 25 cm x 0.46 cm ID, with a mobile phase of 15% water in methanol at a flow rate of 1.0 ml/min.

Verification of qualitative HPLC analysis of the six toxins observed in Mote Marine Laboratory cultures was obtained by inter-laboratory calibration with Dr. Daniel Baden of the University of Miami, Rosenstil School of Atmospheric and Marine Science.

Quantitative analysis of PbTx-2 and PbTx-3 was established with standard solutions of each toxin prepared from purified and

recrystallized toxin extracts. Sufficient quantities of all other toxins were not available to prepare standard HPLC curves for quantitative analysis. For this report, all toxins, other than PbTx-2, were assigned uv response factors identical to PbTx-3 for quantification. Toxins are listed in the figures in order of elution during HPLC analysis: PbTx-3, -6, -2, -7, -5, -1. The other two possible toxins, PbTx-4 and PbTx-8, have not been identified in our samples.

Results and Discussion

Field Samples

Results of toxin analysis for the Florida red tides (Figure 4) show PbTx-2 to be the most abundant toxin (average of 200 $\mu\text{g/l}$), about 4 to 8 times more abundant than PbTx-3 and PbTx-5 (averaging 30 $\mu\text{g/l}$), resulting in a ratio of PbTx-2/3 near 7. The aerosol samples revealed similar patterns except that the relative amount of PbTx-3 increased with respect to PbTx-2 (2/3 ratio = ca. 3), suggesting an enrichment of PbTx-3 in aerosol relative to PbTx-2.

Samples from the North Carolina bloom contained the same three most abundant toxins (Figure 5); however, PbTx-2 was more abundant relative to PbTx-3 in comparison to the Florida samples with a PbTx-2/-3 ratio of 8 to 12. The aerosol sample also exhibited an increase of PbTx-3 over PbTx-2 as compared to the water

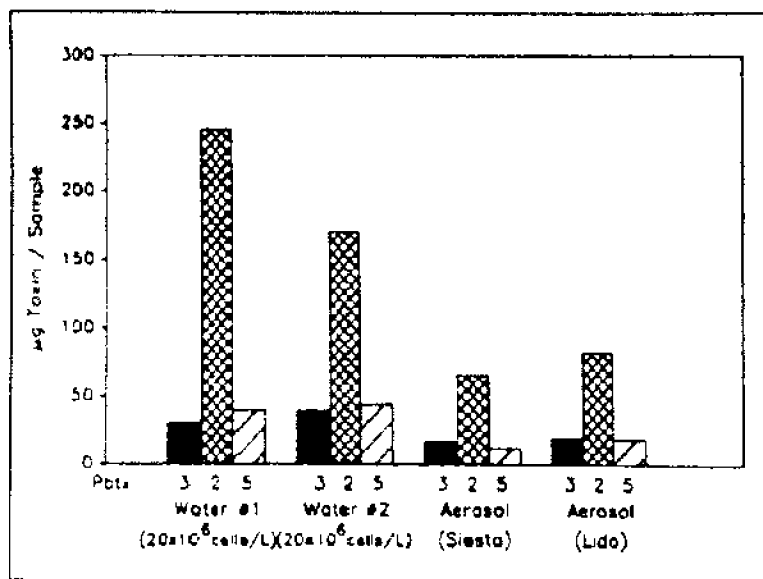


Figure 4. Toxin concentration in Florida red tide blooms, May 1987, water and aerosol samples.

samples (2/3 ratio = ca. 3). Preliminary results of this study first reported by Pierce (1987) are presented here based on revised toxin standards. The Florida red tide blooms were much more intense at 20 to 26 x 10⁶ cells/l than the North Carolina blooms' 5 to 6 x 10⁶ cells/l. However, toxin content per cell abundance was greater for the North Carolina bloom (ca. 22 µg/10⁶ cells) than for the Florida bloom (ca. 14 µg/10⁶ cells).

Toxin Degradation in Seawater

Information about the persistence and rate of change in toxin

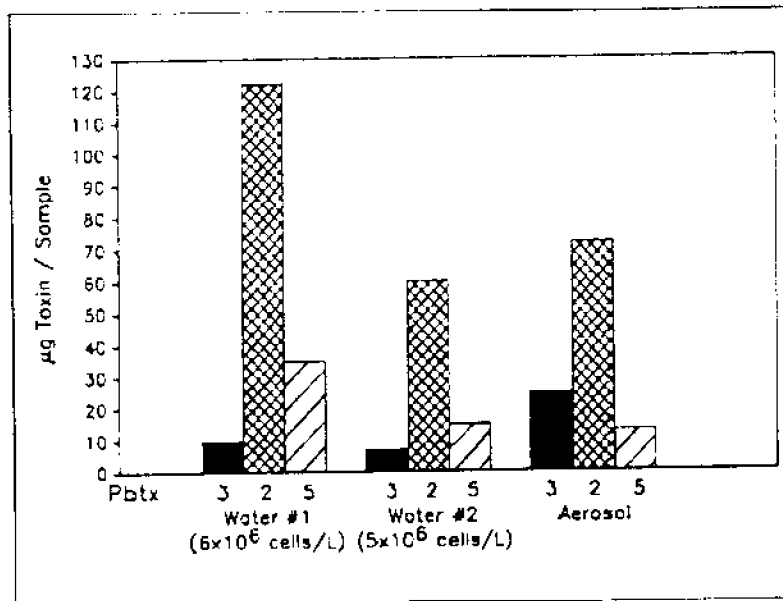


Figure 5. Toxin concentration in North Carolina red tide bloom, November 1987, water and aerosol samples.

composition during a bloom is essential for interpreting field toxin data. Results of the toxin degradation study (Figure 6) show a conversion (reduction) of PbTx-2 to PbTx-3 over a 9-day period with subsequent loss of PbTx-2 by day 21, indicating that toxins may persist in excess of 3 weeks following cell lysis. Thus, differences in toxin composition from one sampling place to another or from one time to another may result from not only different growth stages and concentrations of the *P. brevis* organisms, but also from different degradation sequences of toxins released into the water from lysed cells. Conversion of PbTx-2 to PbTx-3 indicates that the apparent enrichment of PbTx-3 in marine aerosol may be a result of chemical conversion rather than preferential adsorption to bubble surfaces. In view of the marked increase in PbTx-3 over

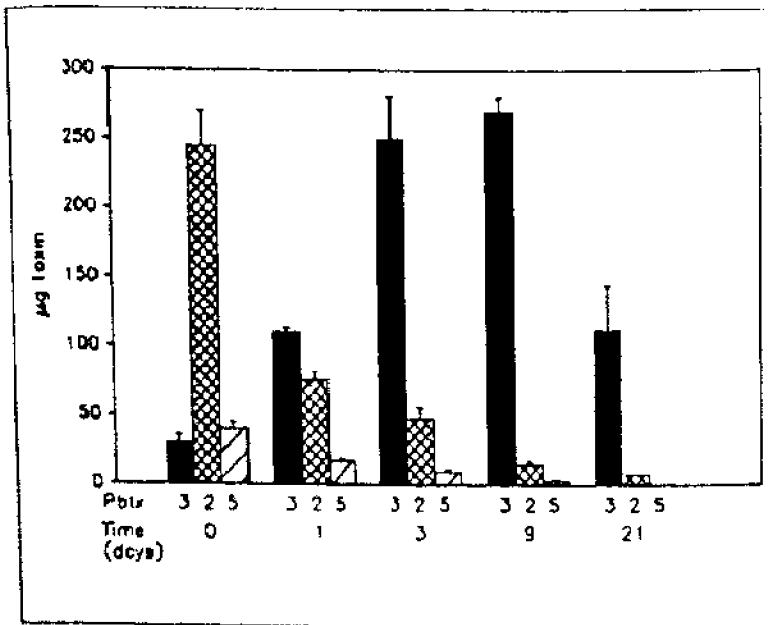


Figure 6. Change in toxin composition in aerobic seawater (30×10^6 cells/l) μg toxin/2l sample, 23°C , $37^\circ/\text{sec}$.

time in water and as observed above in aerosol samples, it is interesting to note that PbTx-3 has been implicated as the most potent respiratory irritant among the *P. brevis* toxins (Baden *et al.*, 1982).

Toxin Enrichment in Bubble-Mediated Foam and Jet Drops

This experiment was performed to establish the role of bubbles in collecting toxins from bulk solution with subsequent transport to the sea-air interface. Specifically addressed was the differentiation between aerosols resulting from direct removal of surface water as chop and spume drops blown aloft by the wind and from bubble concentration and enrichment of toxins in jet and film drops (Woolf *et al.*, 1987). Results (Figure 7 and Table 1) show that the toxins were enriched in the surface foam by a factor of about 3 times that in the original culture, and in jet drops reaching a height of 5 cm above the water surface by an enrichment factor of about 40. These results indicate that the jet drop material impacting the filters was not airborne foam, but resulted from a more highly enriched source such as jet drops produced from bursting bubbles (Blanchard, 1983; 1985).

An apparent increase in PbTx-3 over PbTx-2 in the foam and jet drops would suggest that PbTx-3 may have a greater affinity for the bubble surfaces than does PbTx-2. When considering the

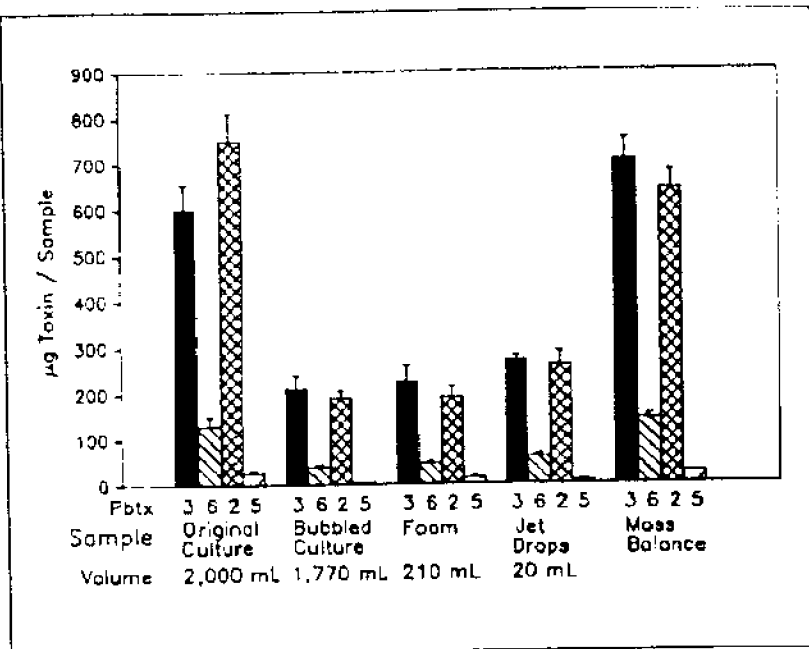


Figure 7. Toxin enrichment in bubble-produced foam and jet drops (*P. brevis* culture, 25×10^6 cells/l), 30-minute sample in bubble chamber at 25°C, 34‰.

entire mass balance, however, it becomes evident that an increase in PbTx-3 was also observed in the remaining culture after removal of toxins by bubbling, which is contrary to selective removal of PbTx-3 by bubbles. Also, the final mass balance showed a decrease in PbTx-2 in proportion to the increase in PbTx-3, providing strong evidence for the conversion of PbTx-2 to PbTx-3, as was indicated in the toxin degradation study above.

The other two toxins found in sufficient quantity to evaluate

Table 1. Toxin enrichment in bubble-mediated surface foam and jet drops.

SAMPLE	VOLUME	PBTX-2	PBTX-3	PBTX-5	PBTX-6
ORIGINAL CULTURE µg/l	2,000 ml	375±27	300±27	12±3	65±10
BUBBLED CULTURE EF ¹	1,770 ml	0.28	0.35	NR ²	0.33
FOAM EF	120 ml	2.4	3.6	5.0	3.3
JET DROPS EF	20 ml ³	35	45	30	46

¹ EF: enrichment factor, µg/l sample ÷ µg/l original culture

² NR: none recovered

³ Volume estimated by difference

foam and jet drops (Table 1). The *P. brevis* culture used for this study contained 25×10^6 cells/l, exhibiting a toxin to cell ratio of $29 \mu\text{g}$ toxin/ 10^6 cells.

Toxin Enrichment in Bubble-Mediated Aerosol

Having established toxin enrichment in jet drops, the continued enrichment during the transition from jet drops to aerosol had to be verified. Results of studies using the aerosol production and collection chamber (Figure 8), show a very similar scenario to that observed above for the jet drops. The uncertainty regarding the actual volume of culture represented precludes calculation of precise enrichment factors. Rough estimates of aerosol volume of 20 to 50 ml results in enrichment factor of 20 to 50 times that in the original solution. Although these calculations show considerable toxin enrichment in aerosol, the magnitude is much less than the 17,000 enrichment estimated for organics from seawater by Blanchard (1975) and by Hoffman and Duce (1974). This discrepancy could be caused by our use of larger, less efficiently enriching bubbles (avg. 1 mm) than are produced by breaking waves (avg. 200-500 μm) (Blanchard, 1985; Monahan, 1986). Also, our study collected more than just the top jet drop which is the most highly enriched top jet drop reported by Blanchard (1985) and Blanchard and Syzdek (1988).

These data show that all of the *P. brevis* toxins recovered exhibited considerable enrichment in the bubble-produced aerosol with no apparent selection for one toxin over another. Culture for this study contained 40×10^6 cells/l, resulting in $29 \mu\text{g}$ toxin/ 10^6 cells. Additional studies with larger quantities of toxin and more precise aerosol volume determinations are needed to obtain data on all of the toxins produced by *P. brevis*.

Conclusions

1. Major toxins biosynthesized by *P. brevis* during red tide blooms along the Florida Gulf Coast were similar to those from a bloom along the North Carolina coast, and were similar to those produced in laboratory-maintained cultures at MML.

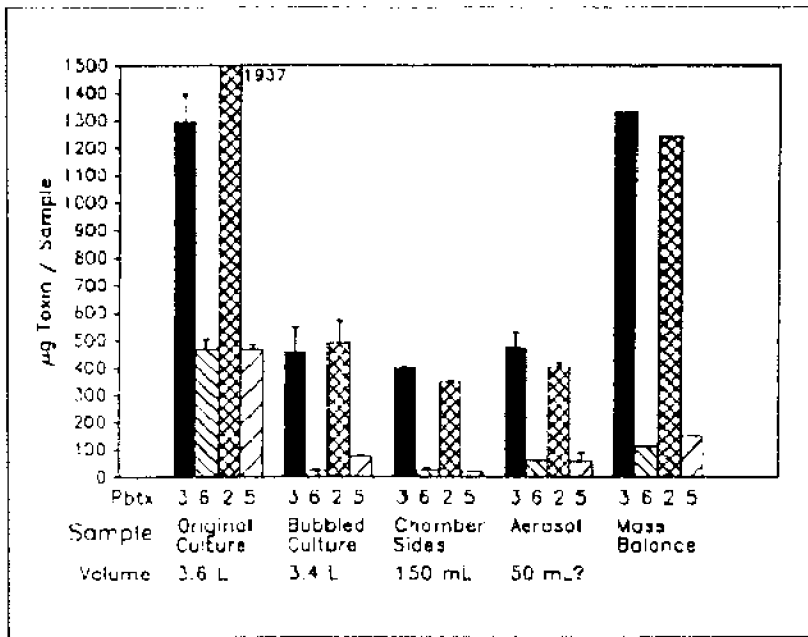


Figure 8. Toxin enrichment in bubble-produced aerosol (*P. brevis* culture, 40×10^8 cells/l) 4-hr sample in lab aerosol chamber with 10 kt air velocity, 24°C , 34% RH

2. Toxins were enriched in surface foam at the sea-air interface by bubble-mediated transport. For PbTx-2 and PbTx-3, foam enrichment factors ranged from 2.4 to 3.6 times the concentrations in the original sample.

3. Toxins were highly enriched in bubble-produced jet drops and aerosol. For PbTx-2 and PbTx-3, enrichment factors ranged from 35 to 45 for jet drops and from 20 to 50 for aerosol.

4. Selective enrichment of one toxin over another was not verified; however, the apparent enrichment of PbTx-3 over PbTx-2 was found to result from the conversion of PbTx-2 to PbTx-3 during the aerosolization process.

5. Larger quantities of red tide-containing seawater and/or lab cultures are needed to investigate bubble-mediated enrichment of other *P. brevis* toxins as well as bacteria and bacteria toxins associated with red tides.

Acknowledgments

This project was funded by the State of Florida, Department of Natural Resources, Florida Marine Research Institute. Additional support in the form of a feasibility grant was provided from the Marine Biomedical Center of the Duke University Marine Laboratory, and to Drs. Joseph and Celia Bonaventura, for investigations relative to the North Carolina red tide episode. A special thanks goes to Mr. Bud Hartman, MML Volunteer handyman for constructing the aerosol production-collection chamber.

References

- Baden, D.G. 1983: Marine food-borne dinoflagellate toxins. *Int. Rev. Cytol.* 82:99.
- Baden, D.G. and T.J. Mende. 1982: Toxicity of two toxins from the Florida red tide dinoflagellate (*Ptychodiscus brevis*). *Toxicon* 20:457.
- Baden, D.G., T.J. Mende, G. Bikhazi and I. Leuny. 1982: Bronchoconstriction caused by Florida red tide toxins. *Toxicon* 20:929.
- Blanchard, D.C. 1975: Bubble scavenging and the water-to-air transfer of organic material in the sea. In: R. Baier (ed.), *Applied Chemistry at Protein Interfaces. Adv. Chem. Ser.* 145:360.
- Blanchard, D.C. 1983: The production, distribution and bacterial enrichment of the sea-salt aerosol. In: P.S. Liss and W.G.N. Slinn (eds.), *Air-Sea Exchange of Gases and Particles*, Hingham: D. Reidel. p. 407.
- Blanchard, D.C. 1985: The oceanic production of atmospheric sea salt. *J. Geophys. Res.* 90:161-163.
- Blanchard, D.C. and L.D. Syzdek. 1988: Film drop as a function of bubble size. *J. Geophys. Res.* 93:3649-3654.
- Blanchard, D.C. and A.H. Woodcock. 1957: Bubble formation and modification in the sea and its meteorological significance. *Tellus* 9:145.
- Buck, J.O. and R. H. Pierce, 1989: Bacteriological aspects of the Florida red tide: A revisit and newer observations, *Est. Coast. and Shelf Sci.* (In press)
- Chou, N.-N, Y. Shimizu, G.D. van Duyn and J. Clardy. 1985: Two new polyether toxins of *Gymnodinium breve* (= *Ptychodiscus brevis*). In: D.M. Anderson, A.M. White and D.G. Baden (eds.), *Toxic Dinoflagellates*, New York, Elsevier, p. 305.
- Duce, R.A. 1983: Biogeochemical cycles and the air-sea exchange of aerosols. In: B. Bolin and R.B. Cook (eds.), *The Major Biogeochemical Cycles and Their Interactions* Wiley-Interscience, NY, p. 427.

- Gershey, R.M. 1983: Characterization of seawater organic matter carried by bubble-generated aerosols. *Limnol. Oceanogr.* 28:309.
- Hoffman, E.J. and R.A. Duce. 1974: The organic carbon content of marine aerosols collected in Bermuda. *J. Geophys. Res.* 79:4474.
- Kientzler, C.E., A. Arons, D.C. Blanchard and A.H. Woodcock. 1954: Photographic investigation of the projection of droplets by bubbles bursting at a water surface. *Tellus* 6:1.
- Lin, Y.Y., M. Risk, S.M. Ray, D. van Engen, J. Clardy, J. Golzk, J.L. James and K. Nakanishi. 1981: Brevetoxin B from the red tide dinoflagellate, *Ptychodiscus brevis* (*Gymnodinium breve*). *J. Am. Chem. Soc.* 103:6773.
- MacIntyre, F. 1974: The top millimeter of the ocean. *Sci. Am.* 230:62.
- Monahan, E.C. 1986: The ocean as a source for atmospheric particles. In: P. Buat-Menard (ed.), *The Role of Air-Sea Exchange in Geochemical Cycling*. D. Reidel, Hingham, MA, pp. 129-163.
- Nakanishi, K. 1985: The chemistry of brevetoxins: a review. In: S. Ellis (ed.) *Brevetoxins: Chemistry and Pharmacology of "Red Tide" Toxins from *Ptychodiscus brevis* (formerly *Gymnodinium breve*)*. *Toxicon* 23:473-479.
- Narita, H., S. Matsubara, N. Miwa, S. Akahane, M. Murakami, T. Goto, M. Nara, T. Noguchi, T. Saito, Y. Shida and K. Hashimoto. 1987: *Vibrio alginolyticus*, a TTX-producing bacterium isolated from the starfish *Astropecten polyacanthus*. *Nippon Suisan Gakkaishi*. 53(4):617-621.
- Padilla, G.M., Y.S. Kim and D.F. Martin. 1975: Separation and analysis of toxins isolated from a red tide sample of *Gymnodinium breve*. In: V.R. Lo Cicero (ed.), *Proceedings of the First International Conference of Toxic Dinoflagellate Blooms*, Wakefield, Massachusetts Science and Technology Foundation, p. 299.
- Pierce, R.H. 1986: Red tide (*Ptychodiscus brevis*) toxin aerosols: a review. *Toxicon* 24:955-965.
- Pierce, R.H. 1987: Cooperative scientific effort identifies red tide toxin. *Environ* X(4):7-12.
- Pierce, R.H., R.C. Brown and J.R. Kucklick. 1985: Analysis of *Ptychodiscus brevis* toxins by reverse phase HPLC. In: D.M. Anderson, A.W. White and D.G. Baden (eds.), *Toxic Dinoflagellates*, Elsevier, NY, p.309.
- Pierce, R.H., R.C. Brown and K.R. Hardman. 1987: *Mote Marine Laboratory Red Tide Program, 1986-1987*. Final Report to the FL Dept. of Natural Resources, Contract #C4149, September 11, 1987. 15 pp.
- Poli, M.A., T.J. Mende and D.G. Baden. 1986: Brevetoxins, unique activators of voltage-sensitive Na channels bind to specific sites in rat brain synaptosomes. *Molec. Pharmac.* 30:129-135.
- Shimizu, Y. 1978: Dinoflagellate toxins. In: J.P. Scheuer (ed.), *Marine Natural Products, Chemical and Biological Perspectives*, Academic Press, NY, p. 1.
- Shimizu, Y. 1982: Recent progress in Marine toxin research. *Pure Appl. Chem.* 54:1973-1980.

- Shimizu, Y., H.N. Chou, H. Banda, G. van Duyne and J.C. Clardy. 1986: Structure of Brevetoxin A (GB-1 Toxin), the most potent toxin in the Florida red tide organism *G. breve* (*Ptychodiscus brevis*). *J. Am. Chem. Soc.* 108:515-516.
- Simidu, U., T. Noguchi, D-F. Hwang, Y. Shida and K. Hashimoto. 1987: Marine bacteria which produce tetrodotoxin. *Appl. Environ. Micro.* 53(7):1714-1715.
- Steidinger, K.A. 1983: A re-evaluation of toxin dinoflagellate biology and ecology. *Prog. Phycol. Res.* 2:148.
- Steidinger, K.A. and E.A. Joyce. 1973: *Florida red tides*. Florida Department of Natural Resources Educational Series No. 17.
- Tester, P.P., P.K. Fowler and J.T. Turner. 1989: Gulfstream transport of the toxic red tide dinoflagellate, *Ptychodiscus brevis*, from Florida to North Carolina. In: E.M. Cooper, E.J. Carpenter and V.M. Bricelj (eds.), *Novel Phytoplankton Blooms: Causes and Impacts of Recurrent Brown Tides and Other Unusual Blooms*, Springer Verlag, Berlin (In press).
- Woodcock, A.H. 1948: Note concerning human respiratory irritation associated with high concentrations of plankton and mass mortality of marine organisms. *Sears Foundn. J. Mar. Res.* 56.
- Woodcock, A.H., C. Kientzler, A. Aronus and D. Blanchard. 1953: Giant condensation nuclei from bursting bubbles. *Nature* 172:1144.
- Wolf, D.K., P.A. Bowyer, and E.C. Monahan, 1987: Discriminating Between the Film Drops and Jet Drops Produced by a Simulated Whitecap, *J. Geophys. Res.*, 92, 5142-5150.

From the Laboratory Tank to the Global Ocean

Edward C. Monahan
Marine Sciences Institute
University of Connecticut
Avery Point, Groton, CT 06340

Abstract

A series of models have been developed to predict the aerosol flux up from the sea surface, the bubble flux up to the sea surface, and the rate of gas transfer through the sea surface. In each case, the process is described explicitly in terms of oceanic whitecap coverage. The laboratory measurements of the contribution of an individual whitecap are combined with assessments of global or regional oceanic whitecap coverage to make the desired estimates of the fluxes of droplets from, bubbles to, and gases through, the ocean surface. While the utility of these models has already been demonstrated, the value of these models, and of this modeling approach, will be enhanced if answers can be obtained for the 24 questions set out in the text.

1. Introduction

When we began our study of sea spray several decades ago, with an initial investigation of the role of spray droplets in the downward transport of forward momentum (Monahan, 1968), we quickly learned that, under the high wind conditions which were of the most geophysical interest, it was extremely difficult to measure the concentration of spray droplets in the lowest meter over the

tossing waves, and came to the conclusion that there was no feasible technique available that could be used to directly measure the downward, or upward, flux of droplets at the very surface of the sea. While in the intervening years, progress has been made in devising instruments for the measurement of the spray droplet population just above the wildly oscillating water surface (e.g., DeLeeuw, 1987), we still have no practical way to count and "clock" the spray particles just as they leave the air-sea interface without altering the natural environment, although recent developments in the application of radar doppler systems hold out some hope that we may soon attain the capability to remotely measure the sea surface droplet flux.

Recognizing that oceanic whitecapping must be closely related to the rate of droplet production at the sea surface, since the role of individual bursting bubbles in producing spray droplets had been graphically demonstrated by Kientzler *et al.*, (1954) and described in some detail by Blanchard (1963), we then set out to describe oceanic whitecap coverage in terms of the controlling meteorological and oceanographic parameters (Monahan, 1971). The ship-mounted photographic system adopted for this task (Monahan, 1969) was used successfully to record whitecaps at considerably higher wind speeds and sea states than those at which the spray camera raft employed in the earlier study could be used.

But in order to be able to estimate the actual rate of aerosol generation at the sea surface from such photographic measurements of oceanic whitecap coverage, we had first to arrive at a physical picture that illuminated the specific relationship between whitecap coverage and surface aerosol flux. Our initial model (Monahan, *et al.*, 1979; 1982) incorporated the idea that the rate of spray production was proportional to the area of the sea surface from which whitecaps disappeared per unit time, which in turn was simply proportional to the fraction of the sea surface instantaneously covered by whitecaps. To obtain a quantitative estimate of the rate of spray droplet generation associated with a given whitecap coverage from such a model, it was also necessary to determine how many spray droplets are produced during the decay of a unit area of surface whitecap, and since it is not feasible to

measure in the field the “crop” of spray droplets injected into the air as a consequence of the decay of a specific whitecap, we resorted to producing “captive” transient whitecaps in hooded whitecap simulation tanks and counting the aerosol particles that appeared in the air within the hoods as a result of the decay of individual whitecaps (Monahan, *et al.*, 1982; 1986). A further refinement involved the recasting of this spray generation model in terms of the rate of reduction of the volume of the aerated plume associated with each whitecap, which resulted in a conceptually more satisfying model than the one relating aerosol flux to the rate of decay of the surface area of a whitecap (Monahan, 1986; 1988).

It is insightful to review these models, and the models being formulated to define the influence of whitecaps on the rates of sea-air gas exchange (e.g., Monahan and Spillane, 1984), and to make explicit the assumptions incorporated in, or “hidden within,” the resulting mathematical expressions. In this fashion, we hope to make clear some of the critical questions still to be answered about these several air-sea exchange processes.

But before we begin our review of the models themselves, we need to consider what is meant by the term, “fraction of the sea surface covered by whitecaps,” and how this quantity may be related to increases in sea surface microwave emissivity, a property of the ocean that can be routinely, and remotely, monitored by existing and proposed satellite systems.

2. Measuring Oceanic Whitecap Coverage

By projecting oblique 35mm photographic images of the sea surface and analyzing them by the standard “manual” technique (Monahan, 1969), it has been possible to assess the fraction of the sea surface covered by mature whitecaps (Stage B of Figure 1), as well as by active whitecaps (Stage A) and aerated spilling waves. As a consequence of their greater horizontal extent, and relatively longer duration, the fraction of the sea surface that is at any instant covered by Stage B whitecaps far exceeds the fraction of the sea surface covered by the higher albedo Stage A whitecaps.

This is demonstrated by the curves plotted on Figure 2, where

HYPOTHETICAL EVOLUTION OF BUBBLE PLUME/CLOUD

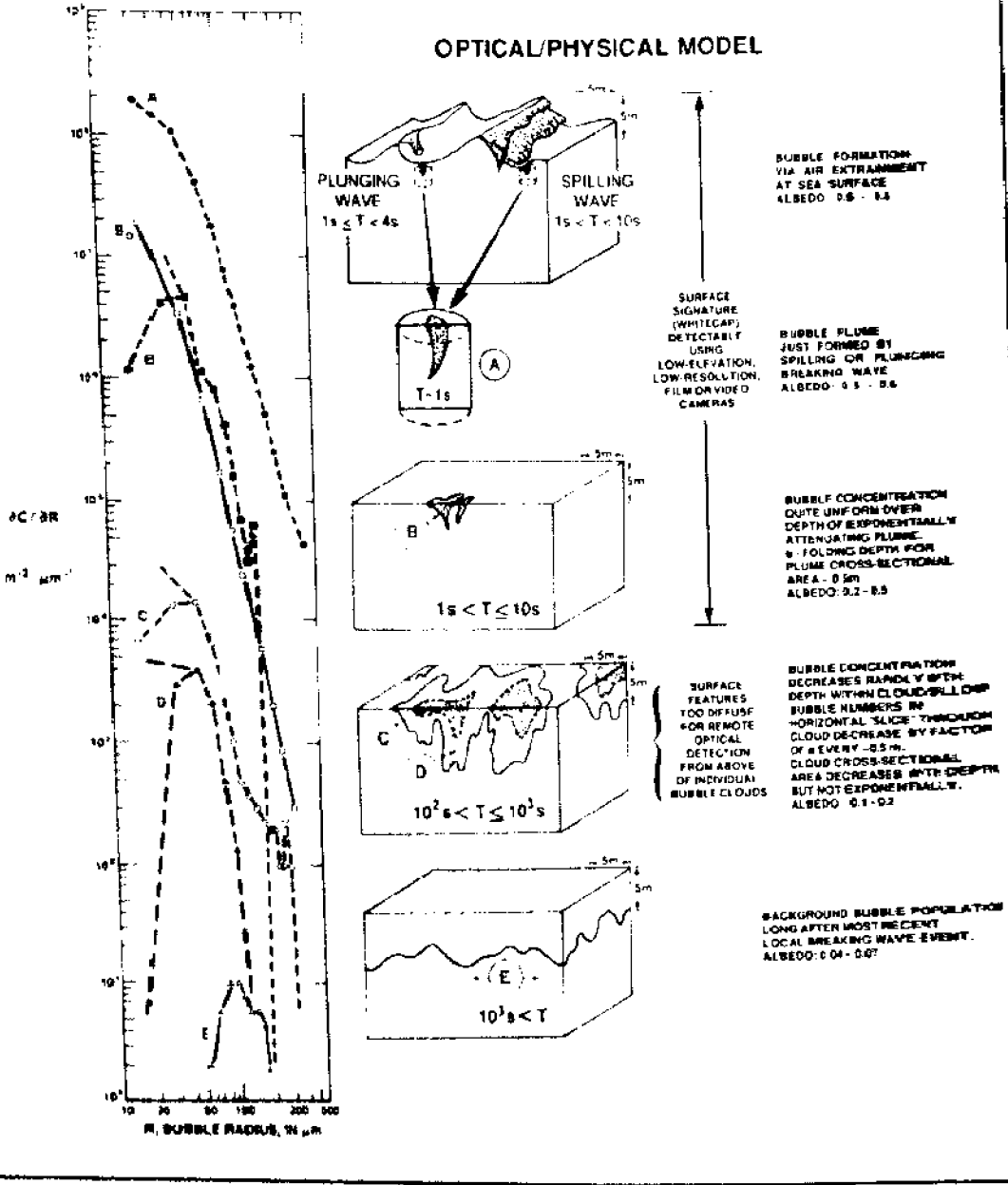


Figure 1. Model of whitecap decay and bubble cloud evolution. Candidate bubble spectra for each stage of bubble plume development shown on left side of panel. Spectrum BD reproduced from Figure 3.

Line B1 corresponds to the whitecap - 10 m elevation wind speed; i.e., $W_b(U)$, expression of Monahan and O'Muircheartaigh (1980), which they obtained by applying the technique of robust Bi-weight fitting to the photographic whitecap data sets found in Monahan (1971) and Toba and Chaen (1973), while Line A1 is a representation of the $W_A(U, \Delta T)$ expression that arose from the analysis, with a Hamamatsu Area Analyzer, of oblique U-matic video recordings of the sea surface taken during the MIZEX 1983 (Monahan, *et al.*, 1985), MIZEX 84 (Monahan and Woolf, 1986), HEXPILOT (Monahan, *et al.*, 1985), and HEXMAX (Monahan, *et al.*, 1988b) experiments. The video-based expression, given here for near neutral atmospheric stability, i.e., for ΔT equals zero, only takes into consideration the high albedo Stage A whitecaps and spilling breakers (Monahan, Wilson, and Woolf, in Monahan, *et al.*, 1988a), effectively excluding the relatively low albedo Stage B whitecaps which of necessity fall below the discrimination brightness level routinely adopted for use with the Hamamatsu Area Analyzer. Line B2, also included on Figure 2, is the $W_b(U, \Delta T)$ expression obtained by Monahan and O'Muircheartaigh (1986) from the analysis of the composite whitecap data base comprised of the photographic results from BOMEX plus other warm seas (Monahan, 1971), the East China Sea and adjacent waters (Toba and Chaen, 1973), JASIN (Monahan, *et al.*, 1981), STREX (Doyle, 1984), and MIZEX 83 (Monahan, *et al.*, 1984). In this instance, ΔT , the surface water temperature minus the deck height air temperature, has again been set equal to zero; i.e., Line B2 represents the $W_b(U)$ expression for near neutral stability.

Only in the Soviet literature can be found the results obtained from the analysis of specific sets of photographic images for both the areas of the sea surface associated with crests and active Stage A whitecaps, and for direct comparison the areas occupied on the same images by foam and passive Stage B whitecaps.

The fraction of the sea surface covered by breaking wave crests found by Bondur and Sharkov (1982) is illustrated by Curve A2, while the fraction of the sea surface they deduced from the same photographs to be covered by striplike foam is presented by curve B3. Bortkovskii's (1987) results for active whitecaps, based on

observations obtained when the sea surface temperature was between 3° and 15° C, are shown as curve A3, while his description of combined whitecap and foam cover for seas in this temperature range is illustrated by curve B4.

Each observer must be explicit as to the effective spatial and contrast resolution of his imaging system, so that a judgment can be made as to whether his results pertain only to Stage A, or to both Stage A and Stage B whitecaps.

The passive microwave radiometers mounted aboard satellites do not resolve individual whitecaps; rather, the elevated apparent brightness temperatures detected by these systems are a consequence of the integrated effect of all the foam batches in their "footprint" on the microwave emissivity of the sea surface.

Individual bubbles, and small bubble clusters, as well as Stage B and A whitecaps (and other features) all contribute to enhancing the emissivity of the ocean.

Q1 - Is the area of the sea surface covered at any instant by optically unresolvable foam patches in a fixed ratio to W_B , or W_A , or neither?

Q2 - Are the W_B/W_A ratios inferred from Figure 2 consistent with the model of the evolution of sub-surface bubble clouds, and of their concentration spectra, depicted in Figure 1?

Q3 - While the various curves illustrated in Figure 2 do appear to fall into two distinct clusters, is it in fact meaningful, or for that matter, possible, to truly distinguish between Stage A and Stage B whitecaps?

Q4 - While it is clear from the results presented by Bondur and Sharkov (1982), and by Monahan and Monahan (1986), that the size distribution of oceanic whitecaps varies with wind speed, with the median size increasing with a freshening of the wind, how does this increase in median whitecap size combine with the increase of whitecap numbers to yield the strong increase in fractional whitecap coverage that is observed to occur with a strengthening of the wind?

Q5 - Given that power-law descriptions of $W_B(U)$ and $W_A(U)$ clearly do not apply at wind speeds below the Beaufort velocity, i.e., at wind speeds lower than the threshold for whitecapping

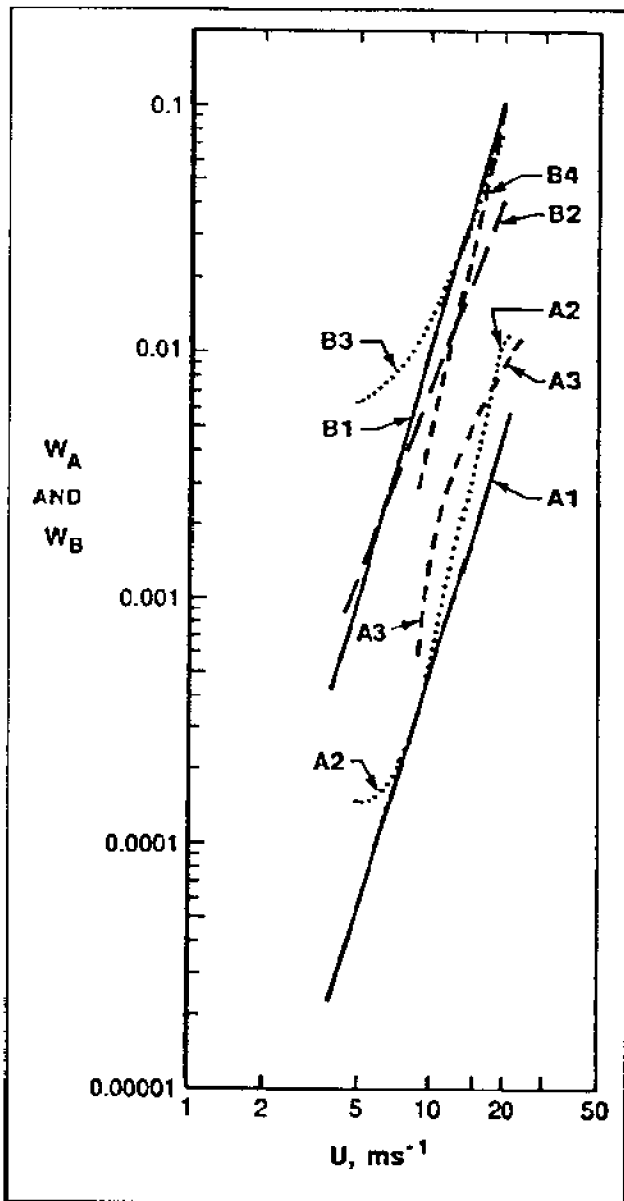


Fig. 2. Wind dependence of Stage A and Stage B whitecap coverage. See text for identity of each labeled curve. Note that both axes bear logarithmic scales.

(Monahan and O'Muircheartaigh, 1986), what is the wind speed above which these power-law expressions likewise do not apply?

Q6 - For a constant 10 m elevation wind speed and uniform atmospheric stability, what is the quantitative effect of changes in the kinematic viscosity, i.e., of changes in sea surface temperature, on whitecap coverage?

Q7 - Can we quantify, via water wave theory, the influence of finite fetch and limited wind duration on W_B and W_A ?

Q8 - While the two-dimensional surface divergence associated with the idealized, buoyant, whitecap bubble plume should mitigate the effect of any surface monolayers on the persistence of

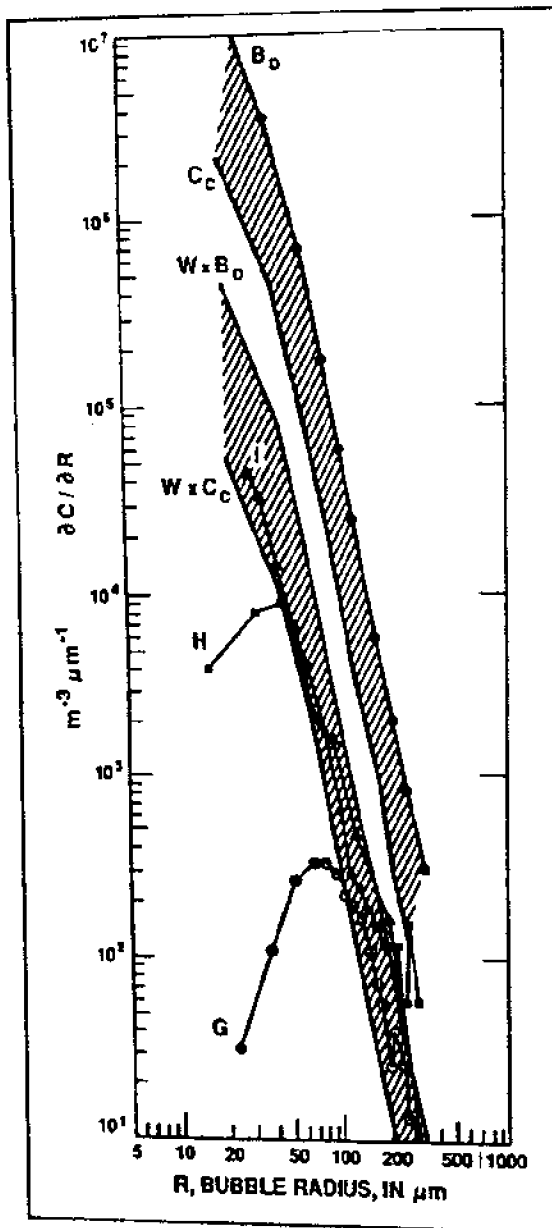


Figure 3. Near-surface resident bubble spectra for winds of $11-13 \text{ ms}^{-1}$. Region $W \times (B)$; range of spectra predicted by Equation 7 for U_{10} of 13 ms^{-1} , i.e., for W_b equal to 0.0241. Curve G, oceanic spectrum, 1.5 depth, $11-13 \text{ ms}^{-1}$ winds, Kolovayev (1976). Curve H, coastal spectrum, 0.7 m depth, $11-13 \text{ ms}^{-1}$ winds, Johnson and Cooke (1979). Curve I, fresh-water wind-wave flume spectrum, 0.05 m depth, 13 ms^{-1} winds, 26.2 m fetch, Baldy and Bourguel (1985). Region (B_D-C_C) at top corresponds to range of spectra model predicts for immediately beneath a whitecap, or for W_b equal to 1.00.

whitecaps, can the actual role of organic material in the oceanic mixed layer, and of surfactant films on the sea surface, in stabilizing whitecap bubbles, and hence in extending the lifetimes of individual whitecaps, be explicated?

3. Whitecap-Dependent Sea Surface Aerosol Generation Models

Our initial expression, incorporating quantities derived from the study of small whitecaps in laboratory tanks and quantities obtained from recording whitecaps at sea (Monahan, *et al.*, 1983; Monahan, 1986) is reproduced, with slight change in notation, as Equation 1.

$$\frac{\partial F_0}{\partial r} = W_B \tau^{-1} \frac{\partial E}{\partial r} \quad (1)$$

Here $\partial F/\partial r$ is the number of spray droplets produced per second, per square meter of sea surface, per micrometer increment in droplet radius, as a consequence of the bursting of whitecap bubbles. In this expression, as elsewhere in our treatment of marine aerosol droplets, all droplet descriptions are in terms of the radii the droplets would have attained if they had been allowed to adjust to their equilibrium size in air with a relative humidity of 80%. The last term on the right-hand side of Equation 1, $\partial E/\partial r$, is the laboratory-derived description of the number of aerosol particles, per micrometer increment in particle radius, introduced into the air within the hood of the tank, normalized by the initial area, A_0 , of the whitecap whose decay resulted in the generation of these particles. As before, W_B is the fraction of the sea surface, for a given set of meteorological and oceanographic conditions, covered by both Stage A and Stage B whitecaps. The remaining quantity, τ , represents the time constant describing the rate of exponential decay of individual whitecaps. While the initial value used for τ , 3.53s, came from the analysis of cine-film records of the decay of small laboratory whitecaps, Nolan (in Monahan, *et al.*, 1988a) has obtained a value of 4.27s for τ by analyzing, with the Hamamatsu Area Analyzer, the decay of a number of individual whitecaps whose lifetimes were documented on the HEXMAX whitecap video tapes. It should be noted that the quotient $W_B \tau^{-1}$ represents the fraction of the sea surface from which whitecaps disappear each second. If the older, laboratory, value for τ is used, then Equation 1 can be restated (Monahan, *et al.*, 1983; Monahan, 1986) as shown in Equation 2.

$$\frac{\partial F}{\partial r} = 3.57 \times 10^5 r^{-3} (1 + 0.057 r^{1.05}) \times 10^{1.19e^{-y^2}} \times W_B$$

$$y = (0.380 - \text{LOG } r)/0.650 \quad (2)$$

This model, which has been used with some success by Burk (1984) and Stramska (1987) as a sea surface source function in their modeling of the aerosol population of the marine atmospheric

boundary layer, has recently been restated, with a revised expression for $\partial E/\partial \tau$, by Woolf, *et al* (1988).

Q9 - Given that the spilling period for a typical whitecap, as recently documented by Nolan, is by no means insignificant when compared to τ , the exponential decay constant, is $W_B \tau^{-1}$ the best measure of the rate of disappearance of bubbles from the sea surface?

Q10 - Given the indications to the contrary recently documented by Woolf (1988), should $\partial E/\partial \tau$ still be taken to be independent of the initial size, A_o , of the source whitecap?

Q11 - Noting that the function $\partial E/\partial \tau$ has been shown to be dependent on sea water temperature, T_w , particularly in the portion of the droplet spectrum below 2 micrometers (Bowyer, 1986 ; Woolf, *et al.*, 1987), should not an explicitly T_w -dependent expression be introduced into future statements of $\partial F/\partial \tau$?

Q12 - Does the absence of a wind in the whitecap simulation tanks influence in any way the number or size of the droplets produced by an individual bursting bubble?

A physically more appealing expression for $\partial F/\partial \tau$, which relates the rate of generation of aerosol particles at the sea surface to the rate at which aerated plume volume is disappearing from, and in a dynamic equilibrium, is being formed in, the oceanic mixed layer, is reproduced in Equation 3.

$$\frac{\partial F_o}{\partial \tau} = W_B v_m \frac{\partial G}{\partial r} \quad (3)$$

Here v_m is the terminal rise velocity of bubbles of radius R_m , the smallest bubbles contributing to the optically resolvable mature whitecap. The product $W_B v_m$ is then the number of cubic meters of aerated plume disappearing per second per square meter of the ocean surface. The term $\partial G/\partial r$ in Equation 3 represents the number of aerosol particles, per micrometer radius increment, injected into the hood of the whitecap simulation tank during the decay of a laboratory whitecap, normalized by the initial volume of the aerated plume associated with this whitecap. This initial volume is simply DA_o , where D is the scale depth, or e-folding depth, of the aerated plume. Note that it is assumed that the cross-

sectional area of such plumes, or whitecap bubble clouds, attenuates exponentially with depth (Monahan, 1986).

Q13 - Does the effective cross-sectional area of the aerated plume beneath a whitecap die off exponentially with depth, given that Thorpe (1982) found that bubble clouds ranged from billowy to columnar in shape?

Q14 - Noting that D is equal to the product $v_m \tau$, is it reasonable to assume that the e-folding depth of oceanic bubble clouds is the same as the scale depth associated with the aerated plume generated in the laboratory tank by a breaking wave event?

Q15 - How sensitive is $\partial E/\partial r$, or $\partial G/\partial r$, to the specific mechanism, and energetics, of air entrainment?

4. Model for Estimating Sea Surface Bubble Flux

As a consequence of the degree of success attained with the sea surface aerosol generation models in predicting the spectral shape and concentration of the marine aerosol populations for various wind conditions (e.g., Monahan, 1986), we felt warranted in attempting to "work backward" from our basic aerosol flux model to attain a bubble flux model, and indeed, an estimate likewise, in terms of W_b , of the near surface bubble population.

This treatment, which can be found in full in Monahan (1988), leads to Equation 4, where $\partial K/\partial R$ represents the number of bubbles arriving and bursting per second, per square meter of sea surface, per micrometer increment in bubble radius.

$$\frac{\partial K}{\partial R} = \frac{\partial F_0}{\partial r} \cdot \frac{\partial r}{\partial R} \cdot P(r) \cdot J^{-1} \quad (4)$$

Here $\partial F/\partial r$ is as defined before, and $\partial r/\partial R$ is simply the rate of increase of droplet radius, r , per unit increment of bubble radius, R . Equation 5, which describes the relationship between the size of the daughter jet drops and the size of the parent bubble, was evaluated using the information obtained by Blanchard (1963) from his study of the bursting of isolated bubbles.

$$r = aR + b = 8.77 \times 10^{-2}R + 0.98 \quad (5)$$

The term $P(r)$ in Equation 4 is the fraction of the bubble generated droplets that is comprised of jet droplets, as opposed to film droplets. Equation 6 is an expression for the jet droplet/film droplet partition function based on the findings presented in Woolf, *et al.*, (1987).

$$P = 1 - e^{-0.343r} = 1 - 0.715e^{-0.030R} \quad (6)$$

The quantity J , which appears in the denominator of Equation 4, is simply a measure of the number of jet droplets produced as a result of the bursting of a single whitecap bubble. Cipriano and Blanchard (1981) assumed in one instance that each bubble produces five jet droplets.

Since available observations are of near-surface bubble populations, $\partial C/\partial R$, we must, if we are to compare our model with such results, deduce the bubble population that would give rise to a specific bubble flux. This can be done by simply dividing the bubble flux expression of Equation 4, $\partial K/\partial R$, by $v_m(R)$, the radius-dependent terminal rise velocities for air bubbles in sea water, as shown in Equation 7.

$$\frac{\partial C}{\partial R} = \frac{\partial F_v}{\partial r} \cdot \frac{\partial r}{\partial R} \cdot P(r) \cdot J^{-1} \cdot v_m^{-1}(R) \quad (7)$$

Here $\partial C/\partial R$ is a measure of the number of bubbles per cubic meter of sea water per micrometer radius increment, and $v_m(R)$, expressed in meters per second is the appropriate terminal rise velocity, i.e., the terminal rise velocity for hydrodynamically "clean" or "dirty" bubbles (Thorpe, 1982).

Noting that there are several published observations of the near-surface bubble population associated with wind speeds of about 13 meters per second, we have evaluated $\partial C/\partial R$, or more specifically, $\partial F_v/\partial r$ (Equation 2), using the W_B value appropriate for this wind speed as determined from Equation 8 (Monahan and O'Muircheartaigh, 1980), where U is the 10 meter elevation wind speed expressed in meters per second.

$$W_B = 3.86 \times 10^{-6} U^{3.41} \quad (8)$$

The near surface bubble population spectra predicted by Equation 7 to be associated with winds of 13 ms^{-1} is represented by the lower hatched band depicted on Figure 3. The upper bound of this range of bubble populations, given by the curve $W \times B_p$, was determined assuming that each bubble produces only one jet droplet; i.e., that J equals one, and that the bubbles are hydrodynamically dirty, and thus rise with the terminal velocity appropriate for a sphere with no tangential relative flow at its immediate surface. Conversely, the lower bound of this range, illustrated by curve $W \times C_c$, was calculated assuming that each bubble gives rise to five jet droplets and that the bubbles are hydrodynamically clean. By way of reference, the band of bubble population spectra predicted by our model for 100% whitecap coverage is also included (Region B_p - C_c) on Figure 3.

Near-surface oceanic bubble spectra have been obtained by Kolovayev (1976), and by Johnson and Cooke (1979), when the wind was blowing 11 - 13 ms^{-1} . It is apparent from Figure 3 that for all bubble radii, R , greater than $120 \mu\text{m}$ Kolovayev's spectrum (curve G) falls essentially within the band of spectra predicted by Equation 7 when the $\partial F / \partial r$ term was evaluated for winds of 13 ms^{-1} . Johnson and Cooke's spectrum (Curve H), on the other hand, is consistent with the model predictions for all R larger than $50 \mu\text{m}$. The discrepancy in the 50 to $120 \mu\text{m}$ radius interval between Kolovayev's results for 1.5 m depth, obtained using Neuimin's semi-automatic cylindrical bubble trap (Glotov, *et al.*, 1961), equipped with a camera and three lamps to illuminate the bubbles, and the results obtained by Johnson and Cooke using at a depth of 0.7 m a camera in a waterproof housing accompanied by three external strobe lamps, may, as was suggested by Johnson and Cooke (1979) be due to some dissolution, and perhaps also some coalescence, of bubbles in this size range during their residence within the Neuimin bubble trap. (It may be assumed that Glotov, *et al.*, would not agree with this interpretation, as they state in their 1962 paper that the bubbles rested against the underside of the

upper lid of their trap "for a sufficiently long time without merging and without altering their sizes.")

Baldy and Bourguel (1985) obtained a further near-surface resident bubble spectrum associated with a wind speed of 13 ms^{-1} , which is reproduced as Curve I on Figure 3. These measurements were made at a depth of 0.05 m and a fetch of 26.2 m in the large wind-wave flume (La Grand Soufflerie) at the Institute de Mecanique Statistique de la Turbulence in Luminy, France, using a sophisticated optical bubble probe (Avellan and Resch, 1983; Resch, 1986) which detects laser light scattered by individual bubbles. With the exception of one point, Baldy and Bourguel's entire spectrum, even at the small radius ($32 \mu\text{m}$) end, falls within the spectral band generated using Equation 7.

In considering the similarity between the band of spectra predicted by Equation 7 and the Baldy and Bourguel spectrum represented by Curve I, and the contrast, particularly apparent for the smaller radii, between Curve I and the other measured bubble spectra, it is tempting to note that the marine aerosol spectrum that was the starting point in the development of the bubble spectrum model represented by Equation 7, was, like the Baldy and Bourguel bubble spectrum, measured with a sensitive laser-based probe that detected the light from individual scatterers, while the spectra of Kolovayev, and of Johnson and Cooke, were determined from the analysis of photographs of highlighted bubbles.

The observation that the Baldy and Bourguel spectrum reflects a much higher concentration of the small bubbles than do the two other spectra measured for the equivalent wind speed is particularly striking when it is noted that the I.M.S.T. wind-wave flume contained fresh water, and, as has been shown in pouring experiments (Monahan and Zietlow, 1969; Scott, 1975a), fresh-water aerated plumes contain fewer small bubbles than do aerated plumes produced by the same mechanical action in salt water. This marked difference between fresh water and saltwater bubble spectra is presumably a consequence of the retardation of bubble coalescence in sea water (Scott, 1975a; 1975b), a conclusion confirmed by Pounder (1986).

The demonstrated ability of the model summarized in Equation

7 to predict the approximate shape and amplitude of the large radius portion of the near-surface, in-situ, bubble spectrum, gives support to our contention that the bubble flux modeling approach set forth in this section, and the aerosol flux modeling scheme described in Section 3, are fundamentally valid, and thus merit further development.

Q16 - Is the relationship found by Blanchard (1963) to pertain between the radius, R , of an isolated bubble breaking at a quiet water surface, and the radius, r , of the daughter jet droplets, still fully valid in the case of whitecap bubbles, which are not isolated and often burst at an agitated sea-air interface?

Q17 - Is the transition between the jet droplet dominated portion of the aerosol spectrum and the film droplet dominated portion adequately described by the laboratory findings of Woolf, *et al* (1987)?

Q18 - Will the function, J , representing the number of jet droplets produced per bursting bubble, upon further laboratory studies prove to be dependent upon R ; i.e., should we expect ultimately to substitute a $J(R)$ term in Equation 7?

Q19 - Is it reasonable to expect that the J , or $J(R)$, expression determined from laboratory studies of the bursting of individual bubbles, be appropriate for use in modelling the relationship between the sea surface aerosol flux and the whitecap bubble flux, given that many whitecap bubbles do not burst in isolation nor on a relatively calm sea surface?

Q20 - Need we consider the possible influence of protracted bubble-surface-lifetime on $\partial F / \partial r$, $\partial r / \partial R$, and $J(R)$, in perfecting our model?

Q21 - Can we, with any confidence, predict when bubbles, of Radius R , in a specified part of the world ocean, will typically prove to be hydrodynamically dirty, and thus behave accordingly?

Q22 - Given the variety of fates that Thorpe (1982) has documented await small bubbles in the open ocean, is there any reason to hope that a model such as the one described above can ever be used to predict the resident population of these smaller bubbles?

Q23 - Can the agreement between the wind dependence found by Farmer and Lemon (1984) for the population of bubbles in

coastal waters, and the wind dependence implicit in Equation 7 (and explicit in Equation 8), be taken as general confirmation of the present modelling approach?

5. The Influence of Whitecaps on Sea-Air Gas Exchange Rates

The thought that the piston velocity, or sea-air transfer rate, for gases such as Rn and CO₂ might be directly dependent upon the average local whitecap coverage came to us as we viewed a poster paper prepared in 1982 by W. M. Smethie of the Lamont Doherty Geological Observatory which included a chart of North Atlantic piston velocities that was strikingly similar in appearance to the charts of North Atlantic monthly average whitecap coverage prepared by M.C. Spillane of University College, Galway (see Spillane, *et al.*, 1986). A subsequent detailed comparison (Monahan and Spillane, 1984) confirmed our original impression. An explicit physical model was set out in which each whitecap was considered to be a low impedance vent that facilitated sea-air gas exchange. The high levels of small-scale turbulence present in a whitecap are perceived to be sufficient to destroy any near-laminar surface layer (Kanwisher, 1963), or "stagnant layer," which would otherwise represent a high impedance layer through which gas could only be transferred by the relatively ineffective process of molecular diffusion. Complementing the effect of the whitecap's buoyant plume in destroying any viscous, laminar, surface sub-layer in the liquid medium, the bubble, and bubble-cusp, roughened sea surface in the interior of a whitecap will instigate boundary-layer separation in the overlying airflow and thus assure the absence of any laminar surface layer in the gaseous medium. The potential energy of the whitecap's buoyant bubble plume is sufficient to continually destroy for a period of many seconds any stagnant layer as it attempts to re-establish itself in the immediate region of the whitecap.

The mathematical expression of this model is found in Equation 9 (Monahan and Spillane, 1984), where k_E is the effective piston velocity through the sea surface, in ms^{-1} , k_M is the piston velocity associated with gas transfer via molecular diffusion

through the viscous surface layer assumed to exist everywhere but in the interior of whitecaps, and k_T is the much higher piston velocity identified with the turbulent transfer of gases through a whitecap vent.

$$k_E = k_M(1 - W_B) + k_T W_B \quad (9)$$

In light of the detailed discussions of gas transfer through smooth and roughened, but not whitecap covered, sea surfaces available in the recent literature (Liss and Merlivat, 1986; Coantic, 1986), it may be more appropriate to rewrite Equation 9, as has been done in Equation 10, to make explicit the wind-dependent nature of k_M .

$$k_E = (k_{M_1} U + k_{M_2} U^2)(1 - W_B) + k_T W_B \quad (10)$$

It should be noted that the last term, $k_T W_B$, is still by far the most strongly wind-dependent term in this expression.

Recent, preliminary, gas exchange experiments carried out in Whitecap Simulation Tank III in the Marine Sciences Institute at the University of Connecticut have shown that the generation of a small whitecap once every 210 seconds, in an instance where the water in the tank is already being continuously stirred, is enough to more than triple the evasion velocity of radon gas when compared to its evasion velocity when the tank is simply being continuously stirred. The effectiveness of whitecaps in stimulating gas exchange can be appreciated when it is noted that the average fraction of the sea water surface in the tank covered by whitecaps during each 210-second cycle of this experiment was 0.1%; i.e., W was just 0.001. Further measurements of this sort will make it possible for us to evaluate k_T , the piston velocity associated with the turbulent transfer of gases via a whitecap vent.

Q24 - Is it reasonable to assume that k_T will be independent of the area of the individual whitecap, or is it more probable that k_T will increase with increasing whitecap size?

6. Conclusions

While the aerosol flux, bubble flux, and gas transfer models described in the previous sections are at markedly different stages of refinement, all show clear promise, and support the contention that a modeling approach in which the individual whitecap, or bubble plume, is taken as the key element enabling us to extrapolate the laboratory tank results to global ocean is a fundamentally valid one.

It is obvious that even the most detailed of our models stands in need of refinement and revision, and it is to be hoped that the answers to the two dozen questions interspersed in the foregoing text will be of particular utility in the further development of these several models.

Acknowledgments

Our investigation of whitecaps in the laboratory and in the field has been supported throughout by the Office of Naval Research. Currently our research on whitecaps, marine aerosol particles, bubbles, bubble plumes, and gas exchange is supported by ONR Contract N00014-87-K-0185 and by ONR Contract N00014-87-K-0069. This paper is Contribution No. 206 from the Marine Sciences Institute of the University of Connecticut.

References

- Avellan, F., and F. Resch, 1983: A Scattering Light Probe for the Measurement of Oceanic Air Bubble Sizes. *Int. Journal of Multiphase Flow*, 9, 649-663.
- Baldy, S., and M. Bourguel, 1985: Measurements of Bubbles in a Stationary Field of Breaking Waves by a Laser-Based Single-Particle Scattering Technique. *J. Geophys. Res.*, 90, 1037-1047.
- Blanchard, D.C., 1963: The electrification of the atmosphere by particles from bubbles in the sea. *Prog. Oceanog.*, 1, 71-202.
- Bondur, V.G., and E.A. Sharkov, 1982: Statistical Properties of Whitecaps on a Rough Sea. *Oceanology*, 1, 274-279.
- Borkovskii, R.S., 1987: *Air-Sea Exchange of Heat and Moisture During Storms*, D. Reidel Pub. Co., Dordrecht, The Netherlands, 194 pp. (revised English edition)

- Bowyer, P.A., 1986: Electrostatic Phenomena Associated With the Marine Aerosol Arising from the Bursting of Whitecap Bubbles, Ph.D. Thesis, National University of Ireland, 155 pp.
- Burk, S.D., 1984: The Generation, Turbulent Transfer, and Deposition of the Sea-Salt Aerosol, *J. Atmos. Sci.* **41**, 3041-3051.
- Cipriano, R.J., and D.C. Blanchard, 1981: Bubble and Aerosol Spectra Produced by a Laboratory 'Breaking Wave.' *J. Geophys. Res.*, **86**, 8085-8092.
- Coantic, M., 1986: A Model of Gas Transfer Across Air-Water Interfaces with Capillary Waves, *J. Geophys. Res.* **91**, 3925-3943.
- deLeeuw, G., 1987: Near-Surface Particle Size Distribution Profiles Over the North Sea. *J. Geophys. Res.* **92**, 14631-14635.
- Doyle, D.M., 1984: Marine Aerosol Research in the Gulf of Alaska and on the Irish West Coast (Inishmore), M.Sc. Thesis, National University of Ireland, 140 pp. (also University College Galway Report No. 6 to the Office of Naval Research).
- Farmer, D.M., and D. D. Lemon, 1984: The Influence of Bubbles on Ambient Noise in the Ocean at High Wind Speeds. *J. Phys. Oceanogr.*, **14**, 1762-78.
- Glotov, V.P., P.A. Kolovayev, and G.G. Neumin, 1962: Investigation of the Scattering of Sound by Bubbles Generated by an Artificial Wind in Sea Water and the Statistical Distribution of Bubble Sizes. *Sov. Phys., Acoustics*, **7**, 341-345.
- Johnson, B., and R.C. Cooke, 1979: Bubble Populations and Spectra in Coastal Waters: A Photographic Approach. *J. Geophys. Res.*, **84**, 3761-3766.
- Kanwisher, J., 1963: On the Exchange of Gases Between the Atmosphere and the Sea. *Deep Sea Res.*, **10**, 195-207.
- Kientzler, C.F., A.B. Arons, D.C. Blanchard, and A.H. Woodcock, 1954: Photographic Investigation of the Projection of Droplets by Bubbles Bursting at the Water Surface, *Tellus*, **6**, 1-7.
- Kolovayev, P.A., 1976: Investigation of the Concentration and Statistical Size Distribution of Wind-Produced Bubbles in the Near-Surface Ocean Layer. *Oceanology*, **15**, 659-661.
- Liss, P.S., and L. Merlivat, 1986: Air-Sea Gas Exchange Rates: Introduction and Synthesis, in *The Role of Air-Sea Exchange in Geochemical Cycling*, P. Buat-Menard, Ed., D. Reidel Publishing Co., Dordrecht, 113-127.
- Monahan, E.C., 1968: Sea Spray as a Function of Low Elevation Wind Speed. *J. Geophys. Res.* **73**, 1127-1137.
- Monahan, E.C., 1969: Fresh Water Whitecaps, *Journal of the Atmospheric Sciences*, **26**, 1026-1029.
- Monahan, E.C., 1971: Oceanic Whitecaps, *J. Phys. Oceanogr.* **1**, 139-144.
- Monahan, E.C., 1986: The Ocean as a Source for Atmospheric Particles, in *The Role of Air-Sea Exchange in Geochemical Cycling*, P. Buat-Menard, Ed., D. Reidel Publishing Co., Dordrecht, 129-163.
- Monahan, E.C., 1988: Whitecap Coverage as a Remotely Monitorable Indication of the Rate of Bubble Injection into the Oceanic Mixed Layer, in *Sea Surface Sound*, B.R. Kerman, Ed., Kluwer Academic Publishers, Dordrecht,

- Monahan, E.C., P.A. Bowyer, D.M. Doyle, M.R. Higgins, and D.K. Woolf, 1985: *Whitecaps and the Marine Atmosphere*, Report No. 8, to Office of Naval Research from University College, Galway, 124 pp.
- Monahan, E.C., R.J. Cipriano, W.F. Fitzgerald, R. Marks, R. Mason, P.F. Nolan, T. Torgersen, M.B. Wilson, and D.K. Woolf, 1988a: *Oceanic Whitecaps and the Fluxes of Droplets from, Bubbles to, and Gases Through, the Sea Surface*, Whitecap Report No. 4, to ONR from MSI, UConn (in press).
- Monahan, E.C., K.L. Davidson, and D.E. Spiel, 1982: *Whitecap Aerosol Productivity Deduced from Simulation Tank Measurements*. *J. Geophys. Res.*, **87**, 8898-8904.
- Monahan, E.C., and C.F. Monahan, 1986: *The Influence of Fetch on Whitecap Coverage as Deduced from the Alte Weser Light-Station Observer's Log*, in *Oceanic Whitecaps and Their Role in Air-Sea Exchange Processes*, E.C. Monahan and G. MacNiocaill, Eds., D. Reidel Pub. and Galway U. Press, 275-277.
- Monahan, E.C., and I.G. O'Muircheartaigh, 1980: *Optimal Power-law Description of Oceanic Whitecap Coverage Dependence on Wind Speed*. *J. Phys. Oceanogr.*, **10**, 2094-2099.
- Monahan, E.C., and I.G. O'Muircheartaigh, 1986: *Whitecaps and the Passive Remote Sensing of the Ocean Surface*. *Int. J. Remote Sensing*, **7**, 627-642.
- Monahan, E.C., I.G. O'Muircheartaigh, and M.P. FitzGerald, 1981: *Determination of Surface Wind Speed from Remotely Measured Whitecap Coverage, a Feasibility Assessment*. *Proceedings of an EARSeL-ESA Symposium, Application of Remote Sensing Data on the Continental Shelf*, Voss, Norway, 19-20 May 1981, European Space Agency, SP-167, 103-109.
- Monahan, E.C., B.D. O'Regan, and K.L. Davidson, 1979: *Marine Aerosol Production from Whitecaps*, Interdisciplinary Symposia, Abstracts and Time-table, International Union of Geodesy and Geophysics, XVII General Assembly, Canberra, Australia, 3-15 December 1979, 423.
- Monahan, E.C., D.E. Spiel, and K.L. Davidson, 1983: *Model of Marine Aerosol Generation via Whitecaps and Wave Disruption*. *Ninth Conference on Aerospace and Aeronautical Meteorology*, 6-9 June, 1983, Omaha, Nebraska, American Meteorological Society, Preprint Volume, 147-158.
- Monahan, E.C., D.E. Spiel, and K.L. Davidson, 1986: *A Model of Marine Aerosol Generation via Whitecaps and Wave Disruption*, in *Oceanic Whitecaps and Their Role in Air-Sea Exchange Processes*, E.C. Monahan and G. MacNiocaill, Eds., D. Reidel Pub. and Galway U. Press, 167-174.
- Monahan, E.C., and M.C. Spillane, 1984: *The Role of Oceanic Whitecaps in Air-Sea Gas Exchange*, in *Gas Transfer at Water Surfaces*, W. Brutsaert and G.J. Jirka, Eds., Water Science and Technology Library, D. Reidel Pub. Co., Dordrecht, 495-503.
- Monahan, E.C., M.C. Spillane, P.A. Bowyer, M.R. Higgins, and P.J. Stabeno, 1984: *Whitecaps and the Marine Atmosphere*, Report No. 7, to the Office of Naval Research from University College, Galway, 103 pp.

- Monahan, E.C., M.B. Wilson, and D.K. Woolf, 1988b: HEXMAX Whitecap Climatology: Foam Crest Coverage in the North Sea, 16 October - 23 November 1986, Proceedings, HEXMAX Workshop, Univ. of Washington Tech. Report (in press).
- Monahan, E.C., and D.K. Woolf, 1986: Oceanic Whitecaps, Their Contribution to Air-Sea Exchange, and Their Influence on the MABL, Whitecap Report No. 1, to ONR from MSI, UConn, 135 pp.
- Monahan, E.C., and C.R. Zietlow, 1969: Laboratory Comparisons of Fresh-Water and Salt-Water Whitecaps, *J. Geophys. Res.* **74**, 6961-6966.
- Younders, C., 1986: Sodium Chloride and Temperature Effects on Bubbles, in *Oceanic Whitecaps and Their Role in Air-Sea Exchange Processes*, E.C. Monahan and G. MacNiocaill, Eds., D. Reidel Pub. and Galway U. Press, 278.
- Zesch, F., 1986: Oceanic Air Bubbles as Generators of Marine Aerosols, in *Oceanic Whitecaps and Their Role in Air-Sea Exchange Processes*, E.C. Monahan and G. MacNiocaill, Eds., D. Reidel Pub. Co. and Galway U. Press, 101-112.
- Scott, J.C., 1975a: The Role of Salt in Whitecap Persistence. *Deep Sea Res.*, **22**, 653-657.
- Scott, J.C., 1975b: The Preparation of Water for Surface-Clean Fluid Mechanics. *J. Fluid Mech.*, **69**, 339-351.
- Spillane, M.C., E.C. Monahan, P.A. Bowyer, D.M. Doyle, and P.J. Stabeno, 1986: Whitecaps and Global Fluxes, in *Oceanic Whitecaps and Their Role in Air-Sea Exchange Processes*, E.C. Monahan and G. MacNiocaill, Eds., D. Reidel Pub. and Galway U. Press, 209-218.
- Stramska, M., 1987: Vertical Profiles of Sea Salt Aerosol in the Atmospheric Surface Layer: A Numerical Model. *Acta Geophysica Polonica*, **35**, 87-100.
- Thorpe, S.A., 1982: On the Clouds of Bubbles Formed by Breaking Wind-Waves in Deep Water, and Their Role in Air-Sea Gas Transfer. *Phil. Trans. R. Soc. London*, **A304**, 155-210.
- Toba, Y., and M. Chaen, 1973: Quantitative Expression of the Breaking of Wind Waves on the Sea Surface. *Records, Oceanogr. Works Japan*, **12**, 1-11.
- Woolf, D.K., 1988: The Role of Oceanic Whitecaps in Geochemical Transport in the Upper Ocean and the Marine Environment, Ph.D. Thesis, National University of Ireland, 330 pp.
- Woolf, D.K., P.A. Bowyer, and E.C. Monahan, 1987: Discriminating Between the Film-Drops and Jet-Drops Produced by a Simulated Whitecap, *J. Geophys. Res.* **92**, 5142-5150.
- Woolf, D.K., E.C. Monahan, and D.E. Spiel, 1988: Quantification of the Marine Aerosol Produced by Whitecaps, Preprint Volume: Seventh Conference on Ocean-Atmosphere Interaction, 31 January - 5 February 1988, Anaheim, California, American Meteorological Society, 182-185.

The Occurrence of Large Salt Water Droplets at Low Elevations Over the Open Ocean

Gerrit de Leeuw,*

Naval Postgraduate School, Dept. of Meteorology, Code 63D1
Monterey, CA 93943, U.S.A.

*Permanent address: TNO Physics and Electronics Laboratory,
P.O. Box 96864, 2509 JG The Hague, The Netherlands.

Abstract

An overview of the occurrence of sea-spray droplets and their concentrations at low elevations over the ocean is presented. The survey is focused on field data obtained in the lower 10 meters above the air-sea interface. Size distributions and profiles are discussed in relation to the production of droplets at the sea-surface and their subsequent dispersal in the surface layer.

1. Introduction

The ocean acts as both a source and a sink for atmospheric aerosols. In turn, the aerosol droplets may transfer water vapor, heat, pollutants and bacteria through the air-sea interface. The airborne droplets are important since they limit the transmission of electromagnetic radiation by scattering and absorption. Hence they affect the performance of electro-optic equipment, and the earth's radiation budget, as well as visibility. Small droplets may act as condensation nuclei and are therefore important in the formation of fog and clouds.

* HEXOS Contribution No. 20

In spite of their meteorological, optical and environmental significance, little is known about the occurrence of aerosols near the air-sea interface. This survey addresses near-surface particle concentrations and profiles of droplet concentrations over the open ocean, and droplet production, dispersion and transport.

2. Particle concentrations near the air-sea interface.

Field data on the concentrations of aerosols near the air-sea interface are sparse. Six individual data sets were published thus far in the open literature (see Table 1). A survey of the size distributions is presented in Figure 1. As yet unpublished results from the HEXMAX experiment in 1986 are presented as well. More common data above 10 m ASL (above sea level) from ship-deck experiments and from coastal experiments are not included. The data were obtained by various methods and under different conditions. They are briefly discussed in the following paragraphs.

Monahan (1968) was the first who measured particle size distributions below the more conventional ship deck level. Using a raft he collected data at a single height of only 0.13 m, i.e. in the ejection zone (cf. section 4). Monahan used a photographic technique to measure particles larger than $90\ \mu\text{m}$ in diameter. Two size distributions were published by Monahan. One is the average of particle size distributions measured near Aruba Island (Netherlands Antilles) in wind force 5-6. The other one was measured in Buzzards Bay (Massachusetts) in wind force 7.

Chaen (1973) collected data from ships in the Indian Ocean and in the Pacific. Aerosols were sampled by two impaction methods. MgO-coated glass slides were exposed at some distance from the ship at 6 m ASL by extending a rod from the bow of the ship. The droplet sizes were determined from the impacts in the MgO coating. Samples at other heights were obtained with impactors placed on the various decks that were accessible. The aerosols were collected on chlorine-sensitive gelatine film. The size of the spot left after developing the film is a measure of the droplet size. The data presented in Figure 1 are from run 10 (2.5 m) and run 10' (0.3 m), both in $6.1\text{-}6.5\ \text{ms}^{-1}$ wind speeds. It is not clear how the

data at 0.3 m were sampled. The data at 2.5 m are typical for those obtained with the impactor.

Preobrazhenskii (1973) measured particle size distributions from a ship at 3 heights: 1.5-2 m, 4 m, and 7 m. Samples were collected on oil-coated glass plates. The data were presented for two ranges of wind speeds: 7-12ms⁻¹ and 15-25 ms⁻¹. Those collected at 1.5-2 m ASL, converted to number concentrations per diameter interval, are presented in Figure 1. At higher elevations the concentrations are lower.

Wu, *et al.*, (1984) measured droplet concentrations from a raft in Delaware Bay at elevations between 0.13 and 1.3 m. Wind speeds were 6-8 ms⁻¹. Droplets in the 30-400 μm diameter range were detected by the extinction of a laser beam when the droplets passed through the sensor volume. Absolute concentrations were not obtained, the data were presented as the normalized frequencies of occurrence (f) of particles in certain size bands.

The normalized droplet spectra are described by two relations. In the jet-droplet ejection zone Wu, *et al.* obtained:

$$\begin{aligned}
 f &\sim D^{-1} & 50 \mu\text{m} < D < 150 \mu\text{m} \\
 f &\sim D^{-2.8} & 150 \mu\text{m} < D < 400 \mu\text{m} & \quad z < 20 \text{ cm} \\
 f &\sim D^{-8} & 400 \mu\text{m} < D
 \end{aligned}
 \tag{1}$$

Above the maximum ejection height of the jet droplets the same relations apply, but for different size ranges:

$$\begin{aligned}
 f &\sim D^{-1} & 10 \mu\text{m} < D < 50 \mu\text{m} \\
 f &\sim D^{-2.8} & 50 \mu\text{m} < D < 200 \mu\text{m} & \quad z > 20 \text{ cm} \\
 f &\sim D^{-8} & 200 \mu\text{m} < D
 \end{aligned}
 \tag{2}$$

D is the particle diameter, and z is the elevation above the instantaneous water surface. The size distributions were found to be independent of both elevation and wind speed.

The relations between f and D for the smallest sizes in eqns. 1

and 2 were obtained from comparisons with the data of Monahan (1968) at a height of 13 cm and Preobrazhenskii (1973) at heights of 1.5 to 2 m and 4 m. The $D^{-2.8}$ relationship appears to fit reasonably well to Preobrazhenskii's data for diameters larger than $50 \mu\text{m}$. At smaller sizes a D^{-1} relation applies. Monahan's data were put together with Preobrazhenskii's data to show that the above

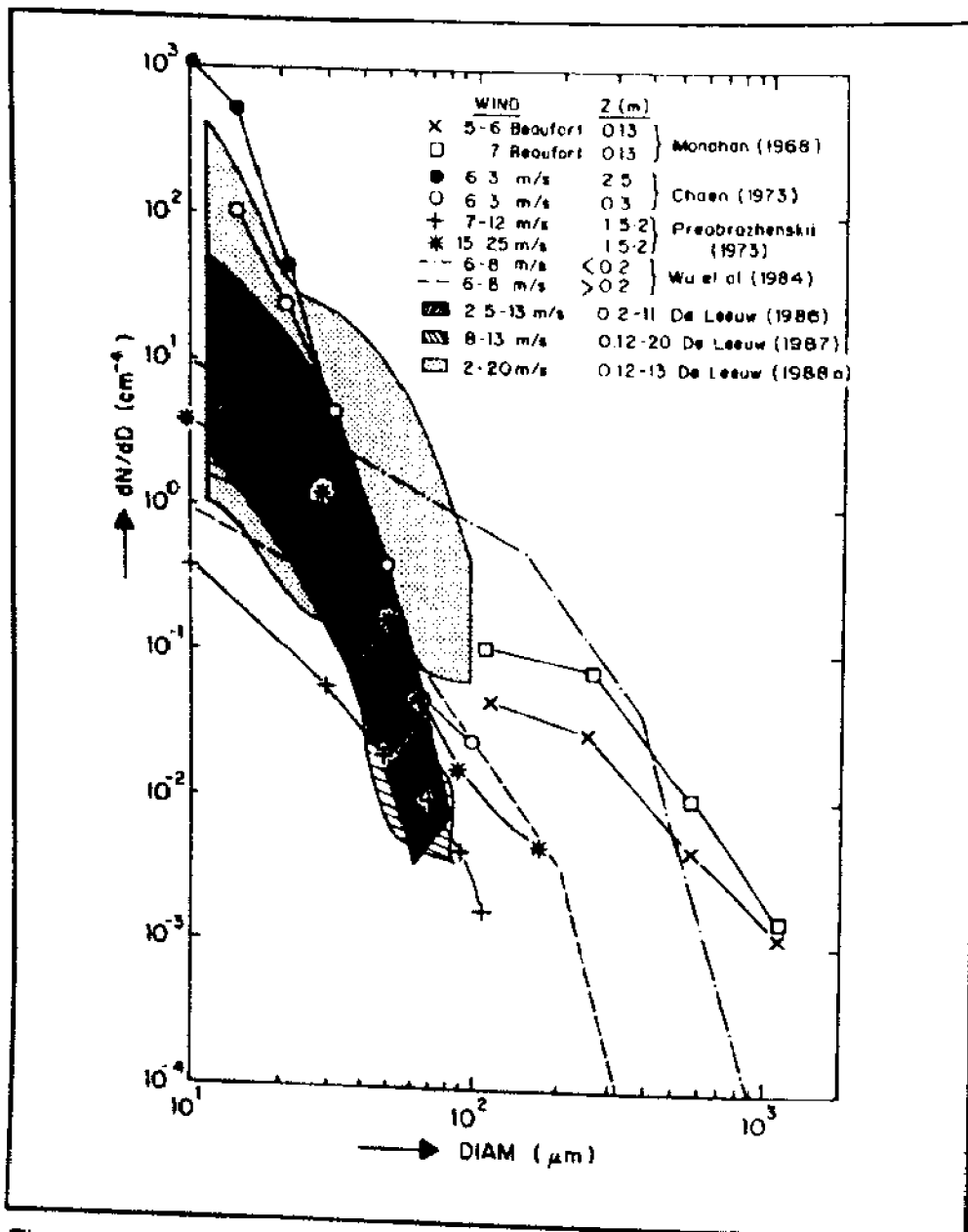


Figure 1. Survey of droplet concentrations in the atmospheric surface layer over the open ocean. The sources are indicated in the legend. Sampling methods, conditions and locations are presented in the text.

Table 1. Near-Surface Droplet Measurements

<u>Author</u>	<u>Technique</u>	<u>Location</u>	<u>Carrier</u>	<u>z (m)</u>	<u>U (ms⁻¹)</u>
Monahan (1968)	optical (photographic)	Aruba, Buzzards Bay	raft	0.13 0.13	10.8 15.5
Chaen (1973)	impactor (Cl sens.) and MgO slides	Indian Ocean, Pacific	ship board	1-3	0.8-16.6
Preobrazhenskii (1973)	oil-coated slides	N. Atlantic	ship board	1.5-7 15-25	7-12
Wu <i>et al.</i> (1984)	laser extinction	Delaware Bay	raft, time dependent	0.13-1.3	6-8
de Leeuw (1986)	impaction (Rotorod)	N. Atlantic	buoy, ship	0.2-11	2.5-13
de Leeuw (1987)	impaction (Rotorod)	North Sea	buoy, tower	0.12-20	1-13
de Leeuw (1989a)	impaction (Rotorod) and light scattering	North Sea	buoy, tower	0.12-13	2-20
de Leeuw (1989b)	light scattering	North Sea	buoy, tower; time dependent	0.12-13	2-20

relations apply also below 20 cm with a division at 150 μm . We note here that the fit to the sparse data points presented by Monahan is arbitrary. Least square fits would yield different relations, with large standard deviations that might include the relations in eqns. 1 and 2 proposed by Wu, *et al.* (1984). Moreover, comparisons with Monahan's (1968) original data show that Wu, *et al.* used data from two different wind speeds measured at different sites. The differences are obvious from Figure 1.

Particles larger than 400 μm were not observed by Wu, *et al.* (1984) above the ejection zone. The size distributions in Figure 1 were plotted at arbitrary concentrations since only the shape could be obtained from Wu, *et al.*

De Leeuw (1986) used rotating impaction samplers mounted on a wave follower to measure particle size distributions in the 10-100 μm diameter range alongside a ship. His stainless steel rods were coated with sprayed Silicone. Size distributions were measured in the North Atlantic at 0.2-2 m ASL (wave following at about 6 m from the ship's hull) and on decks 4, 6 and 11 m ASL. Wind speeds varied from 2.5 to 13 ms^{-1} . Results from all heights and wind speeds are collected in the shaded area in Figure 1.

During the HEXOS experiments in 1984 and in 1986 these measurements were repeated from a tower in the North Sea. In 1984 (HEXPLOT) samples were taken at a distance of 9 m from the legs of the platform (de Leeuw, 1987). During the HEXMAX experiment in 1986 a boom was used to bring the sampler at 13 m from the platform structure (de Leeuw, 1989a). The size distributions measured during these experiments fall within the boundaries indicated in Figure 1. The experiments by de Leeuw were originally intended to measure profiles. These are discussed in the following sections.

3. Surface layer profiles of droplet concentrations over the ocean.

Until recently the particle concentrations were assumed to increase exponentially toward the sea surface (Blanchard and Woodcock, 1980). This was based on a limited data set recorded at

different places and under different atmospheric and oceanic conditions.

Chaen (1973) concluded from his experiments that on the average the vertical distributions of the particle concentrations approach a power law dependence. Preobrazhenskii (1973) concluded that the particle volume decreases exponentially with height.

The profile published by Blanchard and Woodcock (1980) for

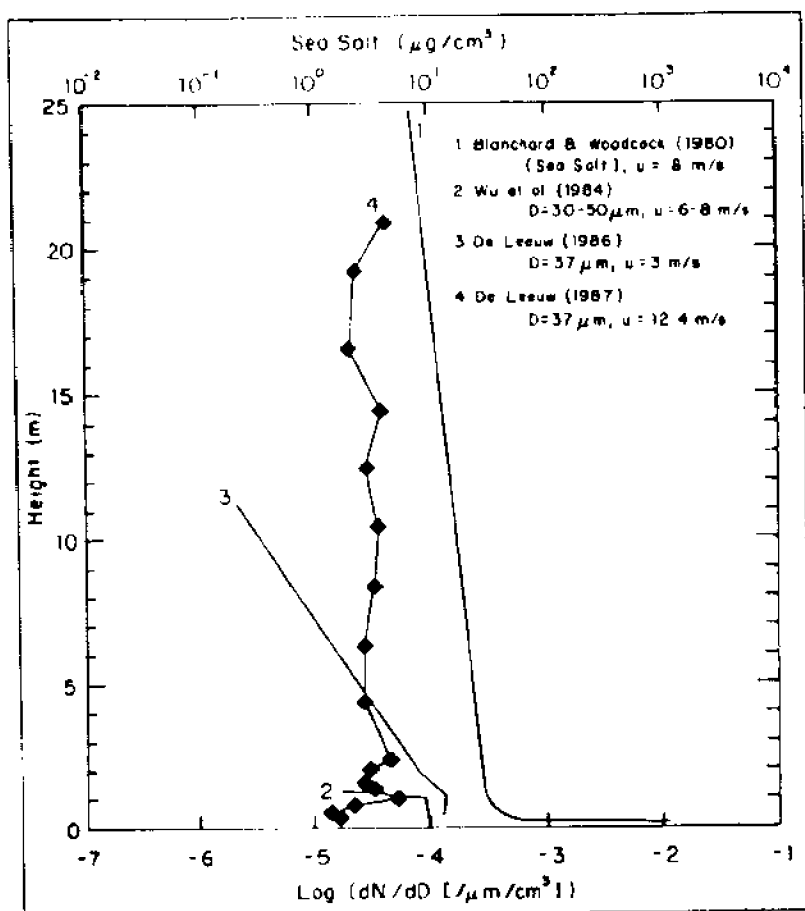


Figure 2. Representative examples of droplet concentration profiles in the atmospheric surface layer over the ocean.

8 ms^{-1} wind speed has been reproduced in Figure 2, together with examples of other profiles discussed below.

Wu, *et al.*, (1984) measured relative profiles of particle concentrations. The $30\text{-}50 \mu\text{m}$ particles were observed to be rather homogeneously distributed within the lowest meter above the instantaneous water surface, with only a small negative gradient, cf. Figure 2. The gradient becomes stronger as particle size increases. Above 1m the concentrations drop dramatically, for all sizes.

From our experiments in the North Atlantic in 1983 (de Leeuw,

1986) it was shown that a logarithmic profile does not generally apply in the lower few meters of the surface layer. In low winds logarithmic profiles were observed for all particle sizes. At wind speeds above approximately 7 ms^{-1} , however, a maximum was observed at heights between 1 and 2 m above the instantaneous water surface, cf. Figure 2.

The maximum was seen to develop with increasing wind speed. The effect is size dependent. For the largest particles ($85 \mu\text{m}$ in diameter) it was not observed, even in the highest wind occurring during this study in the North Atlantic (13 ms^{-1}). On the other hand the number of particles collected for this size range was statistically insufficient.

The observations concerning the shape of the particle concentration profile and the occurrence of a maximum were supported by measurements during the HEXPILOT experiment in 1984 (de Leeuw, 1987). The latter were made with much better vertical resolution than in the North Atlantic. Data were collected from the wave follower at 0.12, 0.20 and 0.35 m and between 0.5 and 3 m (resolution 0.25 m). Data were collected at fixed heights between 1 and 13 m with 1 m resolution. This revealed more detail in the profiles. At the highest wind speed of 12.4 ms^{-1} , the vertical data sequence shows strong evidence for the occurrence of a maximum near 1 m, as well as a less obvious secondary maximum just above 2 m (Figure 2). In the North Atlantic measurements the occurrence of a double maximum might have been overlooked due to insufficient vertical resolution. The analysis of our new experiments in the North Atlantic in 1987 (unpublished) might reveal whether the double maximum also occurs in the open ocean with its longer and higher waves, or that it is a feature specific to shallower waters with limited fetches like the North Sea.

A comprehensive set of data was collected during the HEXMAX experiment in the fall of 1986 (de Leeuw, 1989a, b). Two independent methods were used, based on different physical principles. In addition to the Rotorod impaction sampler, an optical device (called an optical scatterometer) was mounted on the wave follower to measure particle concentrations from the intensity of light scattered in the near forward direction (de Leeuw, *et al.*,

1989). Unfortunately direct comparisons were not possible since both instruments could not be mounted on the wave follower simultaneously. Nevertheless the profiles measured with the scatterometer and with the Rotorod were often similar and the scatterometer data confirm the previously observed occurrence of a maximum in the particle profiles (de Leeuw, 1989a).

On the other hand, the data collected with both the Rotorod and the optical scatterometer are often scattered in the vertical, which might hide the occurrence of a maximum in the profile.

4. Production of sea-salt aerosols and dispersal in the surface layer.

The production and subsequent dispersion of aerosols in the surface layer are discussed in the following sections. Comprehensive documentation exists on the production, cf. the reviews by Blanchard (1983) and Monahan (1986). Some salient features of production are reviewed below.

4.1 Production.

Salt water droplets can be produced at the sea surface by various mechanisms. The bubble mechanism has been studied extensively in the laboratory, cf. Blanchard (1983) for a review. When an air bubble in salt water reaches the surface it stays there for a second or more. Surface tension forces the bubble to reach an equilibrium position before it bursts. Upon bursting the thin film at the surface breaks up into typically 10-1000 particles (the so-called film drops). This applies to bubbles larger than about 2 mm in diameter. Smaller bubbles produce less film drops. The film drop spectrum peaks at 5 μm , and may extend from smaller than 1 μm to larger than 30 μm (Blanchard, 1983).

When the bubble bursts, the surface free energy is converted into kinetic energy of a jet of water which rises from the bottom of the bubble cavity. The water column overshoots the surface and breaks up into typically 1-10 droplets, depending on bubble size. The maximum ejection heights of these so-called jet drops have been observed to be nearly 20 cm for the top drop and only a

fraction of that for the following drops. This applies to 2-mm bubbles, the ejection heights of jet drops originating from smaller or larger bubbles are lower. The size of the top drop is about 10% of the size of the bubble diameter (Blanchard, 1983).

4.2 Consideration of laboratory production estimates and oceanic conditions.

In the ocean, air bubbles are usually formed after the entrainment of air in the water by breaking waves (cf. Monahan and O'Muircheartaigh, 1986, for a review). Precipitation and living organisms may be other sources that will cause more isolated bubbles. In a bubble patch the bubbles may influence each other, giving rise to particle production characteristics different from those in isolated bubbles (Blanchard, 1983; Mestayer and Lefauconnier, 1988). In addition to the bubble mechanism, also direct production of spume drops by wave disruption occurs in the ocean in winds exceeding 9 ms^{-1} (Monahan, *et al.*, 1983).

Obviously the scale heights over the ocean are different from those in a wave tank. Ocean waves are measured in meters, whereas in a wave tank the highest waves may be 10-20 cm. Droplets that are produced at the crest of a wave and are carried along with the wind may soon reach a height of several meters above the instantaneous sea surface. Similarly, the ejection height of jet droplets may not be a useful parameter over the ocean because the surface displacements cause height variations which are more than one order of magnitude larger. On the other hand, the suspension times of the jet drops might be so short (cf. Wu, 1979 for suspension times in still air) that the surface displacements are insignificant on this time scale. Not much wind is required, however, to create enough turbulence to enhance the suspension time appreciably. Numerical calculations by Edson (Edson, *et al.*, 1988; Mestayer, *et al.*, 1989) on the effect of turbulence on particle trajectories in a wave tank show that particles may travel distances on the order of 10 m before they are returned into the water.

The influence of wave-induced surface displacements on atmospheric droplet concentrations has recently been observed over the North Sea (de Leeuw, 1989b). The effects were visible from close

to the surface up to 13 m, the highest elevations where samples were taken. The analysis of these data led to the conclusion that the time scale for transport of the largest particles is on the order of 5 seconds or longer.

The occurrence of wave-induced fluctuations of droplet concentrations was confirmed by wave tank experiments (de Leeuw, 1988). Analysis of the wave tank data might reveal interesting information on the phase relation between aerosol concentrations and waves.

In spite of their limitations, laboratory experiments are very useful to study the physics of droplet production and the subsequent dispersion due to the interactions with the turbulent fields of air flow, humidity and temperature (Mestayer, *et al.*, 1988). In the open ocean such measurements are hard to accomplish.

4.3 Surface production estimates from the open ocean.

The few oceanic surface production estimates were indirectly obtained. One approach is based on a physical model that describes the vertical structure in the mixed-layer. From a fit to particle size distributions measured at elevated heights of 10 m, the surface flux was obtained (Fairall, *et al.*, 1983). The other estimate is from laboratory experiments on the aerosol whitecap productivity, combined with a comprehensive set of field observations of whitecap coverage (Monahan, 1986). Both estimates are in good agreement.

Verification of the predicted surface production rates requires particle concentration profiles (Fairall and Larsen, 1984; Wu, 1979). The model by Fairall, *et al.*, (1983) has been modified (de Leeuw, 1989c) and applied to our surface layer profiles (de Leeuw and Davidson, 1989). In low winds the predictions by the model are correct for small particles, but not for particles larger than 15-20 μm . In high wind the model also overestimates the surface production rates for smaller particles.

5. Particle transport in the surface layer.

Since particles are observed in noticeable concentrations both in the surface layer and in the mixed-layer, some mechanism will

carry them aloft after production at the air-sea interface.

In still air the ejection height is limited to a maximum of 20 cm (Blanchard, 1983) by gravitational forces. However, in nature still air is unlikely to occur. Turbulence is generally considered the driving force that lifts particles off the ejection zone. The oceanic measurements by Wu, *et al.*, (1984), however, indicate a change in the particle spectrum at 20 cm. The particle size distributions measured below 20 cm are considered the production spectrum (Wu, *et al.*, 1984). Particles larger than a certain size (50 μm at the 6-8 ms^{-1} wind speeds of these observations) are not lifted out of the production zone.

To achieve this, turbulence should at least balance the gravitational fall velocity. Hence particles tend to stay in suspension when the following condition is met (Wu, *et al.*, 1984):

$$W/\kappa u_* > 1 \quad (3)$$

W is the gravitational fall velocity, κ is the Von Karman constant and u_* is the friction velocity.

The above condition applies to the data presented in Wu, *et al.*, (1984). Other data which might be used to check on the wind speed dependence of particle concentrations in the surface layer were published in de Leeuw (1986). The critical size derived from these data has been plotted vs. wind speed in Figure 3. The data

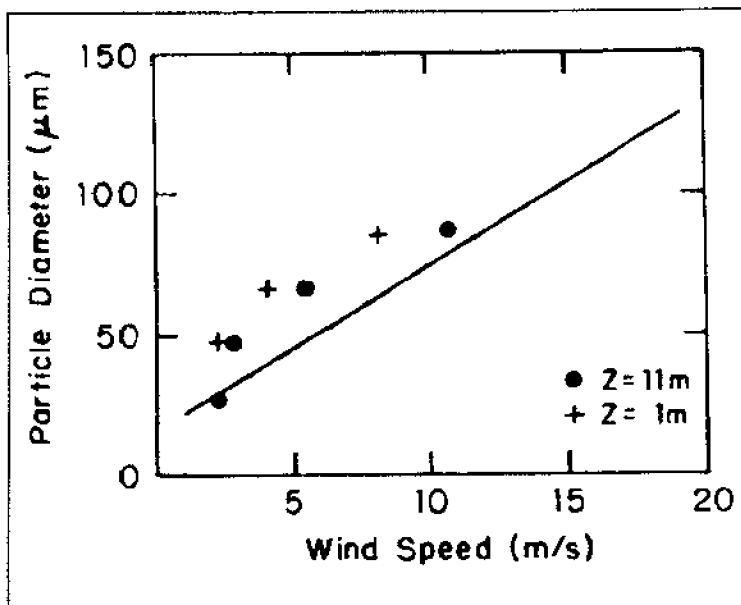


Figure 3. Diameter of largest suspended droplets versus wind speed, for elevations of 1 and 11 m. The solid line indicates where the turbulence intensity κu_* balances the gravitational fall velocity W (eqn. 3, cf. Wu, *et al.*, 1984.)

show that the critical droplet size is somewhat larger than predicted by equation 1. The profiles presented in de Leeuw (1986, 1987) indicate further that close to the sea surface the discrepancy becomes larger, i.e. larger particles escape from the production zone than predicted by equation. 1. To illustrate this, the critical sizes at 1 m have been plotted in Figure 3 as well.

Apparently some other mechanism keeps the particles in suspension, in addition to the turbulence. Based on the changing shape of the profiles as wind speed increases above about 7 ms^{-1} , de Leeuw (1986) proposed the wave rotor model that is schematically presented in Figure 4. In this model particles are temporarily trapped in eddies between wave crests that are caused by flow separation at the stagnation points (cf. Banner and Melville, 1976). This occurs under breaking wave conditions. The onset of white-capping is generally at wind speeds of about 7 ms^{-1} , although

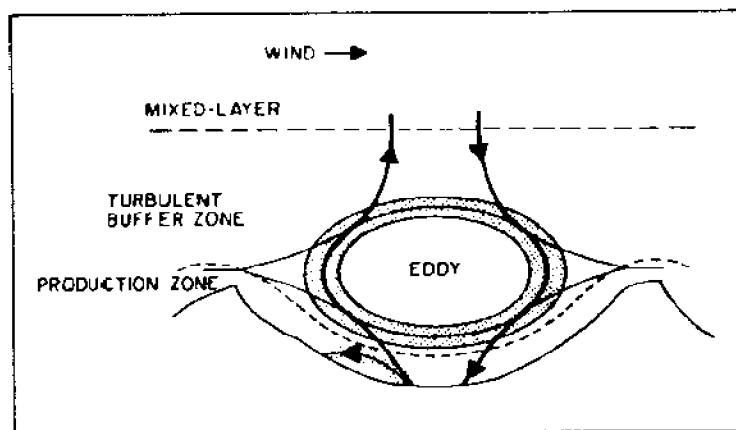


Figure 4. Schematic representation of the wave rotor model (not to scale).

depending on atmospheric conditions it may occur in wind speeds as low as 4 ms^{-1} (Monahan and O'Muircheartaigh, 1986).

In a wave-following coordinate system the air flow is reversed from the wind direction at elevations below the critical layer, i.e. the height where the wind speed equals the wave speed (cf. Kraus, 1972). Droplets ejected from the sea surface are dragged along in this reversed flow. Near the crest the flow has an upward component which gives the droplets some extra lift. If the up-draught is strong enough to lift the droplets above the top of the crest before they impact in the wave surface, the wind drag changes their horizontal direction and they are carried along to the next crest in the direction of the wind. There they may be dragged downward

due to the somewhat enhanced pressure that forces the flow back into the trough. Here the whole process may be repeated.

During this process gravitation and turbulence are also active. If $W > \kappa u$, the particles are dragged downward and are likely deposited into the sea. In the other case, $W < \kappa u$, they might escape the eddy into the mixed-layer. Since these processes are statistical in nature, this distinction is not sharp. Only a fraction of the particles is expected to reach the mixed layer, which depends on size, density and wind speed.

Once in the mixed layer the particles are subject to gravitation and turbulent transport, while entrainment, subsidence and stability also affect the concentrations (cf. Fairall, *et al.*, 1984).

The exchange of particles between the surface layer and the mixed layer is not limited to freshly produced droplets. 'Aged' particles that are trapped in the eddies are subject to the same processes described above. Hence they might be resuspended or deposited. Another interesting possibility is the interaction through coagulation between aged particles and fresh droplets, which might enhance the deposition rate.

In view of the above, the concept of a viscous sub-layer, which is successfully used in the description of air-sea exchange of, e.g., humidity, might be less suitable to aerosol modelling. It is not only the escape of the droplets through the sub-layer that has to be considered, but also the transport of the droplets in the zone of influence of wave-induced eddies. Previously we called this the turbulent buffer zone, since the droplets may be temporarily trapped in the eddies. In effect, this buffer zone may be considered as an elevated and distributed source.

6. Discussion.

Particle size distributions and particle concentration profiles have been measured near the air-sea interface with methods based on different physical principles. Optical techniques employed were photographic (Monahan, 1968), laser extinction measurements (Wu, *et al.*, 1984) and measurements of near-forward laser scattering (de Leeuw, 1989a, b). Passive impaction methods were

used by Chaen (1973) and Preobrazhenskii (1973); active impaction methods were used by Chaen (1973) and de Leeuw (1986, 1987, 1989a). Various coatings were applied to retain the particles. This requires different processing and calibration techniques. The size distributions were measured under a wide range of meteorological and oceanographic conditions, at different locations.

This is reflected in the results displayed in Figure 1. Due to changing meteorological conditions, the concentrations observed during our measurements in the North Atlantic (de Leeuw, 1986) vary over one decade. These data are representative for the average of the other measurements in the same size range. Large differences were observed, however, spanning almost four decades at $10\ \mu\text{m}$ to two decades around $100\ \mu\text{m}$.

The shapes of the surface layer profiles are strongly dependent on wind speed. The occurrence of non-logarithmic profiles under breaking wave conditions was demonstrated by our experiments in the North Atlantic (de Leeuw, 1986). The maximum in the profiles was confirmed by the HEXOS experiments in 1984 (de Leeuw, 1987) and in 1986 (de Leeuw, 1989a, b). The analysis of these profiles led to new insights into the surface production rate (de Leeuw and Davidson, 1989). The application of a viscous sublayer concept might need reconsideration. The use of an effective source strength in mixed-layer models yields correct predictions of the trends in mixed-layer aerosol profiles (de Leeuw, 1989c). Near the surface, however, the predicted concentrations increase faster than indicated by our data (de Leeuw and Davidson, 1989). Hence the surface production rates are overestimated. Better results might be obtained by considering a distributed source function that extends over the region where wave-induced eddies are active. The extent of this region will depend on the meteorological and oceanographic conditions. Empirical relations to estimate the elevated source strengths were presented in de Leeuw (1986). This simple model is based on a single data set consisting of 17 profiles. Inclusion of the HEXOS data is expected to lead to refinements yielding a more reliable model. The results are important to quantify the effects of droplets on, e.g., the processes mentioned in the introduction. When they are trapped in the turbulent buffer zone

more time is available for interaction with the surrounding air parcels.

A wave-rotor model has been proposed to explain the observed non-logarithmic profiles (de Leeuw, 1986). This concept is supported by the observed wind speed dependence of the particle concentrations at various elevations. Theoretically this wave rotor model has not been verified yet. The extension of the numerical calculations by Edson (Edson *et al.*, 1988; Mestayer *et al.*, 1989) to include the wave-induced flow has been outlined in de Leeuw (1989b). This approach can also be used to study the relative importance of the wave rotor mechanism and particle transport by turbulent air flow.

Acknowledgment.

This paper was prepared while the author held a National Research Council Research Associateship at the Naval Postgraduate School. The author thanks Dr. Kenneth L. Davidson for careful reading of the manuscript.

References

- Banner, M.L., and W.K. Melville, 1976: On the Separation of Air Flow Over Water Waves, *J. Fluid Mech.* 77, 825-847.
- Blanchard, D.C., and A.H. Woodcock, 1980: The Production, Concentration, and Vertical Distribution of the Sea-Salt Aerosol. *Ann. of the NY Academy of Science*, pp. 330-347.
- Blanchard, D.C., 1983: The Production, Distribution, and Bacterial Enrichment of the Sea-Salt Aerosol. In: *Air-Sea Exchange of Gases and Particles*. P.S. Liss and W.G.N. Slinn (eds.): Reidel, pp. 407-454.
- Chaen, M., 1973: Studies on the Production of Sea-Salt Particles on the Sea Surface. *Mem. Fac. Fish., Kagoshima Univ.* 22, 49-107.
- de Leeuw, G., 1986: Vertical Profiles of Giant Particles Close Above the Sea Surface. *Tellus* 38B, 51-61.
- de Leeuw, G., 1987: Near-Surface Particle Size Distribution Profiles Over the North Sea. *J. Geophys. Res.* 92, 14631-14635.
- de Leeuw, G., 1988c: Survey of the CLUSE Main Experiment Grand-CLUSE, May 1-June 15, 1988. Physics and Electronics Laboratory TNO, Report FEL 1988-43.
- de Leeuw, G., 1989a: Surface Layer Profiling of Aerosol Concentrations,

BUBBLE-MEDIATED SEA-AIR EXCHANGE

- Particle Size Distributions and Relative Humidity During HEXMAX.
Submitted to *Tellus*.
- de Leeuw, G., 1989b: Investigations on Turbulent Fluctuations of Particle Concentrations and Relative Humidity in the Marine Atmospheric Surface Layer. *J. Geophys. Res.* **94**, 3261-3269.
- de Leeuw, G., 1989c: Modeling of Extinction and Backscatter Profiles in the Marine Mixed-Layer. *Appl. Opt.* **28**, 1356-1359.
- de Leeuw, G., and K.L. Davidson, 1989: Mixed-Layer Profiling with Lidar and Modeling of the Aerosol Vertical Structure. Submitted to *J. Atm. Oceanic Techn.*
- de Leeuw, G., J.A. Boden, L.H. Cohen, M. Deutekom, A.J.T. de Krijger, G.J. Kunz, M.M. Moerman and C.W. Lamberts, 1989: An Angular Scattering Device for the Determination of Turbulent Fluctuations of Aerosol Concentrations. Submitted to *Rev. Sci. Instr.*
- Edson, J.B., C.W. Fairall, S.E. Larsen and P.G. Mestayer, 1988: A Random Walk Simulation of the Turbulent Transport of Evaporating Jet Drops in the Air-Sea Simulation Tunnel During HEXIST. 7th Conf. on Air-Sea Interaction, Jan. 31-Feb. 5, Anaheim, Calif.
- Fairall, C.W., K.L. Davidson and G.E. Schacher, 1983: An Analysis of the Surface Production of Sea-Salt Aerosols. *Tellus* **35B**, 31-39.
- Fairall, C.W., K.L. Davidson and G.E. Schacher, 1984: Application of a Mixed-Layer Model to Aerosols in the Marine Boundary Layer. *Tellus* **36B**, 203-211.
- Fairall, C.W. and S.E. Larsen, 1984: Dry Deposition, Surface Production and Dynamics of Aerosols in the Marine Boundary Layer. *Atmos. Environ.* **18**, 69-77.
- Kraus, E.B., 1972: Atmosphere-Ocean Interaction, Clarendon Press, Oxford.
- Mestayer, P.G., C.W. Fairall, S.E. Larsen, D.E. Spiel and J. Edson, 1989: Turbulent Transport and Evaporation of Droplets Generated at an Air-Water Interface. Proc. Sixth Symp. Turb. Shear Flows, Toulouse, France, Sept. 7-9.
- Mestayer, P., and C. Lefauconnier, 1988: Spray Droplet Generation, Transport, and Evaporation in a Wind Wave Tunnel During the Humidity Exchange over the Sea Experiments in the Simulation Tunnel. *J. Geophys. Res.* **93**, 572-586.
- Mestayer, P.G., C. Lefauconnier, M. Rouault, S. Larsen, C.W. Fairall, J.B. Edson, D.E. Spiel, K.L. Davidson, E.C. Monahan, D. Woolf, G. de Leeuw, H. Gucinski, K.B. Katsaros and J. DeCosmo, 1988: HEXIST NATO Advanced Workshop on Humidity Exchange Over the Sea, De Bilt/Epe, The Netherlands, April 25-29.
- Monahan, E.C., 1968: Sea Spray as a Function of Low-Elevation Wind Speed. *J. Geophys. Res.* **73**, 1127-1137.
- Monahan, E.C., 1986: The Ocean as a Source for Atmospheric Particles. In: P. Buat-Menard (ed.), *The Role of Air-Sea Exchange in Geochemical Cycling*. Reidel, 129-163.

- Monahan, E.C., and I.G. O'Muircheartaigh, 1986: Whitecaps and the Passive Remote Sensing of the Ocean Surface. *Int. J. Remote Sensing* 7, 627-642.
- Monahan, E.C., D.E. Spiel, and K.L. Davidson, 1983: Model of Marine Aerosol Generation Via Whitecaps and Wave Disruption. Ninth Conf. on Aerospace and Aeronautical Meteor., June 6-9, Omaha, Nebr.
- Preobrazhenskii, L. Yu., 1973: Estimate of the Content of Spray Drops in the Near-Water Layer of the Atmosphere. *Fluid Mech.-Soviet Res.* 2, 95-100.
- Wu, J., 1979: Spray in the Atmospheric Surface Layer: Review and Analysis of Laboratory and Oceanic Results. *J. Geophys. Res.*, 84, 1693-1704.
- Wu, J., J.J. Murray and R.J. Lai, 1984: Production and Distributions of Sea Spray. *J. Geophys. Res.* 89, 8163-8169.

.. 6 ..

Relationships Between Marine Aerosols, Oceanic Whitecaps, and Low-Elevation Winds Observed During the HEXMAX Experiment in the North Sea.

Roman Marks and Edward C. Monahan
Marine Sciences Institute
University of Connecticut
Avery Point
Groton, CT 06340

Abstract

During the HEXMAX experiment in October - November 1986, the sea-salt aerosol mass concentration, its size distribution and vertical profile, and the other meteorological parameters describing the Marine Atmospheric Boundary Layer, along with the whitecap coverage and other relevant oceanographic parameters, were investigated.

The sea-salt aerosol mass concentration (S-SAMC) and its vertical profile were measured using isokinetic air filtration units at elevations of 4.5 m, 12 m and 18.3 m. Five size classes of the S-SAMC were sampled using a multistage impactor (Sierra 230). The whitecap coverage data were recorded with a video camera system.

The interrelationships between S-SAMC, wind speed and whitecap coverage were determined. The results demonstrated a marked enhancement of the S-SAMC at 4.5 m elevation when the wind speed exceeded 10 ms^{-1} and at 12 m and 18.3 m elevations

when the wind increased to above 15 ms^{-1} . Correlation coefficients between S-SAMC and wind speed were found to increase with wind speed and with increasing sizes of the sea-spray aggregates dispersed in air.

1. Introduction

Sea-spray generation processes have been investigated and closely correlated with wind speed (e.g. Woodcock, 1953, Blanchard, 1963, Garbalewski, 1980, and others). In the initial stage the turbulent components of the air flow over the sea surface generate fine ripples and capillary waves, which create rough surface elements. Through such rough elements in a high frequency range, the energy of air turbulence is transferred to the developing wind waves. In a random wave field those waves that have developed to the critical steepness will dissipate energy by breaking and forming whitecaps. This is the main source of bubbles at the sea surface. It is these bubbles which generate jet and film drops upon bursting and affect the turbulent diffusion of heat and moisture. When the wind-wave-whitecap system reaches a high state of development the tearing of drops and water parcels from the wave crests contributes further to the sea-spray flux to the atmosphere.

During heavy storms or hurricanes water parcels from wave crests as well as rough elements of the surface are mechanically dislodged, creating an air/sea mixing zone. Furthermore, the sea-spray production processes may be modified by other peripheral conditions. These include wave breaking in shallow water, or at obstacles (i.e. icebergs), air bubble advection in the ocean surface layer, supersaturation of the sea water, wave-wave interaction, atmospheric precipitation, stability at the air/sea interface, and other meteorological and oceanographic conditions. An attempt to correlate sea-salt concentration with wind speed and other meteorological factors has been made by Lovett (1978). It was found that total sea-salt concentration could be represented as a function of the wind speed by the equation $\ln Q = 0.16u + 1.45$ (Q = sea-salt concentration in μgm^{-3} and u = wind speed in ms^{-1}). Exton *et al.*, (1983) conducted field experiments at a coastal site on the island

of South Uist in the Outer Hebrides. They suggest that the size distribution of the sea-salt could be sub-divided into two ranges separated at $r \sim 0.3 \mu\text{m}$, the lower corresponding to long range aerosol and the higher to locally-produced aerosol.

The complex interrelations between 10 m elevation winds, whitecaps and marine aerosols were investigated by Monahan *et al.*, (1983). They report the positive dependence of aerosol concentration upon whitecap cover, increasing with droplet radius. The total mass of the sea-salt aerosols as a function of wind speed $u(10)$ and whitecap coverage were determined by Marks (1987). In this study, the static stability at the air/sea interface was found to inhibit the sea-salt aerosol production. Vertical profiles of the sea-salt aerosols have been investigated by Chaen (1973), Pre-abrazhenskii (1973), Blanchard and Woodcock (1980), Blanchard *et al.* (1984), de Leeuw (1986) and Stramska (1987). Furthermore, some laboratory studies on the size distribution of particles in profiles have been done by Wu (1979), Koga and Toba (1981) and Koga (1984). Both the particle concentration and its variation with height are strongly dependent on wind speed, and the average concentration gradients decrease with decreasing particle diameter at a given wind speed (de Leeuw, 1986).

The present investigation was carried out to combine the S-SAMC and whitecap coverage data obtained during the HEXMAX experiment. This effort is part of the intercomparison of the various data sets collected to study the evaporation and spray-droplet fluxes from the sea at the moderate- to high-wind speeds.

2. Measurements

Data were collected from the Dutch research platform Noordwijk, located 9 km offshore in the North Sea.

The S-SAMC observations consisted of measurements at three heights; 4.5 m, 12 m and 18.3 m, and the measurement of sea-salt size distribution at 12 m elevation. For profile measurements a semi-isokinetic air filtration unit with adjustable air speed at the inlet was used. A High Volume Cascade Impactor (5 stages), Sierra 230, was used for the size distribution measurements.

Whatman 41 filters were used for the actual collection of the aerosol sampled by both instruments. The air-filtration-unit inlets were oriented in the direction of the oncoming wind.

To collect a sufficient amount of aerosol, both sampling units were operated in ambient air for 0.5-3 hours. After each run, eight exposed filters were unloaded and pressed to get pills of about 1 cm diameter.

Neutron activation analysis was carried out on a total of 750 pills. Irradiation was performed for 10 minutes at a thermal neutron flux of about $10^{13} \text{ sec}^{-1} \text{ cm}^{-2}$ using the reactor at the GKSS Research Centre (Fed. Rep. of Germany). The concentration of Na was determined from the intensity of the 1368 keV Gamma-Ray emission of Na-24 as measured with a Ge(Li) detector.

The whitecap coverage was recorded using a video camera, a SONY Trinitron Model DXC 1800 P, and a color portable video recorder (SONY Model V0-4800PS). The line-of-sight of the camera was set 20° below the horizontal. The camera shelter itself was fixed on the exterior of the platform at an elevation of about 12 m above the surface of the North Sea. The fraction of the sea surface covered by young (stage A) whitecaps has been determined for 159 periods during the experiment by analyzing the video images with a Hamamatsu Area Analyzer (Model C1143-00).

Background meteorological and oceanographic data were automatically recorded at 10-minute intervals by the platform data acquisition system. The wind speeds measured 28 m above the mean sea level were adjusted to the 10 m elevation wind speed equivalent using the logarithmic wind profile law.

3. Sea-salt aerosol-total mass concentration data

The aerosol data obtained using the air filtration unit at 12 m elevation were subdivided into five classes according to the different air advection patterns present during the experiment. These classes were partitioned using 1000 mb air mass trajectories and included air flow from a SW-NNW sector, from NNW-N sector, from the English Channel, from the coastal zone, and from land. In Fig. 1 the five classes of S-SAMC are presented as a function of

BUBBLE-MEDIATED SEA-AIR EXCHANGE

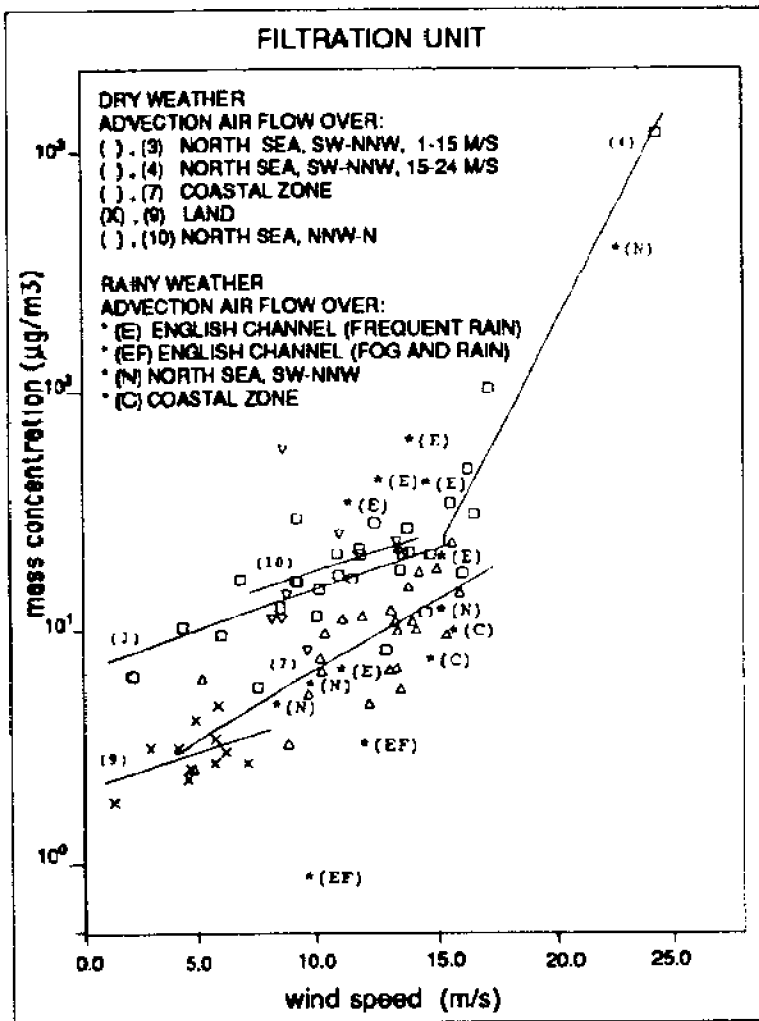


Fig. 1. Sea-salt aerosol mass concentration of the filtration-unit versus 10 m wind speed for different advection air flows. Measurements were taken at 12 m elevation during dry (points and curves) and rainy (points denoted by letters) weather conditions. Curves 3,4,7,10 are described in Table 1.

the wind speed $u(10)$ for dry and rainy weather conditions. The S-SAMC data in dry weather, associated with air advection from SW-NNW sector (curves 3 and 4), from a NNW-N sector (curve 10) as well as from the English Channel (in spite of rainy weather condition), (points denoted by E), indicated a considerably higher mass concentration than did the S-SAMC data associated with air mass advection from the coastal zone (curve 7) or land (curve 9). In the latter case the air had to travel over the sea a distance of 10-20 km.

Samples collected during rainy weather are indicated in Fig. 1 by letters which correspond to advection air flow over: the English Channel (E class for frequent rain, and EF class for fog and rain), the North Sea, SW-NNW (N class) and the coastal zone (C class). Generally, the S-SAMC data collected during rainy weather at 12 m elevation showed lower concentrations and larger variations,

identified with samples collected during foggy weather conditions (see points denoted by EF on Fig. 1).

To study the influence of wind speed $u(10)$ on S-SAMC the samples collected when the air was advecting from the SW-NNW sector (representing for the most part winds from over the North Sea) were partitioned into two categories. The first included the S-SAMC values measured when the wind speed were between 1 and 15 ms^{-1} (see curve 3 on Fig. 1), and the second category included the S-SAMC values obtained when the wind was between 15 and 24 ms^{-1} (see curve 4 on Fig. 1). The differences in the slope of these two curves show that the S-SAMC undergoes a marked enhancement when the wind speed exceeds 15 ms^{-1} (see Table 1).

Curve No.	Data Set	No. of points	Wind range (u in ms^{-1})	Curve fit	Corr. coeff.
3	North Sea SW-NNW	24	1-15	$M=5.6145 \text{ EXP}(0.0823 u)$	0.60
4	North Sea SW-NNW	6	15-24	$M=0.0229 \text{ EXP}(0.4562 u)$	0.95
7	Coastal zone	25	4-17	$M=1.4176 \text{ EXP}(0.1417 u)$	0.72
9	Land	11	1 - 8	$M=1.7704 \text{ EXP}(0.0735 u)$	0.46
10	North Sea	7	7-14	$M=6.9267 \text{ EXP}(0.0786 u)$	0.21

Table 1. Least squares exponential curve estimates fitted to the data of sea-salt aerosol mass concentration $M(\mu\text{gm}^{-3})$ versus 10 m wind speed $u(\text{ms}^{-1})$, (measurements taken at 12 m elevation).

This initial analysis shows some remarkable differences in S-SAMC associated with different air advection patterns over the North Sea. These differences support the hypothesis that sea-salt aerosol over the North Sea is of a mixed type, originating from both Atlantic and locally emitting sources. Nevertheless, the

BUBBLE-MEDIATED SEA-AIR EXCHANGE

S-SAMC can be related to the air/sea interaction conditions over the North Sea itself, especially when wind speeds exceed 10 ms^{-1} . In order to compare five earlier studies with our own, the data have been expressed in the form $\ln(M)=au+\ln(b)$ and are presented in Table 2. The associated value of the quantity a determined from our studies is seen to agree well with those obtained by Woodcock and Lovett, under similar sampling conditions.

Authors	Latitude	Site and Approximate sampling height	Max u (ms^{-1})	a (sm^{-1})	b (μgm^{-3})
Woodcock 1953	20°N	Cloud base over Pacific Ocean (500m)	35	0.16	2.57
Tsunogai <i>et al</i> 1972	40°N-60°S	Ship on Pacific Ocean	18	0.62	0.33
Lovett 1978	50°N-60°N	Weather ship Atlantic Ocean 5-15 m	20	0.16	4.26
Kulkarni <i>et al</i> 1982	19°N	W. Indian coast 1.8 km inland, 1.2m	8	0.27	5.35
Exton <i>et al</i> 1983	57°N	Hebridean beach facing Atlantic 15 m	20	0.17	14.30
Present	52°N	North Sea Noordwijk platform 4.5 m	24	0.35	1.17
		12 m	24	0.17	2.39
		18.3 m	24	0.16	2.65

Table 2. Published relationships between airborne salt concentration M in μgm^{-3} , and wind speed u in ms^{-1} , assuming a relationship of the form $\ln(M)=au+\ln(b)$ where a and b are constants.

4. Five size classes of the sea-salt aerosol

Recognizing that the pumping system of the multi-stage impactor was too weak to sample at the correct rate during heavy wind conditions, the S-SAMC data obtained from the multi-stage

impactor were corrected using the simultaneously measured data from the isokinetic air filtration unit. This was done by multiplying the original results obtained from each of five impactor stages $M(i, x=1, 2, 3, 4, 5)$ by the ratio $R=M(F)/M(I)$ where $M(F)$ and $M(I)$ are the total the S-SAMC obtained from the filtration unit and from the multi-stage impactor respectively. Data processed in this manner for the five size classes of S-SAMC were plotted in Fig. 2 as a function of wind speed $u(10)$ for those samples collected when the air advection was from the SW-NNW sector over the North Sea. The results, delineated by the ten estimates fitted to the S-SAMC data as $\ln(M)$, show that giant particles (see stage 1), in the size range $7.2-30 \mu\text{m}$ in diameter, increase in concentration with wind speed more rapidly than does the concentration of smaller particles represented by the stages 2, 3, 4, and 5 which correspond to size ranges $3.0-7.2 \mu\text{m}$, $1.5-3.0 \mu\text{m}$, $0.95-1.5 \mu\text{m}$ and $0.49-0.95 \mu\text{m}$ respectively. This is more obvious for wind speeds $1-15 \text{ ms}^{-1}$ (range A in Fig. 2). The few data collected for wind speeds $15-24 \text{ ms}^{-1}$ (see range B in Fig. 2) are too scarce to give statistically

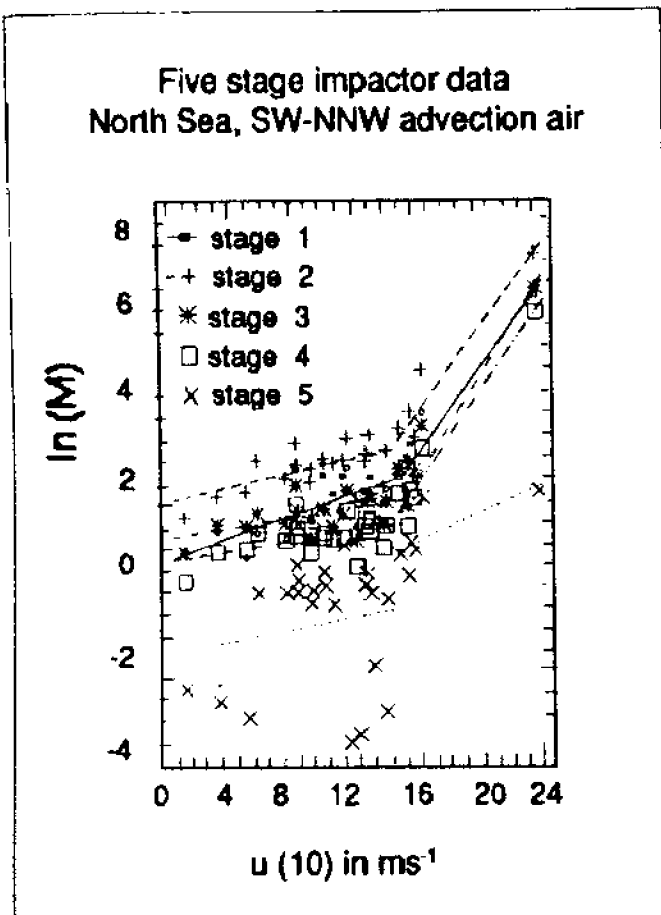


Fig. 2. Five size classes of sea-salt aerosol mass concentration plotted as a $\ln(M)$ versus $u(10)$ wind speed. Measurements taken at 12 m elevation. Curves are described in Table 3.

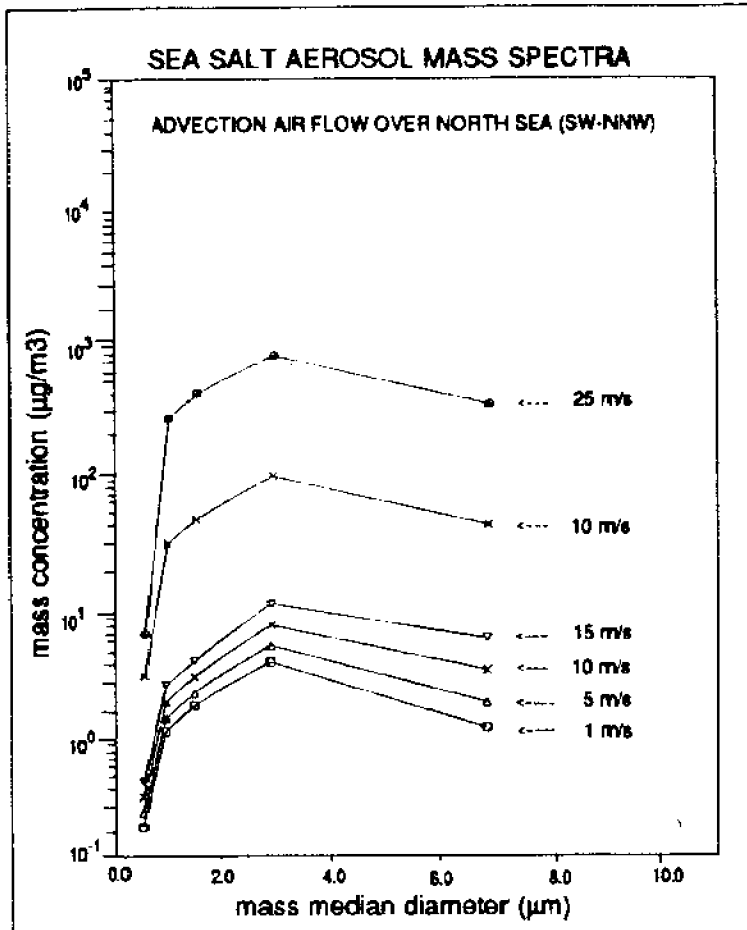


Fig. 3. Comparison of estimated spectra of sea-salt aerosol mass at 12 m elevation for different wind speeds.

significant results. The S-SAMC data of stage five (0.49-0.95 μm) were found to have the largest variation and the lowest correlation with wind speed.

To present the spectra of the S-SAMC in Fig. 3 the S-SAMC estimated for each of the impactor stages (see Table 3) were plotted versus the mass median diameter of that stage for measurements taken at 12 m elevation. Fig. 3 shows a gradual widening of the mass spectrum towards the bigger sized particles as wind speed increases. Furthermore, the correlation coefficients between S-SAMC and wind speed were found to increase with wind speed towards increasing sizes of the sea-spray aggregates (see curve fits in Table 3 and Table 5).

5. Vertical profiles of the sea-salt aerosol mass concentration.

As a first approach the profiles of the S-SAMC data were studied as a function of wind speed. Results plotted in Fig. 4 for

Curve No.	Data set/ Wind range	Size cut-off in μm / stage no.	Curve fit	Corr. coeff.
31/1	North Sea	7.2-30 /1	$\ln(M) = -0.1511 + 0.1143 u$	0.69
31/2	SW-NNW	3.0-7.2 /2	$\ln(M) = 1.1159 + 0.0695 u$	0.55
31/3		1.5-3.0 /3	$\ln(M) = 0.3783 + 0.0467 u$	0.46
31/4	Range A	0.95-1.5 /4	$\ln(M) = -0.1011 + 0.0480 u$	0.44
31/5	1-15 ms^{-1}	0.49-0.95/5	$\ln(M) = -2.0908 + 0.0620 u$	0.16
31/1	North Sea	7.2-30 /1	$\ln(M) = -5.3906 + 0.4550 u$	0.94
31/2	SW-NNW	3.0-7.2 /2	$\ln(M) = -4.5049 + 0.4543 u$	0.95
31/3		1.5-3.0 /3	$\ln(M) = -5.7850 + 0.4772 u$	0.96
31/4	Range B	0.95-1.5 /4	$\ln(M) = -6.3053 + 0.4774 u$	0.97
31/5	15-24 ms^{-1}	0.49-0.95/5	$\ln(M) = -2.2902 + 0.1552 u$	0.71
32/1	North Sea	7.2-30 /1	$\ln(M) = 1.844 + 0.104 \ln(W)$	0.39
32/2	SW-NNW	3.0-7.2 /2	$\ln(M) = 2.521 + 0.079 \ln(W)$	0.37
32/3		1.5-3.0 /3	$\ln(M) = 1.295 + 0.059 \ln(W)$	0.31
32/4	Range A	0.95-1.5 /4	$\ln(M) = 0.801 + 0.056 \ln(W)$	0.30
32/5	1-15 ms^{-1}	0.45-0.95/5	$\ln(M) = 0.043 + 0.109 \ln(W)$	0.45
32/1	North Sea	7.2-30 /1	$\ln(M) = 1.844 + 0.104 \ln(W)$	0.39
32/2	SW-NNW	3.0-7.2 /2	$\ln(M) = 2.521 + 0.079 \ln(W)$	0.37
32/3		1.5-3.0 /3	$\ln(M) = 1.295 + 0.059 \ln(W)$	0.31
32/4	Range A	0.95-1.5 /4	$\ln(M) = 0.801 + 0.056 \ln(W)$	0.30
32/5	1-15 ms^{-1}	0.45-0.95/5	$\ln(M) = 0.043 + 0.109 \ln(W)$	0.45

Table 3. Least squares curve estimates fitted to the $\ln(M)$ data of five size classes of S-SAMC $M(\mu\text{gm}^{-3})$ versus 10 m wind speed $u(\text{ms}^{-1})$ and $\ln(W)$ white-cap coverage W (fraction).

three elevations, 4.5 m, 12 m and 18.3 m, show a marked enhancement in concentration at 4.5 m elevation of the S-SAMC when the wind speed exceeds about 10ms^{-1} , and at 12 m and 18.3 m elevations when the wind speed exceeds 15ms^{-1} . The average vertical profiles of the S-SAMC were calculated using the curve fits 25, 26 and 27 (described in Table 4) and are shown for different wind speed conditions in Fig 5. The profiles illustrate that when the wind speed exceeded 10ms^{-1} the S-SAMC gradient between 4.5 m and 12 m elevations increased dramatically with increasing wind speed. At the same time the gradient of the S-SAMC between 12 m and 18.3 m appears to increase slightly with increasing wind speed.

Air-filtration unit data
North Sea, SW-NNW advection air flow

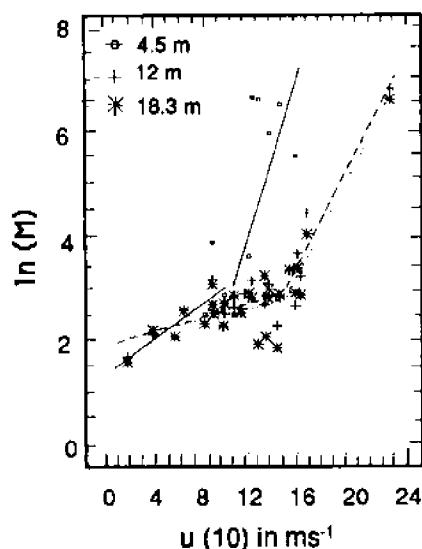


Fig. 4. Distribution of sea-salt aerosol mass concentration at three heights- 4.5 m, 12 m, 18.3 m above the mean sea level plotted as $\ln(M)$ against $u(10)$ wind speed. Curves are described in Table 4.

6. Variation of sea-salt aerosol mass concentration with whitecap coverage

Values of S-SAMC (M in $\mu\text{g m}^{-3}$), at 4.5 m, 12 m and 18.3 m height obtained almost simultaneously with whitecap coverage (W fraction) are plotted as $\ln(M)$ against $\ln(W)$ in Fig. 6. The S-SAMC data were again partitioned into low-wind-speed (range A) and high-wind-speed (range B) data. For the 4.5 m S-SAMC data the split (range A / range B) was made at 10 ms^{-1} . For the 12 m and 18.3 m S-SAMC data the split was made at 15 ms^{-1} . Curves fitted to the data from both range A and range B and for all three heights are included in Fig. 6. The results show a marked enhancement of the S-SAMC at 4.5 m elevation when whitecap cover exceeds about 5.73×10^{-4} (which corresponds to $W_A(u(10)=10 \text{ ms}^{-1})$) and at 12 m and 18.3 m elevations when W_A exceeds about 2.03×10^{-3} (which corresponds to $W_A(u(10)=15 \text{ ms}^{-1})$).

To complete the presentation of the results, the S-SAMC data obtained from the multi-stage impactor at 12 m elevation were

Curve No.	Data set	Height in m	Wind range (u in ms ⁻¹)	Curve fit	Corr. coeff.
25/A 25/B	North Sea SW-NNW	4.5	1-10 10-16	ln(M)=1.2512+0.1793 u ln(M)=-5.3887+0.7917 u	0.76 0.76
26/A 26/B	North Sea SW-NNW	12	1-15 15-24	ln(M)=1.8540+0.0729 u ln(M)=-3.7904+0.4573 u	0.59 0.95
27/A 27/B	North Sea SW-NNW	18.3	1-15 15-24	ln(M)=1.9355+0.0591 u ln(M)=-3.6587+0.4403 u	0.45 0.97
28/A 28/B	North Sea SW-NNW	4.5	1-10 10-16	ln(M)=3.00+0.048 ln(W) ln(M)=9.39+0.852 ln(W)	0.21 0.39
29/A 29/B	North Sea SW-NNW	12	1-15 15-24	ln(M)=3.24+0.078 ln(W) ln(M)=9.81+1.218 ln(W)	0.40 0.88
30/A 30/B	North Sea SW-NNW	18.3	1-15 15-24	ln(M)=3.680+0.139 ln(W) ln(M)=9.27+1.2314 ln(W)	0.66 0.95

Table 4. Least squares curve estimates fitted to the ln(M) data of five size classes of S-SAMC M(μgm^{-3}) versus 10 m wind speed u(ms⁻¹) and ln(W) white-cap coverage W (fraction).

obtained from the multi-stage impactor at 12 m elevation were plotted as ln(M) versus ln(W) in Fig. 7. The results, described by the ten least squares linear curve fits show that S-SAMC within the measured size ranges of 0.49-30 μm (stages 1, 2, 3, 4 and 5) undergoes a marked enhancement when W_A exceeds a value of 2.03×10^{-3} (which corresponds as above to $W_A(u(10)=15 \text{ ms}^{-1})$).

7. Conclusion

The sea-salt aerosol mass concentrations over the North Sea show remarkable differences that depend on whether the air is advected from the English Channel, from the SW-NNW sector, from the NNW-N sector, from coastal zone, or from land. This indicates that S-SA over the North Sea is of a mixed type, originating from both Atlantic and locally emitting sources. The sea-salt aerosol associated with air advected from the NNW-N sector, as

BUBBLE-MEDIATED SEA-AIR EXCHANGE

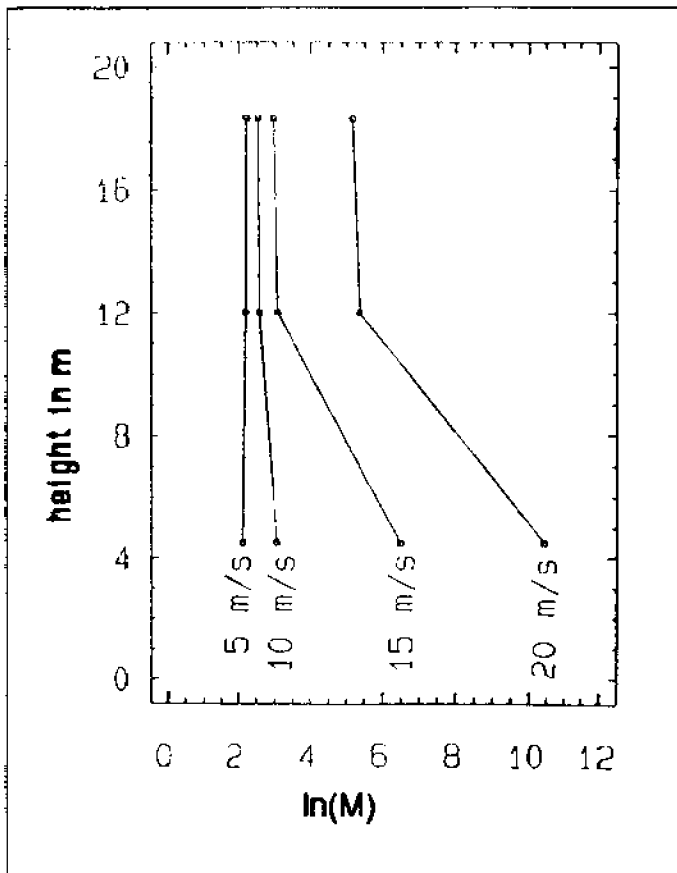


Fig. 5. Comparison of vertical profiles of sea-salt aerosol mass concentration for different wind speeds.

aerosol associated with air advected from the NNW-N sector, as well as from the English Channel, were found to have a considerably high mass concentration than that associated with air masses advected from other sectors. In both of these high concentration cases the wind fetch over the sea was not limited by contact with land. This supports the proposition that fetch is one of the parameters influencing the aerosol emission from the sea surface and the aerosol loading of a given air mass. A marked enhancement of the S-SAMC was observed at 4.5 m elevation when the wind speed $u(10)$ exceeded 10 ms^{-1} and at 12 m and 18.3 m elevations when the wind speed was greater than 15 ms^{-1} . In addition, the vertical gradients of S-SAMC between 4.5 m, 12 m and 18.3 m were small under conditions of light to moderate winds (i.e. $u(10)$ less than 10 ms^{-1}). When the wind speed exceeded 10 ms^{-1} the vertical gradient of the S-SAMC between 4.5 m and 12 m elevation increased dramatically with increasing wind speed. This could be interpreted as a reflection of the increasingly important contribution to the atmospheric salt budget of spume drops, (see also Monahan *et al.*,

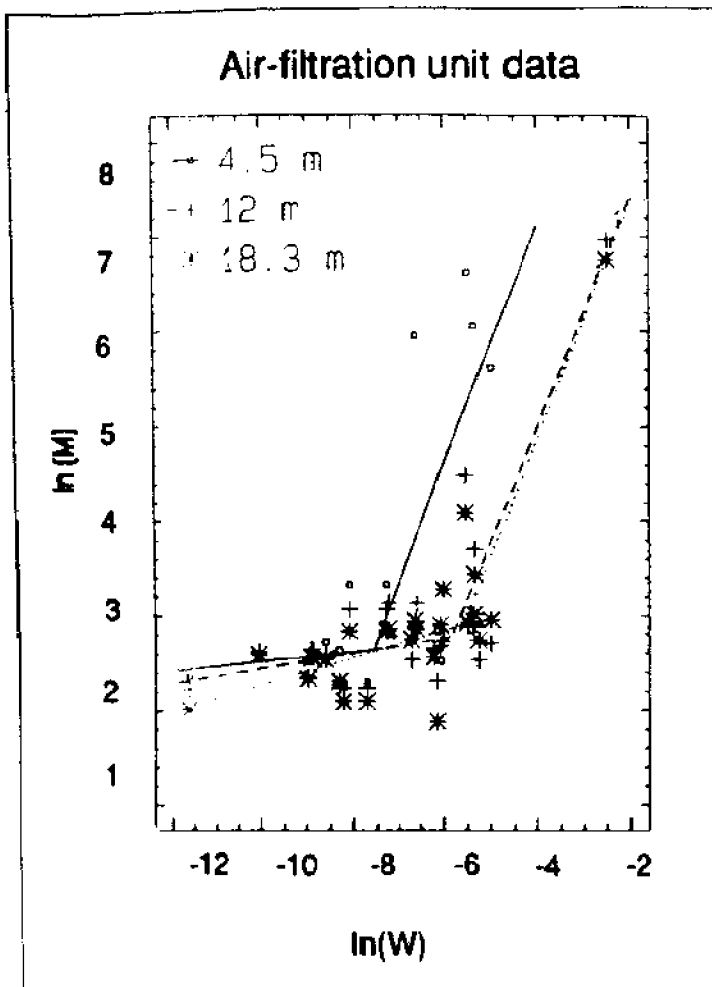


Fig. 6. Distribution of sea-salt aerosol mass concentration at 4.5 m, 12 m and 18.3 m elevations plotted as $\ln(M)$ versus whitecap fraction as $\ln(W)$. Curve fits are described in Table 4.

1983). At the same time the magnitude of the S-SAMC gradient between 12 m and 18.3 m showed only a slight tendency to increase with increasing wind speed. Analysis of the five size classes of the S-SAMC showed a gradual widening of the aerosol size spectrum towards bigger sizes of particles when the wind speed increased. The S-SAMC of particles larger than about $1 \mu\text{m}$ were found to be sensitive to both wind speed and whitecap coverage. Furthermore, the correlation coefficients between the S-SAMC and both $u(10)$ and W_A increase with increasing wind speed (see Table 5). Sea-salt particles within the size range $0.49\text{-}0.95 \mu\text{m}$ seem to be mostly advected from afar, but their mass concentration was also found to increase with whitecap coverage and wind speed, especially under high-wind-speed conditions.

The fractional whitecap coverage was found to be directly correlated to the S-SAMC. This is more evident when whitecap

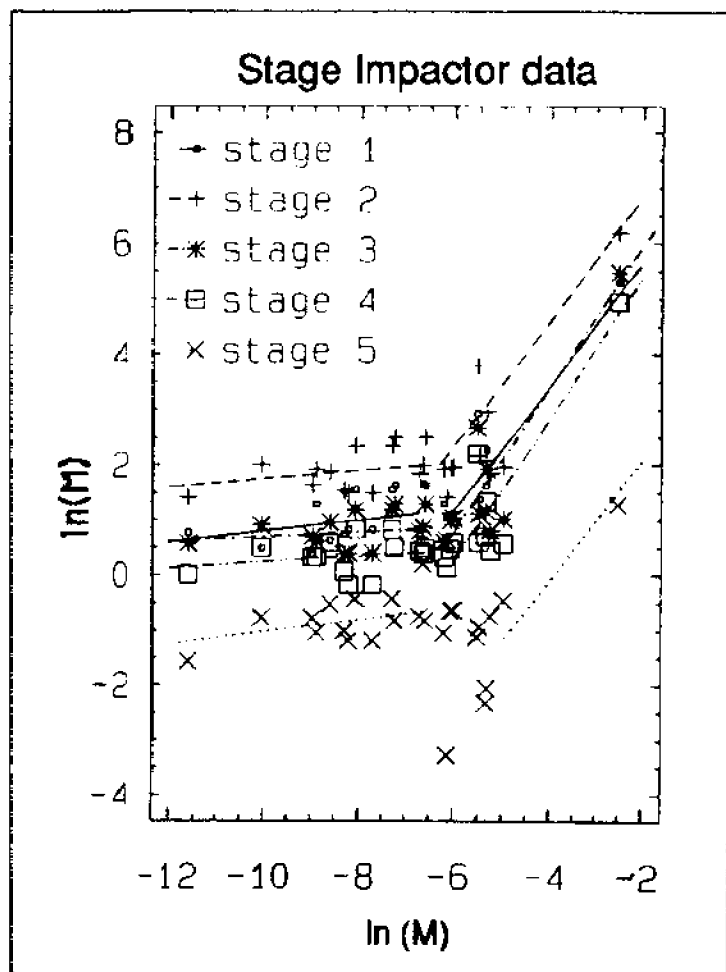


Fig. 7. Five size classes of sea-salt aerosol mass concentration plotted as $\ln(M)$ versus whitecap coverage as $\ln(W)$. Curve fits are described in Table 3.

coverage fraction exceeds a value of 5.73×10^{-4} for the S-SAMC data measured at 4.5 m elevation and when W_A exceeds about 2.03×10^{-3} for the S-SAMC data measured at 12 m and 18.3 m elevations. Within the high-wind-speed range, correlation coefficients between S-SAMC and W_A were found to be even better than between S-SAMC and $u(10)$, (see $M(W_A)$ and $M(u(10))$ fits in Table 5). In essence, this result is consistent with the recently published work by Monahan, (1988), which suggested that whitecap coverage should be more directly related to bubble injection rate and sea surface aerosol flux than to either $u(10)$ or wind friction velocity.

The results outlined herein are part of the HEXMAX Experiment and will be subject to further analysis.

Size cut-off points in μm / Height	Wind speed $u(10)$ range in ms^{-1}	Correlation coefficients			
		Exp. fit $M(u(10))$	Exp. fit $M(W)$	Lin. fit $M(u(10))$	Lin. fit $M(W)$
7.2-30 12 m	1-15 15-24	0.69 0.94	0.07 0.88	0.78 0.96	0.02 0.99
3.0-7.2 12 m	1-15 15-24	0.56 0.95	0.12 0.84	0.67 0.96	0.05 0.99
1.5-3.0 12 m	1-15 15-24	0.46 0.96	0.17 0.92	0.60 0.96	0.12 0.99
0.95-1.5 12 m	1-15 15-24	0.43 0.97	0.21 0.92	0.39 0.96	0.15 0.99
0.49-0.95 12 m	1-15 15-24	0.16 0.71	0.20 0.78	0.32 0.95	0.14 0.99
Total mass 4.5 m	1-10 10-16	0.69 0.66	0.04 0.42	0.54 0.59	0.01 0.35
Total mass 12 m	1-10 15-24	0.65 0.95	0.13 0.89	0.72 0.96	0.07 0.99
Total mass 18.3 m	1-15 15-24	0.59 0.96	0.48 0.91	0.74 0.96	0.47 0.99

Table 5. List of the correlation coefficients of exponential and linear least squares estimates fitted to the sea-salt aerosol mass concentration (M) data of five size classes and vertical profiles, versus $u(10)$ wind speed and whitecap coverage (W) data.

Acknowledgments

The research on sea-salt aerosol was supported by the GKSS Research Centre (Federal Republic of Germany). We especially thank Professor H. Grassl and Dr. B. Schneider for their support and assistance in carrying out the aerosol measurements and analysis.

The whitecap investigation at the Marine Sciences Institute, University of Connecticut, is supported by the U.S. Office of Naval Research via contract N00014-87-K-0185. We would like to thank Professor G.R. Rumney for beneficial comments and Miss M. A. Archer who typed this paper.

References

- Blanchard, D. C. 1963: The electrification of the atmosphere by particles from bubbles in the sea. *Progress in Oceanogr.* **1**, 71-202.
- Blanchard, D. C., and Woodcock, A. H., 1980: The production concentration and vertical distribution of the sea-salt aerosol. *Ann. N. Y. Ac. Sci.*, 330-347.
- Blanchard, D. C., and Woodcock, A. H., and Cipriano, R. J., 1984: The vertical distribution of the concentration of sea-salt in the marine atmosphere near Hawaii. *Tellus*, **36 B.**, 118-123.
- Chaen, M., 1973: Studies on the production of sea-salt particles on the sea surface. *Mem. Fac. Fish.*, Kagoshima Univ. **22.**, 49-107.
- de Leeuw, G., 1986: Vertical profiles of giant particles close above the sea surface. *Tellus*, **38B**, 51-61.
- Exton, H.J., and Latham, J., and Park, P.M., and Smith, M.H., and Allan, R.R., 1983: The production and dispersal of marine aerosol. *Oceanic whitecaps*, E.C. Monahan and G. Mac Niocaill (eds.), 175-193.
- Garbalewski, C., 1980: *Dynamika morskich ukladow rozproszonych*. Inst. of Oceanology, Polish Academy of Sci.
- Koga, M., and Toba, Y., 1981: Droplet distribution and dispersion processes on breaking wind waves. *Sci. Rep. Tohoku Univ., s. 5, (Tohoku Geophys. J.)* **28**, 1-25.
- Koga, M., 1984: Dispersal of droplets over breaking wind waves under the direct action of wind. *J. Oceanogr. Soc. Japan*, **40**, 29-38.
- Lovett, R.F., 1987: Quantitative measurement of airborne sea-salt in the North Atlantic. *Tellus*, **30**, 350-364.
- Marks, R., 1987: Marine aerosols and whitecaps in the North Atlantic and Greenland sea regions. *Dt. hydrogr. Z.* **40**, 71-79.
- Monahan, E. C., Fairall, C. W., Davidson, K. L., Boyle, P. J., 1983: Observed inter-relations between 10 m winds, ocean whitecaps and marine aerosols. *Quart. J. Roy. Meteor. Soc.*, **109**, 379-392.
- Monahan, E. C., 1988: Whitecap coverage as a remotely monitorable indication of the rate of bubble injection into the oceanic mixed layer. *Sea Surface Sound*, B. R. Kerman (ed.), Kluwer Academic Publisher, Dordrecht, 85-96.
- Preobrazhenskii, L. Yu., 1973: Estimate of the content of the spray-drops in the near-water layer of the atmosphere. *Fluid. Mech. Soviet Res.*, **2**, 95-100.
- Stramska, M., 1987: Vertical profiles of sea-salt aerosol in the atmosphere surface layer: a numerical model. *Acta Geophys. Pol.*, **35**, 87-100.
- Woodcock, A. H., 1953: Salt nuclei in marine air as a function of altitude and wind force. *J. Met.* **10**, 362-371.
- Wu, J., 1979: Spray in the atmospheric surface layer: review and analysis of laboratory and oceanic results. *J. Geophys. Res.* **84**, 1693-1704.

Enhancement of Sea-to-Air Moisture Flux by Spray-Droplets Associated with Breaking Waves and Bubble Entrainment: Emulations in IMST Wind-Wave Tunnel.

Patrice G. Mestayer

Institut de Mécanique Statistique de la Turbulence
Unité Mixte C.N.R.S.- Université D'Aix-Marseille II
12, Avenue du Général Leclerc, 13003 Marseille, France

Abstract

Deep-ocean wave breaking and the transformations that it provokes in ocean upper layers, surface micro-layer and atmospheric surface layer represent such a complex ensemble of interrelated phenomena that the laboratory experimental approach to their study is neither simple nor even universally recognized. Nevertheless, the large Air-Sea Interaction Simulation Tunnel at IMST appears to be the key facility for a series of fundamental studies of the processes involved in breaking waves, air-bubble entrainment and spray-droplet generation and the subsequent enhancements of sea-to-air fluxes of gases, moisture and aerosols. The experimental approach delineated by these studies is illustrated by the presentation of the program focused on the generation, transport and evaporation of bubble-mediated spray-droplets in turbulent fields.

I. Introduction

Deep-ocean-breaking waves induce such a large number of associated phenomena that their presence can be considered as

defining a fully different domain of study of the air-sea interactions: most of the relationships that describe the surface transfers in calmer sea states are no longer, or not fully, valid. The dynamics of the wave breaking have a direct influence on the generation of currents and turbulence in the water body, hence on all phenomena depending on the mixing of oceanic upper layers. The surface geometry and its disruption probably have some influence on the dynamics of the atmospheric surface layer and on surface wind stress. Moreover, breaking waves disrupt the chemical and organic surface films; they produce and they entrain air bubbles in the water body. Due to their entrainment under the surface, their physico-chemical exchanges with water at various depths, and their bursting at the surface, these bubbles are responsible for sea-to-air exchanges of gases, moisture and dry nuclei that cannot be described by the same relationships as the surface transfers.

The interconnections of phenomena of very different natures, e.g. the strong influence of the water and surface-film chemistry on gas and moisture exchanges, increase the complexity of sea-to-air exchanges by about one order of magnitude. The scarcity of reliable observations in the open sea, in addition to the large number of variables known to be strongly interconnected makes it dangerous to deduce relationships from mere statistics.

On the other hand, it has often been claimed that this large number of interconnected variables makes it useless to study any part of the phenomena in isolation in the laboratory. This point of view is based on the idea that the results from incomplete simulations are statistically nearly never representative of the "real world" or that their representativeness is, at best, poorly known. Nevertheless, it is true that in the laboratory the purely statistical approach is quite handy but of little use when the laws of similarity with "real world" phenomena are either unknown or inconsistent.

-oOo-

The most usual approach in tunnel simulations can be called the "scale model." The processes under scrutiny can be described by relationships that can be written in a dimensionless form by means of a limited number of independent scaling parameters, that

then depend on a small number of dimensionless variables, the similarity parameters. The laboratory simulation then consists of (i) determining the ranges of values of the similarity parameters that can be explored in the facility, (ii) determining the values of the dimensionless functions in those ranges by means of a statistically representative number of measurements, using either or both of the two basic properties of laboratory facilities: stationary and/or ergodicity. In this context, the quality and quantity of results are determined only by sensor capabilities and hourly costs.

Most laboratory facilities are designed to scan a range of values of only one similarity parameter, occasionally two in combination, but very rarely more than two. The large air-sea interaction simulation facility at IMST Luminy Laboratory has the capability of scanning quite independently a handful of similarity parameters; among which are Reynolds numbers of the macroscopic flow, e.g. fetch Reynolds numbers $Re_x = U X/\nu$ and roughness Reynolds number $Re_z = u_z z/\nu$, and of the turbulence micro-structure, e.g. turbulence Reynolds number $R_\lambda = u' \lambda/\nu$ based on velocity fluctuation rms u' and Taylor microscale λ ; Richardson number or stability parameter z/L based on Monin-Obukhov length L ; Nusselt and Sherwood number (dimensionless surface fluxes of heat and vapor); wave age c/U , Froude number $(g H_{1/3}/U^2)^{-1}$ and dimensionless fetch gX/U^2 . Coantic, *et al.*, (1981) have demonstrated that the extended capability of this unique facility was the key to the extension and quasi-continuity of the simulations that had been realized by that time. The results that they reported ranged from atmospheric surface layer and wavefield dynamic structures to the surface transfers of mechanical energy, momentum, sensible heat, vapor and gases.

When studying the breaking wave dynamics and moreover the phenomena associated with, or generated by, breaking waves, the "scale model" approach does not work anymore due to the incompatibility of the various similarity parameters. Then what? Should we completely dispense with laboratory study? As we do not know enough to design numerical models of these phenomena that are altogether complete, realistic and tractable, without including too many useless calculations, must we rely only on the merely

statistical approach, with the danger of artificially correlating uncorrelated observations?

There are still two approaches to laboratory studies, that can be called "partial simulations" and "process studies". Very close in experimental practice, they differ mainly from an epistemological point of view and this makes them produce very different results. They both realize laboratory experiments that do not respect all similarities. With the concept of "partial simulation" in mind, the experimenter is aware that his laboratory experiment is not really a simulation, but he considers his results to be nevertheless pertinent for the real phenomena. Of course, this concept is both fruitful and dangerous: fruitful because it can bring new insights by rapidly producing new results; dangerous because it can produce results that are actually fully foreign to the problem. This is why this approach always brings endless discussions about the validity and the utility of the results. In fact, many people claim that all laboratory simulations are in essence only partial simulations: this generalization leads the pessimistic ones to consider therefore that all laboratory simulations are useless, and the optimistic ones that any partial simulation can be useful. Of course, we shall follow neither of those; but let us only note that the concept of partial simulation cannot be driven too far without hazards, especially that of passing over a critical value of one of the similarity parameters.

The last approach to laboratory experiments proceeds from a different point of view. In a "process study" the experimental work is usually not the central one, although it can be essential. The major effort of the study consists in defining the means to isolate a given process in order to build a theoretical or, more often nowadays, numerical model able to simulate it properly. The construction of the model of course implies the design of simplifying hypotheses. Most of those can be drawn from previous works but some can be tested by building up specific experiments. In this approach it is not by chance that the experiments look artificial; it is just that they *are* artificial. Actually they can have very little in common with the appearance of the process in the real world: they only pertain to the world of the model and the results of the measurements to the qualitative or quantitative hypotheses of the model.

But, of course, very often the phenomena in the laboratory experiments do look somewhat like some phenomena of the real world. In that case, as we must give up the concept of "simulation," we should probably develop the concept of "emulation." Indeed the laboratory experiment is much more than a simple imitation: quite often it can be "better" than the original because it is purer, it is isolated from its untractable envelope of associated phenomena.

This approach is not new. Most often the emulations realized in the context of a process study take place in ad hoc facilities built on purpose with modest sizes and life expectation. In the domain that is under examination here we should note two interesting process studies associated with emulations: Melville's (1982) study of the instabilities leading deep-water waves to breaking, and Beard and Pruppacher's (1971) study of the evaporation of small water drops falling in air.

The "process study" concept can be extended to the cases when the model is not pre-existent to the emulation but the emulation is built for the purpose of providing model foundations, and not for an abortive partial simulation.

-o0o-

The IMST large wind-wave flume has been built to simulate the ocean-air surface processes, and Coantic *et al.* (1981) showed that it has largely fulfilled its mission. It is certainly not able to produce a complete simulation of deep-water wave breaking because this phenomenon implies not only surface processes but also underwater and above-surface interacting processes. Nevertheless it presents such capabilities that it appeared these last years as the key to a rather complete series of process studies ranging from high steepness wave instabilities to spray-droplet evaporation. The noteworthy advantage is that all associated emulations were realized in the same facility. Let's hope that connections can be realized between these various process studies.

First, we would like to briefly describe this series of independent studies. Then we shall describe the spray-droplet emulation program and see how it can contribute to determining the enhancement of sea-to-air moisture flux.

2. Wave breaking emulations and process studies at IMST

Most of the research programs related to breaking waves are not finished yet. Therefore, it is not yet time to draw conclusions from these efforts, nor the time to synthesize them. Nevertheless, it is interesting to see how the capabilities of the facility helped start these process studies.

1. The non-linear wave dynamics have long since been studied at IMST by developing in parallel the theoretical and experimental approaches (e.g. Ramamonjiarisoa *et al.*, 1978; Ramamonjiarisoa and Mollo-Christensen, 1979). The more recent efforts are characterized by the development of performative numerical algorithms to compute wave characteristics. In particular this numerical development allows the computation of the three and two dimensional superharmonic instabilities of deep water gravity waves leading to the wave breakings (Kharif and Roux, 1984; Kharif, 1987; Kharif and Ramamonjiarisoa, 1988). Interestingly, as very steep wave instabilities cannot yet be properly obtained and measured in the wave flume, the validity of the numerical technique has been assessed by the experimental emulation of a different process, the apparition of some superharmonic three dimensional instabilities on moderately steep waves (Viguiet, 1985).

2. Inside the same theoretical frame, a program to investigate the geometrical and kinetic characteristics of emulated two-dimensional gravity waves is being developed. This program is based on a semi-lagrangian visualization system: a lighting device able to illuminate a 10 mm-thick longitudinal slice of a wave profile about one wavelength long, and a 16 mm movie camera taking 500 frames-per-second are fixed on a carriage moving along the tunnel at about the wave celerity. The digital analysis of the profiles allows following the transformations of the wave geometrical characteristics just before and during the breaking, e.g. their local steepness (Bonmarin and Ramamonjiarisoa, 1985). This study is currently being extended in two directions: (i) calculations of the energy exchange during the breaking; (ii) determination of the air

mass entrained during wave breaking and its kinematic further behavior (Bonmarin, 1986).

3. Air entrainment is considered to be the process associated with wave breaking that has consequences more difficult to predict. This is especially important for the studies of heat, vapor and gas exchanges between sea and atmosphere. In at least two simulation programs, the limits of the simulations have been clearly hit from the outset of breaking waves. The vapor transfer study of Resch and Selva (1977, 1979) is a most typical and successful simulation study. One of their most interesting results is their determination of the relationships between the Sherwood number, representing the vapor surface flux, the fetch Reynolds number $Re_x = U_{\infty} X / \nu$ and a bulk Richardson number Ri_g characterizing the density stratification. Their large set of fine statistics yields $Sh = 0.0073 Re_x^{0.9} (1 - 17 Ri_g)$. But, as soon as they observed breaking waves, their data abruptly deviated from this relationship and indicated an acceleration of the vapor flux at least as strong as $Sh \propto Re^2$ (Resch and Selva, 1977). This is a brutal change of dependency, obviously more brutal than the changes observed over the sea (Friehe and Schmitt, 1976; Francey and Garrat, 1978), an obvious sign of similarity termination.

Let us nevertheless note here that Coupiac (1979) managed to extend the similarity. To take into account some of the effects of the wave-wind coupling, he considered the dependency of vapor flux on the wave age cU_{∞} and steepness H/λ . His study yields:

$$Sh = 0.004 Re_x^{.92} (1 - Ri_g) (c / U_{\infty})^{-.147} \quad (1)$$

with no definite influence of wave steepness. But of course, the validity range of this similarity law does not encompass the breaking wave outset.

4. In a gas exchange simulation study, Merlivat and Memery (1983) also abruptly met a similarity limit. They were measuring the dependency of nitrous oxide and argon transfer velocities on wind speed or friction velocity, and wave age. The transfer

velocity k_L is a normalized surface flux defined by:

$$k_L = FS^{-1}(c_a - c_w)^{-1} \quad (2)$$

where F is the gas flux through the area S and c_a and c_w are the gas concentrations in air just above surface and in the water just under surface, respectively. For $U < 9 \text{ ms}^{-1}$, they observe clear linear variation of k_L with wind speed for both gases. But for higher wind speeds ($U > 9 \text{ ms}^{-1}$) they put in evidence a sudden jump of the values of k_L up to a factor of 3, due to the outset of breaking waves and the entrainment of air bubbles through which extra gas transfer takes place.

Memery and Merlivat's (1983) work represents a typical example of the "process study" approach. Facing this similarity limit, they gave up the similarity concept sustaining relation (2), to design a model of the bubble contribution to the flux itself. Provided relatively crude assumptions on the bubble dynamics in the sub-wave turbulent field, the bubble generation process and the bubble spectral distribution, this model focuses on the water-bubble gas transfer and the bubble transport to the surface. It emphasizes the important role of gas solubility and the difference of the role of concentration gradient in wave-wind tunnel and at the ocean-atmosphere surface. Finally it introduces the effect of surfactants. The tunnel data, that were obviously dangerous to directly "export" to the ocean conditions, provide a good test bed for the model that is shown to be in good agreement with the rare observations made at sea.

5. Various attempts to describe the near-surface bubble population by general similarity laws have been recently summarized by Wu (1988): the bubble concentration would vary proportionally to the exponential of depth z and to wind speed at power 3.5, its spectral distribution being universally proportional to r^{-4} for radii r larger than $50 \mu\text{m}$. Unfortunately these relationships do not appear to be clearly supported by physical bases but result essentially from statistical combinations of experimental data. Moreover the experimental observations are not numerous, their results are quite scattered and they differ in nature, e.g. measurements of global

concentrations, of bubble spectra, of acoustic scattering cross section, so that they take a common statistical significance only inside the author's reducing and a-priori "model". The handiness of such relationships should not mask the fact that although they look like similarity laws, they are not.

To explore the mechanisms of generation and dispersion of the bubbles and their significance for predicting bubble populations close under and at the surface, Baldy (1987, 1988) and Baldy and Bourguel (1985, 1987) adopted a "process study" approach in adequacy with IMST tunnel emulation capabilities. In a first stage Baldy and Bourguel (1985) developed a technique to estimate several local statistical characteristics of bubbles produced by breaking waves in the tank, such as concentration probability functions, crossing frequencies, arrival time intervals and speed distributions. This technique is based on the adaptation of a laser-based single-particle probe previously studied by Avellan and Resch (1982) to the flume experimental conditions of sampling time, bubble density and probe position. But an important part of the technique stands in the original software that they specially designed for IMST Luminy Laboratory numerical system to acquire and process on-line the probe peculiar signal, in order to record the only data necessary to estimate the upper-mentioned statistical characteristics. In particular this real-time software accounts for the laser beam light nonuniformity, oblique crossing and multiple reflexion problems.

In a second stage Baldy and Bourguel (1985 and 1987) fully documented a small number of breaking wave conditions, at all depths from the deepest bubble observation to the surface, with even measurements between wave troughs and crests. The high statistical significance of the data thus obtained allowed Baldy (1988) to ascertain the relative importance of the two main mechanisms, production and dispersion, in two different depth zones.

Because the statistical characteristics obtained by the measurements are in principle exactly representative only of the documented flume breaking-waves, the last stage consists of incorporating understanding of the mechanism so deduced into a general model of the generation-dispersion process, and to test it

with tunnel and ocean data (Baldy, 1987).

6. It has already been shown elsewhere that the direct tunnel simulation of spray-droplet production by breaking waves is at best misleading because it involves several similarities that cannot be verified simultaneously in a laboratory facility (Monahan *et al.*, 1982). This is even more true if we do not consider the droplet generation at the surface itself but above the waves, in connection with their potential production of water vapor on the one hand and aerosols on the other hand (Mestayer and Lefauconnier, 1988). Yet, it appears possible to short-circuit most of the phenomena in order to study only the mechanisms of interaction between the spray-droplets and their turbulent environment, that are finally responsible for the production of vapor and aerosols. Companion to the larger cooperative program HEXOS that primarily relied on the statistical approach of in-situ measurements, HEXIST is a process study program based on simultaneous efforts in model development and emulation documenting, in IMST large flume and other facilities like the whitecap simulation tank of the Marine Sciences Institute, at the University of Connecticut.

3. The HEXIST Program

HEXOS (Humidity Exchange Over the Sea) is a large cooperative program of research on sea-atmosphere exchanges of momentum, heat, vapor and aerosols during gale and storm winds (Katsaros *et al.*, 1987). As a companion program, HEXIST (HEXOS Experiments In Simulation Tunnel) focuses on small-scale processes that are both inherent to these conditions of the marine atmospheric surface layer and difficult to study in isolation in-situ. The central point of interest is the evaporation of spray-droplets during their transport by turbulence in the turbulent fields of temperature and water vapor concentration of the atmospheric surface layer.

The program has been built to take advantage of both emulation capabilities of IMST large flume and of ongoing studies by participants. This is why we basically set aside in this program such processes as large droplet "chopping" by higher winds

(Monahan *et al.*, 1983), the behavior of isolated bubbles and bubbles in plumes (see previous section and Monahan's review in this issue), the dynamics of air in the zone between wave troughs and crests (Baldy, 1977; Davidson and Frank, 1973) and their relationships with aerosol concentrations very close to the surface (de Leeuw, 1986 & 1987), the entrainment of dry aerosols above the marine surface layer (Fairall *et al.*, 1983 and 1984; Fairall and Larsen, 1983).

In its present state, the HEXIST program deals mainly with the following processes:

1. the production of bubble mediated spray-droplets,
2. the transport of spray-droplets by turbulence,
3. the evaporation of droplets in a turbulent field of water vapor concentration,
4. the flux of water vapor in the presence of spray-droplets,
5. the structure of the turbulent fields in the presence of evaporating droplets.

HEXIST originated in 1982 when the members of the HEXOS Dissipation Group decided to try to separate the effects of droplets, sea state and wind speed on the flux estimates, in the controlled environment of IMST tunnel. We stumbled at first over the obvious impossibility of realizing an exact simulation, and it was not until 1984 that the concept of the parallel development of numerical models and artificial tunnel emulations really took shape.

In November 1984, we realized a first series of measurements of the vertical profiles of \bar{U} , \bar{T} , \bar{q} in the presence of breaking waves produced by the combined actions of the hydraulic wave generator and high winds. These measurements demonstrated that the effects of droplet evaporation were measurable and could even be large (Lefauconnier, 1985).

In December 1984, the first HEXIST Planning Meeting, held at the Naval Postgraduate School (Monterey, California), established the connection with the cooperative work made in the tank in Galway (Monahan *et al.*, 1982), the study of the generation of droplets by a simulated whitecap and the decay of the droplet spectrum for zero-wind conditions. We then decided to

concentrate our efforts on the droplet evaporation process and to set aside the important problem of the influence of the wavy mobile surface. In the tunnel we should produce sprays by artificial bubbling devices and dispense with generating breaking waves.

In 1985, three campaigns of measurements took place in March (HEXIST O), June (HEXIST 1) and July (HEXIST 2).

In these experiments, the droplets were produced by a simulated whitecap. This whitecap was generated by a "spray bubbler" consisting of an array of porous ceramic elements similar to those found in aquariums. The spray bubbler produced a continuous and reproducible whitecap of approximately one square meter corresponding to an upwind whitecap fraction of roughly 2% (the equivalent of a 13 ms^{-1} oceanic wind speed). Droplets were then measured at several different fetches downwind of the whitecap under various conditions in order to study the effects of wind speed and humidity on the above processes.

The feasibility campaign of measurements HEXIST O allowed determination of the experimental procedures. It furnished basic data about the background dust spectra, the spray-droplet production by the spray bubbler, compared to that of the breaking waves, and the bulk effects of the turbulent transport and evaporation of these droplets (Mestayer and Lefauconnier, 1988).

The informal HEXIST meeting number 2 was held at IMST at the end of HEXIST O (March 1985). We then drew technical conclusions from the feasibility experiments, refined HEXIST 1 and 2 planning, and cast the bases of our numerical models.

The extensive cooperative experimental documentation of the impact of the local source of droplets was realized in two successive campaigns in June-July 1985. During HEXIST 1, about 300 size-concentration droplet spectra were obtained with the CSAS ($1.5 \mu\text{m}$ to $12 \mu\text{m}$ radii) and OAP (6 to $150 \mu\text{m}$) spectrometers, with winds ranging from 0 to 13 ms^{-1} , relative humidities from 98 to 55 %, distances from the droplet source to the probes from 0 to 9 m . During HEXIST 2, 9 conditions were repeated for measurements of the vertical profiles of U , T , q means and turbulence statistics (Fairall *et al.*, 1986; Mestayer *et al.*, 1988.a).

In 1985-86 the PSU group started the development of a random

walk Lagrangian model to describe the turbulent advection of evaporating droplets from a local source in connection with HEXIST 1 data (Edson, 1987). The IMST group reduced the turbulence data from HEXIST 2 and worked out the bases of a droplet "spectral" model in homogeneous turbulent flow (Mestayer and Lefauconnier, 1988).

A workshop on measurements and modeling the sea spray and its effects on scalar fields and fluxes was held at Pennsylvania State University on April 28-29, 1986, to review the experimental "certainties" and the existing relevant numerical models.

Foreseen in 1985, the second part of the HEXIST program was decided and planned during this workshop. This decision resulted from the following conclusions:

- On the one hand, HEXIST 0 demonstrated that a field of breaking waves, spread over several tens meters, noticeably transforms the vertical profiles of ρ_v and T (Mestayer and Lefauconnier, 1988).
- But HEXIST 2 demonstrated that our turbulence probes were not able to quantify the transformation of the turbulent fields due to the evaporation of droplets generated by a 1-m² spray bubbler local source.
- On the other hand, HEXIST 1 and the Lagrangian model demonstrated that the whitecap simulation by means of the spray-bubblers was a convenient technique to evaluate the droplet behavior (Edson, 1987).
- But the construction of an Eulerian model describing the humidity field-evaporating droplets interactions, necessary to evaluate the transformations of the turbulent scalar fields and the final vapor flux, is too complex in HEXIST the 1-2 geometry: a .8-m wide plume inside a .75-m high, 2-m wide boundary layer.

We therefore decided to i) increase the number of droplets and the air-droplet interaction domain, ii) realize a flow geometry for which the air dynamics can easily be described in a first order numerical model, iii) keep the independency of the transfer processes of heat, vapor and spray droplets. We choose the geometry of a fully-developed boundary-layer of spray droplets matching the boundary-layer of temperature and vapor concentration over the

water surface (Mestayer *et al.*, 1988.b). In the tunnel, the homogeneous transfer of droplets at the surface is realized by immersing a 30-m long spray bubbler net.

This configuration is currently studied by means of the CLUSE Eulerian "spectral" model in development at IMST (Rouault *et al.*, 1988) and the PSU Lagrangian model, extended to describe the behavior of the droplets generated by an homogeneous surface source.

A full experimental documentation of this configuration has been realized during a 6-week cooperative experiment that gathered together all participants in the program. This documentation includes droplet concentrations with several types of spectrometers, mean profiles of U , T , q , and u' , w' , θ' , ρ'_v spectra, structure functions and fluxes. In addition, we measured some bubble spectra, water chemicals and surfactants effects on the bubble production, and variations of droplet production with water temperature. We also realized one test of the wave-rotor model (de Leeuw, 1988) over periodic waves produced by the hydraulic wave generator.

Furthermore, short independent experiments, PETIT CLUSE 1 to 4, are devoted to improve the determination of the statistical relationships between the spectrum of the generated droplets and the spectrum of the parent bubbles. These experiments took place in 1988 and 1989 in IMST-Luminy 2-m³ glass aquarium and in the whitecap simulation tank of the Marine Sciences Institute of the University of Connecticut.

4. First results on water vapor flux enhancement

In a program coupling tunnel emulations and numerical models, the final results are produced only by the end of the program. Nevertheless we can mention a few global calculations obtained during the HEXIST studies.

Mestayer and Lefauconnier (1988) estimated the total amount of water vapor released by droplet evaporation, by integrating the measured droplet volume concentration spectra over all radii. These integrations give estimations of the total concentration of

liquid water M_e present in the air. Their data indicate for instance that, at $U = 3 \text{ ms}^{-1}$, at a distance D of 5m from the droplet source, these total liquid water concentrations were $M_e = 3.5 \cdot 10^{-6} \text{ kgm}^{-3}$ at a relative humidity of 95% and respectively $2.1 \cdot 10^{-6} \text{ kgm}^{-3}$ at 85% and $1.05 \cdot 10^{-6} \text{ kgm}^{-3}$ at 50%. From these numbers, global evaporation rates \dot{M}_v can be estimated by means of relation:

$$\dot{M}_v = \partial M_v / \partial t = -\partial M_e / \partial t = -\Delta M_e / \Delta t \quad (3)$$

or
$$\dot{M}_v(\text{RH}\%) = [M_e(95\%) - M_e(\text{RH}\%)] / [D / U_d] \quad (4)$$

By taking $U_d = 0.75 U$, they obtained $\dot{M}_v(85\%) = 0.74 \cdot 10^{-6} \text{ kgm}^{-3}\text{s}^{-1}$ and $\dot{M}_v(50\%) = 1.3 \cdot 10^{-6} \text{ kgm}^{-3}\text{s}^{-1}$.

On the other hand, surface fluxes of water vapor can be obtained by the method previously used by Coantic *et al.* (1981), Resch and Selva (1979), Coupiac (1979) and others, i.e. by measuring the mean water vapor concentrations and applying the relationships described in Section II:

$$\frac{J_o X}{\rho_a D_v (q(o) - q_\infty)} = \text{Sh}(Re_x, Ri_{g,c} / U_\infty) \quad (5)$$

By this method, Mestayer and Lefauconnier (1988) estimated for $U = 7.5 \text{ ms}^{-1}$ and $\text{RH} = 55\%$ a surface flux J_o of $2.5 \cdot 10^{-6} \text{ kgm}^{-2}\text{s}^{-1}$ without the droplets and an increase of this flux by $0.3 \cdot 10^{-6} \text{ kgm}^{-2}\text{s}^{-1}$ in the presence of the droplets, i.e. a 14% increase. But they also showed that, in this case of droplets generated by a local simulated whitecap the increase in water vapor concentration is limited to the lowest 20 cm of the air boundary-layer, in accordance with the estimations of \dot{M}_v . In the case of high-wind breaking-waves spread over the first 20 meters of the tank they measured an increase of the mean water vapor concentration of the order of 0.25 gkg^{-1} up to the top of the boundary-layer. This appears to correspond to a flux increase of the order of $70 \cdot 10^{-6} \text{ kgm}^{-2}\text{s}^{-1}$ due to the droplets evaporating all along these 20 meters, while the surface flux was of the order of $3.3 \cdot 10^{-6} \text{ kgm}^{-2}\text{s}^{-1}$: a 2000% increase (due to an artificially

low surface flux)! Nevertheless, it is important to realize that this water vapor flux due to the development of spray droplet evaporation ($70 \cdot 10^{-6} \text{ kg m}^{-2}\text{s}^{-1}$) is of the same order of magnitude as typical oceanic surface fluxes, while droplet concentration spectra were also comparable to those measured over the ocean surface (Mestayer and Lefauconnier, 1988). Without making presumptions as to our final results this illustrates well the importance of the process, already confirmed by the calculations of Fairall *et al.* (1988).

Acknowledgments

This work is supported by the Centre National de la Recherche Scientifique and the National Science Foundation under the U.S. - France Cooperative Science Program. A.M. Rugiero deserves special thanks for preparing this manuscript.

References

- Avellan, F. and F. Resch, 1982: A scattering light probe for the measurement of oceanic bubble sizes. *Int. J. Multiphase Flow*, **8**, 649-663.
- Baldy, S., 1977: Etude Statistique sur les mecanismes de transferts dynamiques a travers une interface air-eau. These de Docteur-Ingenieur, Univ. Aix-Marseille II, France.
- Baldy, S., 1987: Les mecanismes de generation et de dispersion des bulles provenant du deferlement des vagues ; Observations, analyses et modele. These de Doctorat Es-Sciences, IMST, Univ. Aix-Marseille II, France.
- Baldy S., 1988: Bubbles in the close vicinity of breaking waves : statistical characteristics of the generation and dispersion mechanism. *J. Geophys. Res.*, **93**, 8239-8248.
- Baldy, S. and M. Bourguel, 1985: Measurements of bubbles in a stationary field of breaking waves by a laser-based single-particle scattering technique. *J. Geophys. Res.*, **90**, 1037-1047.
- Baldy, S. and M. Bourguel, 1987: Bubbles between the wave trough and wave crest levels. *J. Geophys. Res.*, **92**, 2919-2929.
- Beard, K.V., and H.R. Pruppacher, 1971 : A wind tunnel investigation of the rate of evaporation of small water drops falling at terminal velocity in air. *J. Atmos. Sci.*, **28**, 1455-1464.
- Bonmarin, P., 1986: Laboratory observation of the splash up and the air entrainment by the deep water plunging breaker. *Flow Visualization IV*, V. Veret, edit., Springer-Verlag, 797-802.

BUBBLE-MEDIATED SEA-AIR EXCHANGE

- Bonmarin, P. and A. Ramamonjariosa, 1985: Deformation to breaking waves of deep water gravity waves, *Experiments in Fluids*, 3, 11-16.
- Coantic, M., A. Ramamonjariosa, P. Mestayer, F. Resch and A. Favre, 1981: Wind-water tunnel simulation of small-scale ocean-atmosphere interactions. *J. Geophys. Res.*, 86, 6607-6626.
- Coupiac, C., 1979: Contribution à l'étude de l'influence des vagues sur l'évaporation. These de Docteur-Ingenieur, IMST, Univ. Aix-Marseille II, France.
- Davidson, K.L. and A.J. Frank, 1973: Wave-related fluctuations in the air-flow above natural waves. *J. Phys. Ocean.*, 3, 102-119.
- de Leeuw, G., 1986: Vertical profiles of giant particles close above the sea surface. *Tellus* 38B, 51-61.
- de Leeuw, G. 1987: Near-surface particle size distribution profiles over the North Sea. *J. Geophys. Res.*, 92, 14631-14635.
- Edson, J. B., 1987: Lagrangian model simulations of the turbulent transport and evaporation of spray droplets in a wind-wave tunnel. Unpublished M.S. Thesis, Dept. of Meteorology, Pennsylvania State University, University Park, PA 16802, U.S.A.
- Fairall, C.W. and S.E. Larsen, 1983: Dry deposition, surface production and dynamics of aerosols in the marine boundary layer. *Atmos. Envir.* 18, 69-77.
- Fairall, C.W., K.L. Davidson and G.E. Schacher, 1983. An analysis of the surface production of sea-salt aerosols. *Tellus*, 35B, 31-39.
- Fairall, C.W., K.L. Davidson and G.E. Schacher, 1984. Application of a mixed layer model to aerosols in the marine boundary layer. *Tellus*, 36b, 203-211.
- Fairall, C.W., J.B. Edson and M.A. Miller, 1988: Heat fluxes, whitecaps and sea spray. *Remote sensing in the air-sea interactions*. Plant and Goernhaert, eds. (in press).
- Fairall, C.W., S.E. Larsen, P.G. Mestayer and D.E. Spiel, 1986: Measurements of spray droplet transport and evaporation during HEXIST. Sixth A.M.S. Conference of Ocean-Atmosphere Interaction, Miami, Florida; Jan. 13-17, Bull. of American Meteorological Society.
- Francey, R.J. and J.R. Garrat, 1978: Eddy flux measurements over the ocean and related transfer coefficients. *Boundary Layer Meteorol.* 14, 153-166.
- Friehe, C.A. and K.F. Schmitt, 1976: Parameterization of air-sea interface fluxes of sensible heat and moisture by the bulk aerodynamics formulas. *J. Phys. Ocean.* 6, 801-809.
- Katsaros, K.B., S.D. Smith, and W.A. Oost, 1987: HEXOS—Humidity Exchange Over the Sea, a program for research on water-vapor and droplet fluxes from sea to air at moderate to high wind speeds. *Bull. Am. Meteorol. Soc.* 68, 466-476.
- Kharif, C., 1987: A comparison between three and two dimensional instabilities of very steep gravity waves. *J. Theoret. Appl. Mech.* 6, 843-864.
- Kharif, C. and B. Roux, 1984: Stability of steep gravity waves. *J. Theoret. Appl. Mech.* 3, 717-723.
- Kharif, C. and A. Ramamonjariosa, 1988: Deep-water gravity wave instabilities at large steepness. *Phys. Fluids* 21, 1286-1288.

- Lefauconnier, C., 1985: Influence des embruns sur le flux de vapeur d'eau à la surface de la mer, rapport de stage I.T.M., Ecole d'Ing. de la Meteorol. Nat., Toulouse, France.
- Memery, L. and L. Merlivat, 1985: Modelling of gas flux through bubbles at the air-water interface. *Tellus*, 37B, 272-285.
- Merlivat, L. and L. Memery, 1983: Gas exchange across an air-water interface: experimental results and modeling of bubble contribution to transfer. *J. Geophys. Res.* 88, 707-724.
- Melville, W.K., 1982: The instability and breaking of deep-water waves. *J. Fluid Mech.* 115, 165-185.
- Mestayer, P. and C. Lefauconnier, 1988: Spray droplet generation, transport and evaporation in wind-wave tunnel during the humidity exchange over the sea experiments in the simulation tunnel, *J. Geophys. Res.* 93, 572-586.
- Mestayer, P.G., J.B. Edson, C.W. Fairall, S.E. Larsen and D.E. Spiel, 1988a: Turbulent transport and evaporation of droplets generated at an air-water interface. *Turbulent Shear Flows* 6, Springer-Verlag, 129-147.
- Mestayer, P.G., C. Lefauconnier, M. Roualt, S.E. Larsen, C.W. Fairall, J. B. Edson, D.E. Spiel, K.L. Davidson, E. C. Monahan, D. Woolf, G. de Leeuw, H. Gucinski, K.B. Katsaros and J. DeCosmo, 1988b: HEXIST, Proceedings NATO Advanced Workshop on Humidity Exchange Over the Sea. W.A. Oost, S.D. Smith and K.B. Katsaros, eds., Tech. Rep., Dept. Atmos. Sci., Univ. of Wash., Seattle, WA.
- Monahan, E.C., K.L. Davidson and D.E. Spiel, 1983: Whitecaps aerosol productivity deduced from simulation tank measurements, *J. Geophys. Res.* 87, 8898-8904.
- Monahan, E.C., D.E. Spiel and K.L. Davidson, 1983: Model of marine aerosol generation via whitecaps and wave disruption. Ninth Conference on Aerospace and Aeronautical Meteorology, Am. Inst. of Aeraunot. and Astronaut., Omaha, Nebr.
- Ramamonjisoa, A., S. Baldy and I. Choi, 1978: Laboratory studies on wind-wave generation, amplification and evolution. *Turbulent Fluxes Through the Sea Surface, Wave Dynamics and Prediction*, Edited by A. Favre and K. Hasselmann. Plenum, New York. pp. 403-420.
- Ramamonjisoa, A. and E. Mollo-Christensen, 1979: Modulation characteristics of sea surface waves. *J. Geophys. Res.* 84, 7769-7775.
- Resch, F. and J.P. Selva, 1978: Study of momentum transfers, heat and water vapor fluxes under different stability conditions. *Turbulent Fluxes Through the Sea Surface, Wave Dynamics and Prediction*. Edited by A. Favre and K. Hasselmann. Plenum, New York. pp. 81-89.
- Resch, F. and J.P. Selva, 1979: Turbulent air-water mass transfer under varied stratification conditions. *J. Geophys. Res.*, 84, 3205-3217.
- Rouault, M., P.G. Mestayer and R. Schicstel, 1988: The CLUSE numerical model of spray droplet surface flux, transport and evaporation in laboratory boundary layer. Proceedings NATO Advanced Workshop on Humidity Exchange Over the Sea. W.A. Oost, S.D. Smith and K.B. Katsaros, eds.,

BUBBLE-MEDIATED SEA-AIR EXCHANGE

Tech. Rep., Dept. Atmos. Sci., Univ. of Washington, Seattle, WA.

Viguier, P., 1985: Une etude des perturbations superharmoniques d'onde de Stokes. These de Doctorat, IMST, Univ. Aix-Marseille II, France.

Wu, J., 1988: Bubbles in the near-surface ocean: a general description. *J. Geophys. Res.* 93, 587-590.

.. 8 ..

Modeling the Droplet Contribution to the Sea-to-Air Moisture Flux

C.W. Fairall and J.B. Edson
505 Walker Building
Department of Meteorology
Pennsylvania State University
University Park, PA 16802

Abstract

Assessing the importance of sea spray for air-sea moisture transfer is a formidable observational and modeling problem. From a modeling perspective, the primary roadblock is the wide range of size scales (from droplet microphysical to atmospheric boundary layer) that must be considered. Both ensemble average budget equation and Monte Carlo simulation approaches are being pursued. It is now clear that the total droplet evaporation is dominated by rather large droplets (on the order of 50 μm radius) which are so massive that their turbulent transport is affected by inertia. This further complicates the modeling task. Application of ensemble average and Monte Carlo models to this problem is still in its infancy. To date, only somewhat idealized cases (fresh water, ad hoc concentration profiles, laboratory situations, etc.) have been examined. The oceanic droplet source strength as a function of wind speed also represents an important uncertainty. The current state of knowledge suggests that droplets significantly enhance the moisture transfer efficiency at wind speeds in excess of 15 ms^{-1} .

1. Introduction

1.1 Opening comments

The importance of droplets in air-sea transfer at high wind

speeds has long been recognized. For example, Wu (1974) estimated that at a 10 m wind speed of 15 ms^{-1} , as much water is lost from the oceans by evaporation of droplets as is lost by direct evaporation of the interface. The evaporating droplets distort the normal sensible/latent heat flux balance. In the absence of droplets, all of the surface moisture flux appears as a latent heat loss by the ocean and increases the salinity at the surface. Both effects destabilize the ocean mixed-layer. Sensible heat entrained at the top of the marine boundary layer is available to directly heat the ocean. In the presence of whitecaps, the droplet component of the moisture flux neither directly cools the ocean nor does it change the salinity. Instead, it consumes a fraction of the entrained sensible heat. Thus, the dynamics of the oceanic and atmospheric boundary layers are changed.

Water can be transferred from the ocean to the atmosphere by direct evaporation or the evaporation of sea spray with subsequent transport to the troposphere by turbulence and large scale convection. Above the droplet evaporation zone, this transfer appears as a water vapor flux. Within the evaporation zone, the flux is partitioned between vapor flux and liquid (i.e., droplet) flux. Within the evaporation zone the evaporation influences the profiles of temperature and moisture. Evidence that this process is important is relatively sparse, primarily because of the difficulty of the measurements. If we assume that the total (liquid plus vapor) flux is roughly constant with altitude, then the appearance of the liquid flux in the evaporation zone would probably have the effect of reducing the vapor flux. Evidence for this has been observed in aircraft vapor flux profiles over the ocean which often indicate a maximum in the vapor flux in the lower boundary layer (Nicholls and Readings, 1979).

Another obvious manifestation of sea spray effects on the heat fluxes is expected to appear in the heat transfer coefficients (C_H and C_E). It is generally believed that droplet evaporation should lead to some increase in the neutral moisture transfer coefficient at high wind speeds. The anticipated effect on the heat transfer coefficient is not obvious and could be quite sensitive to the reference height used.

1.2 Bulk transfer perspective

By correlating simultaneous measurements of vertical velocity and specific humidity fluctuations, the latent heat flux (for example) can be determined near the surface

$$H_L = \rho L_e \overline{w'q'} \quad (1)$$

where ρ is the density and L_e the latent heat of vaporization of water. Through similarity theory (Fairall *et al.*, 1987) the surface flux, H_{Lo} , can be expressed in terms of bulk atmospheric properties and the transfer coefficient, C_E

$$H_{Lo} = \rho L_e C_E \bar{u} [q_s - \bar{q}(z)] \quad (2)$$

where \bar{u} is the mean wind speed and \bar{q} the specific humidity at height z , and q_s the surface specific humidity. C_E can be thought of as the efficiency of moisture transfer from the sea surface in response to the forcing by windspeed and air-sea humidity difference.

The bulk moisture transfer coefficient has a value on the order of 1×10^{-3} for measurements made at 10 m, and is expected to decrease slowly with increasing windspeed over ice (Joffre, 1982) or over water (Liu *et al.*, 1979) because of increased sheltering of the surface by the roughness elements. The effects of sea spray on evaporation of the ocean can be expected to show up as an enhancement of the 'drop free' C_E with increasing windspeed. In the summaries of transfer coefficient measurements given by Anderson and Smith (1981) there are very few measurements for winds above 10 ms^{-1} and most of those are not from the open ocean but from beach sites where there are probably surf effects. Francey and Garratt (1979) found both transfer coefficients to increase with increasing wind speed; surprisingly, the sensible heat coefficient increased faster than the moisture coefficient. In a recent survey of bulk parameterizations by Blanc (1985), only one of ten schemes projected scalar transfer coefficients that decreased with increasing wind speed.

1.3 Scope

This paper will focus on the influence of sea spray on the scalar heat fluxes near the sea surface and the relevant physics that must be considered to model that influence. It is believed that for realistic wind speeds, the droplets have little effect on the stress. We will not discuss effects (such as the wind speed dependence of the heat transfer roughness length) that fall within the conventional similarity treatment. Section 1.2 gives the conventional scaling approach to the scalar heat fluxes in the absence of droplets and provides a framework for breaking down the droplet problem in terms of interfacial processes (droplet production), molecular diffusion, turbulent and mean slip transport processes, and droplet evaporation. As we shall see, there are two different approaches to dealing with the random processes: (1) ensemble average budget equations or (2) 'Monte Carlo' (i.e., randomly forced but deterministic) simulations.

Our discussion of these issues will begin at the surface and proceed upwards. In section 2 we will briefly discuss the droplet source strength of the ocean. In section 3 we will discuss droplet microphysics, including evaporation/condensation and the size spectral representation of droplet concentration. In section 4 we will present the ensemble average conservation equation for droplets, including evaporation and transport effects, and briefly discuss past applications of this approach. In section 5 we will examine the Monte Carlo simulation approach.

2. Background On Droplet Production

2.1 Whitecaps, bubbles and droplets

Sea spray droplets are primarily produced by the bursting of air bubbles produced by breaking waves (whitecaps). When a whitecap bubble bursts at the surface, it produces two types of droplets: film drops from the ejection of the thin bubble film and jet drops which are formed from the destabilization of the vertically rising jet of water from the collapsing bubble cavity (Blanchard, 1975). Cipriano and Blanchard (1981) find that most of the droplets smaller than 10 μm originate as film droplets. Jet drops are

typically 1/10th the size of the parent bubble (those which produce jet drops range between 0.1 to 2.0 mm diameter range). One to five jet drops are produced per bubble while the much smaller film drops are produced in the hundreds. The rate of production of jet drops on a microphysical scale is much better known than that for film drops, which is still the subject of debate (e.g., Cipriano *et al.*, 1987). It is now known that the larger size droplets (greater than 10 μm radius) dominate the liquid water production by sea spray (Stramska, 1987; Miller, 1987; Edson, 1987), so our poor understanding of film droplets will not handicap the analysis of the effects on the heat fluxes (the same is not true if one's interest is in Aitken nuclei, optically relevant aerosols, or cloud condensation nuclei).

There is also considerable evidence that bubbles are not the only source of droplets. At wind speeds in excess of 13 ms^{-1} there is a rapid increase in the observed sea salt aerosol concentrations at large sizes (Monahan *et al.*, 1983; Fairall *et al.*, 1983). It has been postulated that this increase is due to the additional production of droplets by the so-called 'spume' mechanism where the strong turbulence simply blows the foam patch right off the top of a breaker. This phenomenon can be easily observed at high winds and its appearance threshold constitutes a criteria for sea state 7.

2.2 Oceanic droplet source strength

The droplet surface source strength is crudely defined as the number of drops of a given size interval produced by each square centimeter of the ocean per second. Clearly, this strength is a function of sea state as characterized by whitecap fraction and/or wind speed. Additional information is required to define the source function because at each size the particles are ejected with a distribution of initial vertical velocities (Blanchard and Woodcock, 1957). The usual approach is to assume that the droplets magically appear at the top of their most probable trajectory (Edson, 1987). In other words, the droplets are treated as being created by a distribution of elevated sources. The typical ejection height is on the order of 5 cm. This approach is justifiable because the time scale for this process is quite small compared to the

turbulent transport time scales. More than one study of large droplet concentrations near the ocean surface (Preobrazhenskii, 1972; de Leeuw, 1986) has shown the droplets to be rather uniformly distributed in the vertical below the typical wave height. de Leeuw attributes this to strong mixing by the 'rotor' flow induced by the motion of the wave (in a wave following coordinate system the rotor appears as an eddy in the wave trough). Strictly speaking, this is a transport issue and is not related to the source function but it may be of relevance in inferring the source function from indirect measurements.

Three approaches have been taken to establish the source strength: convolution of the bubble spectra with ejection height, laboratory simulations of whitecaps, and budget computations from marine measurements of particles. In the interest of brevity, we will only discuss the bubble spectra approach (see Fairall *et al.*, 1987, for more detail). Edson (1987) used this approach as the source function for input to a Lagrangian model of a droplet plume from a laboratory whitecap produced in the wind tunnel at IMST, Marseille, France. In this approach, the number/cc/sec of bubbles in a given size interval reaching the surface is simply the product of the bubble concentration spectrum, n_b , and the bubble rise speed, w_b . Thus, the number source strength spectrum, s_{ni} , is

$$s_{ni}(r) = n_b(a)w_b(a)N_e(a) \quad (3)$$

where N_e is the average number of droplets ejected well out of the diffusion sublayer by a bubble of radius a and r is the average radius of the droplet ejected by a bubble of radius a ($r \approx a/10$). The subscript n implies that this is a number density spectrum and the subscript i designates that this is a source that is realized as a distribution within a few centimeters of the interface. Assuming a power law for the bubble size spectrum (Monahan and Zietlow, 1969), the observed droplet concentrations (Fig. 1a) were obtained by adjusting the bubble spectrum (Fig. 1b). Of course, this only yielded the source function for a foam patch produced in a tank in wind tunnel, but the basic approach holds promise for the future

as measurements of oceanic bubble spectra become more reliable and reproducible. A comparison of recent results (Monahan, 1988; Miller and Fairall, 1988) from all three methods suggests that, as the methods are refined, the agreement is improving and a reasonable consensus is anticipated in the near future.

3. Droplet Microphysics

3.1 Evaporation

Consider a single droplet of mass, m_p , given by

$$m_p = \frac{4}{3} \pi \rho_p r^3 \quad (4)$$

We assume that the particle is a saltwater solution so that

$$\rho_p = \rho_w + (\rho_o - \rho_w) r_o^3 / r^3 \quad (5)$$

where ρ_w is the density of water, ρ_o the density of the particle with all water removed to produce a dry radius, r_o .

If the water vapor pressure exerted by the droplet, e_p , is greater than its surroundings, e , then the droplet will evaporate at a rate given by (Pruppacher and Klett, 1978)

$$\partial m_p / \partial t = -4 \pi f_p D_v r [e_p(r, r_o, T_p) - e] / (R_v T) \quad (6)$$

where f_p is a ventilation factor. The droplet vapor pressure can be converted to an effective saturation vapor density or specific humidity, q_p , at the surface of the droplet to yield

$$\partial m_p / \partial t = -4 \pi f_p D_v r \rho (q_p - q) \quad (7)$$

From Fitzgerald (1975) we estimate q_p by

$$q_p = q_{sat}(T_p) \left[1 - \gamma r_o^3 / (r^3 - r_o^3) \right] \quad (8)$$

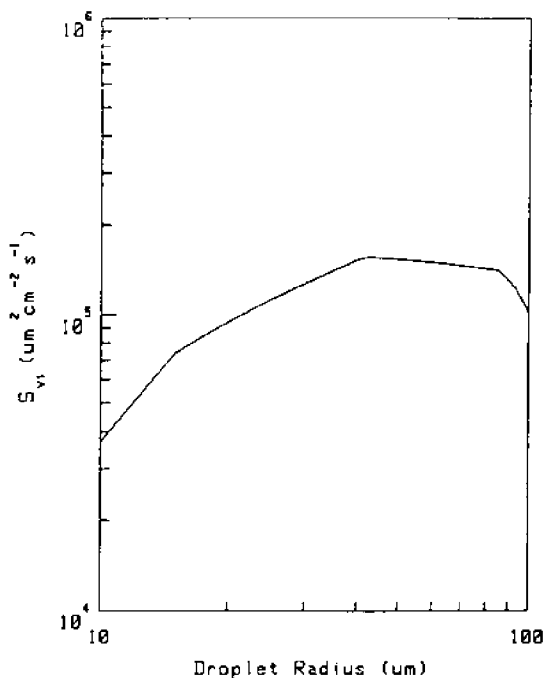
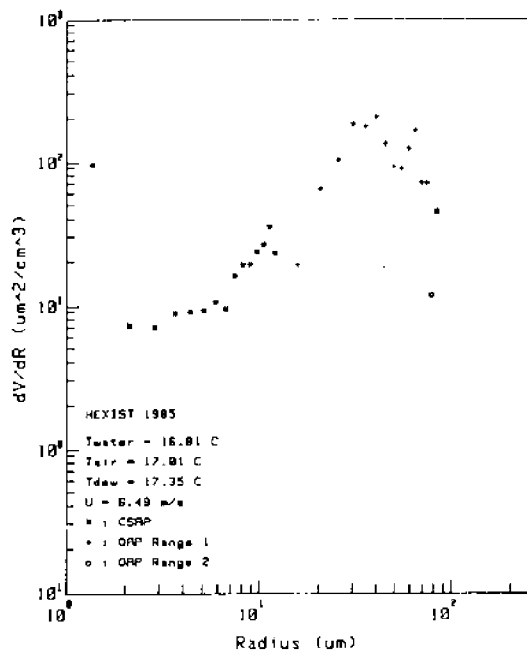


Figure 1. Sample spray droplet concentration parameters from the HEXIST experiment (upper panel). The concentration variables are expressed as the volume (μm^3) per radius increment (μm). (a) Droplet volume concentration ($\text{vol}/\mu\text{m}^3/\text{cm}$) versus radius (upper panel).

(b) Droplet source strength, s_{vi} , as a function of droplet radius for the spray bubblers used in the HEXIST experiment. The source is expressed in units of droplet volume (μm^3) per square centimeter of ocean per second per μm radius increment.

where q_{sat} is the saturation value for pure water with no surface curvature at the droplet temperature, T_p , and γ a parameter that depends on the chemistry of the dry component ($\gamma \approx 1$ for sea salt).

A spray droplet released from the ocean will lose water mass by evaporation until it approaches a state of equilibrium. A pure water droplet will completely evaporate but a salt water droplet will usually retain a considerable amount of water in equilibrium. The equilibrium condition is defined by setting $\partial m_p / \partial t = 0$. From (6) and (8) this defines an equilibrium particle size, r_e ,

$$r_e / r_o = G_e(S) = [1 + \gamma / (1 - S)]^{1/3} \quad (9)$$

where we have assumed that $T_p \approx T$ in equilibrium and S is the ambient water vapor saturation ratio.

The rate of change of size of an evaporating droplet is obtained by taking the derivative of (4) and combining it with (6) and (7); this can be written

$$\dot{r}_p = -A q_{sat}(\tau) r^{-1} \left\{ (1 - \alpha) \left[1 - \gamma / \left[(r / r_o)^3 - 1 \right] \right] - S \right\} \quad (10)$$

where

$$A = f_p D_v \rho / \rho_w \quad (11)$$

The factor α is necessary because the evaporating droplet is assumed to be at the 'wet bulb' temperature (Pruppacher and Klett, 1978), T_w ,

$$\alpha = L_v / (R_v T^2) (T - T_w) \quad (12)$$

Edson (1987) has shown that the time for even 100 μm droplets to reach the wet bulb temperature is small compared to the turbulence integral time scale at the particle ejection height.

3.2 The particle size spectral density

In Section 4 we will discuss the transport of particles or droplets in terms of a particle concentration variable. A variety of

particle concentration variables are used in the literature, the simplest is the total number concentration, $N(r)$, which is the total number of particles per unit volume of air with radius smaller than r . The size spectral density, $n(r)$, is the number per unit volume with radius greater than $r-dr/2$ but less than $r+dr/2$ and is directly related to $N(r)$

$$N(r) = \int_0^r n(r') dr' \quad (13)$$

These distributions describe the salt water solution droplets as they appear under ambient conditions. We can define a quasi-conservative variable in terms of the mass of salt in the particles m , equivalently, the dry radius of the particles. For example, we can define the size spectral density that would result if the particles were dried out completely as $n_o(r_o)$. The total number of droplets per unit volume with dry radius less than r_o is $N_o(r_o)$ so that

$$N_o(r_o) = \int_0^{r_o} n_o(r'_o) dr'_o \quad (14)$$

2. Ensemble Average Models

2.1 Budget equations

Following Fairall *et al.* (1987), we can write the simple one-dimensional, ensemble average budget equations for the standard meteorological variables as

$$D\bar{\theta} / Dt = -\partial(\overline{w'\theta'}) / \partial z - (L_e / c_p) \bar{E} \quad (15a)$$

$$D\bar{q}_v / Dt = -\partial(\overline{w'q'_v}) / \partial z + \bar{E} \quad (15b)$$

$$D\bar{q}_l / Dt = -\partial(\overline{w'q'_l} - \langle w_s \rangle \bar{q}_l) / \partial z - \bar{E} \quad (15c)$$

where the primes denote turbulent fluctuations, θ is the potential temperature, q_v the specific humidity (vapor), q_l the specific humidity (liquid), $\langle w_s \rangle$ the volume averaged fall velocity, and E the total evaporation rate

$$E = -(4\pi\rho_w / \rho) \int_0^\infty r^2 [\bar{r}_p \bar{n}(r) + \overline{r'_p n'(r)}] dr \quad (16)$$

Note that the molecular diffusion terms have been dropped because they are only relevant in the diffusion sublayer (within a mm of the interface). The liquid water content is the integral over the droplet distribution

$$\bar{q}_l = (4\pi\rho_w / 3) \int (r^3 - r_o^3) \bar{n}(r) dr = (4\pi\rho_w / 3) \int r^3 \bar{n}(r) dr \quad (17)$$

The droplets interact with the basic thermodynamic variables (15a and 15b) through the droplet evaporation term (E).

In the same simplified 1-dimensional form, the particle budget equations become

$$D\bar{n}_o / Dt = -\partial [\overline{w'_n n'_o} + \overline{w'_s n'_o} - \overline{w_s n_o}] / \partial z + \bar{s}_{no} \quad (18a)$$

$$D\bar{n} / Dt = -\partial (\bar{r}_p \bar{n} + \overline{r'_p n'}) / \partial r - \partial [\overline{w'_n n'} + \overline{w'_s n'} - \overline{w_s n'}] / \partial z + \bar{s}_n \quad (18b)$$

where w_s denotes the particle slip velocity (relative to the fluid).

Standard formulae are available for the mean value of w_s as a function of particle size (Pruppacher and Klett, 1978). The concentration-slip covariance term is responsible for the inertial impaction deposition mechanism (Slinn *et al.*, 1978) and also leads to reduced turbulent transport for large particles.

Again, note that the terms believed to be negligible above the molecular sublayer have been dropped from these expressions. Also note that the basic liquid water conservation equation (15c) can be obtained from (18b) by converting number density to mass density and integrating over all radii.

While n_o is a quasi-conservative variable, $n(r)$ is not because the droplets change their size while evaporating. Thus, (18a) is a simple conservation equation, but the analogous equation for the non-conservative variable, $n(r)$, requires the additional radius time derivative terms on the right hand side. Hence, two budget equations are required; one to keep track of the salt (18a) and one to

keep track of the salt plus water (18b). Notice that in order to use (10), we must be able to specify the value of r_0 that is appropriate for each value of r . This is done by finding the value of r such that

$$N(r) = N_0(r_0) \quad (19)$$

4.2 Modeling the covariance terms

Ensemble average models are often classified by the method used to model the covariance terms that appear in (15) and (18). We could form budget equations for the covariances, but these would contain third-order covariances. If we terminate this infinite hierarchy of equations by approximating the third-order terms as combinations of second and first-order variables, then this is referred to as a second-order closure model. A simpler approach is to use the conventional eddy-diffusion coefficient (or, first-order closure) model, often referred to as K-theory.

Following the analogy of the molecular diffusion flux expression, the turbulent flux is written

$$\overline{w'q'_v} = -K_h \partial \bar{q}_v / \partial z \quad (20)$$

where K_h is the scalar gradient diffusion coefficient. Within the realm of Monin-Obukhov similarity theory (Fairall *et al.*, 1987), we can write

$$K_h = \kappa z u_* / \Phi_h(z/L) \quad (21)$$

where u_* is the friction velocity, κ the von Karman constant (0.4), L the Monin-Obukhov stability length scale, and Φ_h the dimensionless scalar gradient function. Since the droplet effects on the heat fluxes will only be important under rather strong wind conditions, we can be confident in using the neutral approximation to (21)

$$K_h = \kappa z u_* \quad (22)$$

The K-theory approach is considered to be particularly appropriate for the droplet transport problem because K-theory is at its best in the surface layer. For very large droplets, K is partially compensated by the concentration - slip velocity covariance (Mestayer, this proceeding), which is a manifestation of their sluggish response to turbulent fluctuations.

4.3 Applications to droplet problems

Meteorology has a rich history of numerical model simulations of atmospheric boundary layer structure and dynamics. Many different types of models have been used: mixed-layer (zero-order closure), eddy diffusion (first-order closure), second-order closure, and large eddy simulations (LES).

Most boundary layer models have a total vertical domain of several km and no attempt is made to resolve surface layer structure. Instead, the lower boundary conditions and the lowest level of the model atmosphere are related to the surface fluxes by Monin-Obukhov similarity as previously described. Such models could be used for our purposes by nesting a high resolution surface layer and solving the equations presented in Section 4.1, but, as yet, this has not been done.

Burk (1984) made a major step in this direction when he simulated sea salt aerosol structure within a second-order closure ABL model, but he did not add a high resolution surface layer. He simplified the computational process by transporting the aerosols with an eddy diffusion coefficient (rather than solving the second-order particle covariance equation). Evaporation was not treated explicitly but the particles were assumed to be in a state of evaporative equilibrium using a function similar to (10). Thus, only the dry concentration budget equation (18a) was used. Since Burk was primarily interested in evaluating aerosol profiles throughout the ABL, near surface evaporation was not looked at and evaporation did not feedback onto the scalar profiles. In his simulations, the mass mode radius was relatively independent of wind speed (from Beaufort Force 3 to BF5) with a typical value of $3 \mu\text{m}$ (dry).

Pioneering work on the effects of droplets on the profiles of the means and fluxes for temperature and humidity has been done

using a surface layer first-order closure model developed specifically for this application (Ling and Kao, 1976; Ling *et al.*, 1978; Ling *et al.*, 1980). The budget equations were non-dimensionalized using wave height, wind speed, and air-sea temperature and humidity differences and solved for equilibrium conditions (zero time derivatives). The earlier work used only a single, fixed droplet size, but later papers allowed 5 droplet sizes (5, 20, 40, 70, and 150 μm radius). The droplets were assumed to be pure water so (18a) was not used and the $r'n'$ covariance term was neglected. The surface source function, based on laboratory measurements, was assumed to have a quadratic windspeed dependence but a wind speed independent shape. Since the surface source function appears to be much larger than those discussed in section 2, it is not surprising that substantial effects of droplets on the surface evaporation were found.

Stramska (1987) has developed a K-theory model to study sea salt aerosol profiles that falls somewhere between the Burk and Ling models in philosophy. As did Burk, Stramska used the surface source model for particles smaller than 15 μm radius from Monahan *et al.* (1982) and assumed that these particles are in an evaporative equilibrium state. However, the evaporation necessary to maintain this equilibrium is allowed to feedback onto the moisture and temperature profiles. As it turns out, these particles produce a negligible effect on the mean scalar profiles (this is consistent with conclusions of Ling *et al.*, 1980). The effects of larger droplets at high wind speeds (20 ms^{-1}) were examined by introducing an ad hoc droplet profile based on near surface data and an assumed decrease in the vertical. An evaporation equation similar to (10) was used assuming the droplets were pure water. This led to an increase in temperature of about 2° K and an increase in humidity of about 5%. Stramska did not assume dynamic equilibrium but started with an initial profile and integrated the budget equations in time. This permitted a study of the equilibrium response time of the aerosols as a function of size. The results were very similar to that of Fairall *et al.* (1983) with 10 μm radius particles requiring a few hours to reach dynamic equilibrium. The larger the particle, the shorter the response time because the

removal process (gravitational fallout) increases with size.

5. Monte Carlo Models

5.1 Lagrangian Markov chain

The most common form of Monte Carlo simulation applied to transport of droplets is the Lagrangian (i.e., a reference frame moving with the particle) Markov chain. Markov chain simulations were used by Reid (1979), Legg and Raupach (1982), and Ley and Thomson (1983) to successfully model dispersion of neutrally buoyant particles within the surface layer. The Markov chain is a finite difference form of the Langevin equation; the Langevin equation being given by

$$\frac{dw}{dt} = -\frac{w}{\tau} + \zeta(t) \quad (23)$$

where w is the particle's vertical velocity, τ is a time scale for the motion, and $\zeta(t)$ is a random forcing function due to turbulence.

The above authors assume that the motion of the particles is passive, i.e., they assume that the particles are of such size that they follow the turbulent motion of the atmosphere exactly. With this assumption, the timescale in (23) is the Lagrangian integral time scale of the turbulence, and the random forcing function is derived observing the constraints that

$$\overline{w'(t)} = 0 \quad (24a)$$

and

$$\overline{(w'^2)^{1/2}} = \sigma_w \quad (24b)$$

where σ_w is the standard deviation of the atmospheric vertical velocities.

The 'passive contaminant' assumption is not valid for the jet drops ($\sim 10 - 100 \mu m$ radius) that we are interested in for the sea spray problem. Gravitational and inertial effects must be included in order to realistically simulate their trajectories. This is

accomplished by assuming that the particle's vertical velocity is composed of a mean fall velocity plus a velocity fluctuation

$$w_p(t) = -\bar{w}_s + w'_p(t) \quad (25)$$

The particle velocity statistics are modeled such that

$$\overline{w'_p(t)}_t = 0 \quad (26a)$$

and

$$(\overline{w_p'^2})^{1/2} = \sigma_p = \eta \sigma_w \quad (26b)$$

where σ_p is the standard deviation of the vertical velocity of the particle. The parameter η^2 is the ratio of the particle and atmospheric variances, and is derived by integrating the ratio of their respective velocity spectra. Its value is always less than one due to inertial effects.

The particle's vertical velocity is then defined using the appropriate finite difference form of the Langevin equation

$$w_p(t + \Delta t) = (1 - \Delta t / \tau_p) w_p(t) + \mu(t + \Delta t) \quad (27)$$

where τ_p is now the particle integral time scale, and $\mu(t + \Delta t)$ is the random forcing function, which by definition is uncorrelated with $w_p(t)$. As with the Lagrangian integral time scale, we define the particle time scale as

$$\tau_p = \int_0^{\infty} R_p(t) dt \quad (28)$$

where R_p is the particle autocorrelation function (Meek and Jones, 1973).

Their function shows that increasing fall velocity tends to decrease correlation, while inertial effects tend to offset this effect by "damping" vertical motion, thereby causing the particle to remain in a more correlated region of space. The relative

importance of either effect is dependent on the particle's size.

The initial formulation of the model does not include fluctuations in the streamwise velocity for simplicity ($\overline{w'_p u'_p} = 0$). With this in mind, the necessary form of the random forcing function is found by taking the mean and then variance of both sides of (27) and solving for μ . If we consider only those terms of first order t , this results in

$$\mu = \Gamma \sigma_p \left(\frac{2\Delta t}{\tau_p} \right)^{1/2} - \frac{\Delta t}{\tau_p} \bar{w}_s \quad (29)$$

where Γ is a random number with unit variance, zero mean and Gaussian distribution, and we have assumed that all other moments of $\mu(t+\Delta t)$ are zero. The equation for the particle's vertical velocity can then be written

$$w_p(t + \Delta t) = (1 - \Delta t / \tau_p) w_p(t) + \Gamma \sigma_p \left(\frac{2\Delta t}{\tau_p} \right)^{1/2} - \frac{\Delta t}{\tau_p} \bar{w}_s \quad (30)$$

5.2 HEXIST simulations

A Lagrangian model has been developed for application to a series of measurements of artificially generated spray droplets in the air-sea simulation tunnel at the IMST in Marseille (Edson, 1987; Edson *et al.*, 1988). The purpose of this experiment (given the name HEXIST) was to simulate the turbulent transport of evaporating jet drops within the oceanic surface layer. An artificial whitecap was created in the water in the tank by a matrix of tropical fish tank aerators. Since we are dealing with a plume of droplets generated from a small area source, the one-dimensional ensemble average approach is not applicable.

In the HEXIST Lagrangian model, droplets are created above the simulated whitecap region in numbers determined by the surface source function. As each droplet is carried down the tunnel by the mean wind, its path is followed as it reacts to turbulent fluctuations in the vertical wind. Under non-saturated conditions, the particle is allowed to change size by evaporation. At fixed locations downwind of the source (chosen to coincide with

locations of the measurements), particle concentration profiles can be computed by counting the number of particles of a given size that pass through a given height interval.

The droplets are released at an ejection height described above, and then advected along (see Fig. 2) using (30) and

$$w_p(0) = \gamma \sigma_p - \bar{w}_e \quad (31a)$$

$$z(t + \Delta t) = z(t) + w_p(t + \Delta t) \Delta t \quad (31b)$$

$$x(t + \Delta t) = x(t) + \bar{u}(z(t + \Delta t)) \Delta t \quad (31c)$$

where $\bar{u}(z)$ is the horizontal wind speed at height z taken from a logarithmic profile generated from tunnel observations. The height of the viscous sublayer is used as a lower limit, below which the particles are "absorbed" by the water surface. The sublayer thickness is defined as $\nu/\kappa u_*$, where ν is the kinematic viscosity of air.

The effects of evaporation are modeled using diagnostic equations for the particle's radius (see (10)) and surface temperature, in conjunction with standard diabatic profiles of temperature and specific humidity. The droplet surface temperature is derived using an equation from Pruppacher and Klett (1978), which includes the effects of evaporative cooling and conductive heat flux from air to drop. As stated above, this temperature is found to quickly reach the equilibrium value resulting from the two effects, so that the droplet is essentially at the wet-bulb temperature for most of its transit time.

By keeping track of the particle's position and radius, the dynamics of a shrinking particle are simulated. As expected, the equation of the droplet's motion as its radius shrinks to zero reduces to the Langevin equation in discrete form used implicitly by Reid (1979), Legg and Raupach (1982), and Ley and Thomson (1983). Vertical profiles of particle volume spectra, $v(r)$, are then generated (Figs. 3 and 4) at the desired heights and distances downwind of the source (see Edson *et al.*, 1988). The source

BUBBLE-MEDIATED SEA-AIR EXCHANGE

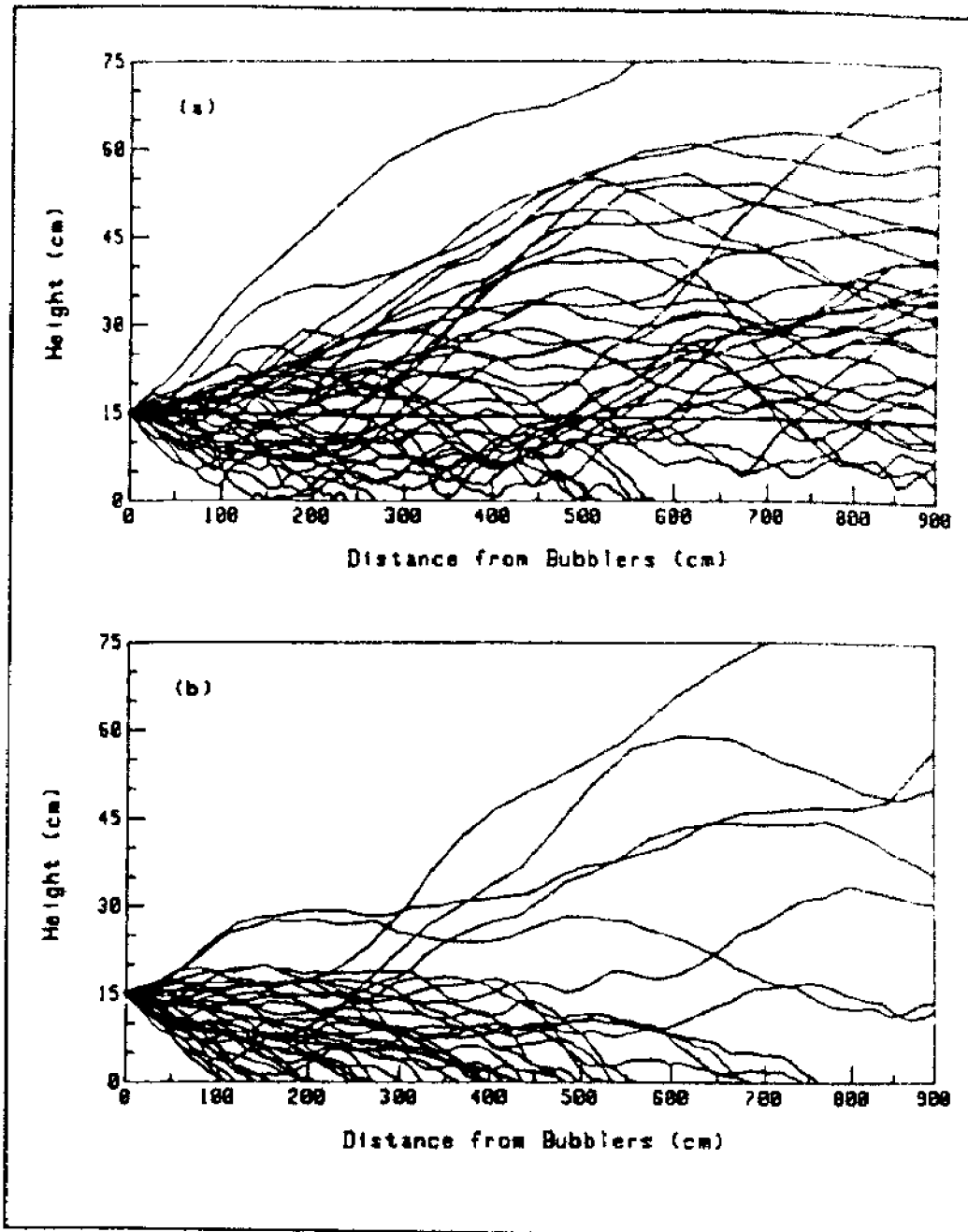


Figure 2. Lagrangian model simulation of 50 droplet trajectories for the HEXIST experiment at 9 m/s nominal wind speed. The vertical axis is the droplet height (cm) and the horizontal axis is the droplet distance (cm) downwind of the source. The upper panel is a family of trajectories for a 50 μm radius droplet, the lower panel is for a 10 μm radius droplet. Both are released from 10 cm for comparison.

function is found by comparing the non-evaporating spectra with their equivalent measured spectra, and adjusting the source function until a reasonable fit is obtained. Once obtained, the source function is fixed so that true comparisons between the modeled and measured data may be made. Notice in Figs. 3 and 4 that the greater fetch causes the droplet concentrations to become more well-mixed by the turbulence because of the greater time the mixing process has had to operate. The effects of evaporation are difficult to judge from these figures because they are expressed in terms of spectra. Depending on the slope of the spectrum, evaporation can cause an increase or decrease in concentration at a specific radius. This can be seen by examining (18b).

6. Discussion

The contribution of sea spray to the evaporation efficiency of the ocean as a function of windspeed is very difficult to determine experimentally. In the short term, we can learn quite a bit by modeling the relevant processes in a manner which realistically represents the conditions over the ocean. So far, only a few first steps have been taken in this direction and the results are inconclusive. Realistic droplet microphysics (including salt) and upper boundary layer processes (entrainment and advection) are potentially very important and have not really been considered. It is also not clear if the Monte Carlo or ensemble average approach is preferable.

We can state that droplet evaporation in the IMST simulation experiment was fairly modest. In a state of near dynamic equilibrium, we can write the total vertical water transport at the height z as the sum of vapor and evaporation terms

$$\text{Total Flux } (z) = \overline{w'q'_v} + \int_z^{\infty} \overline{E}(z) dz \quad (32)$$

Well above the droplet zone the water flux is borne entirely by turbulent transport of vapor (evaporation is zero). Examples from HEXIST measurements (Fig. 5) of the droplet evaporation

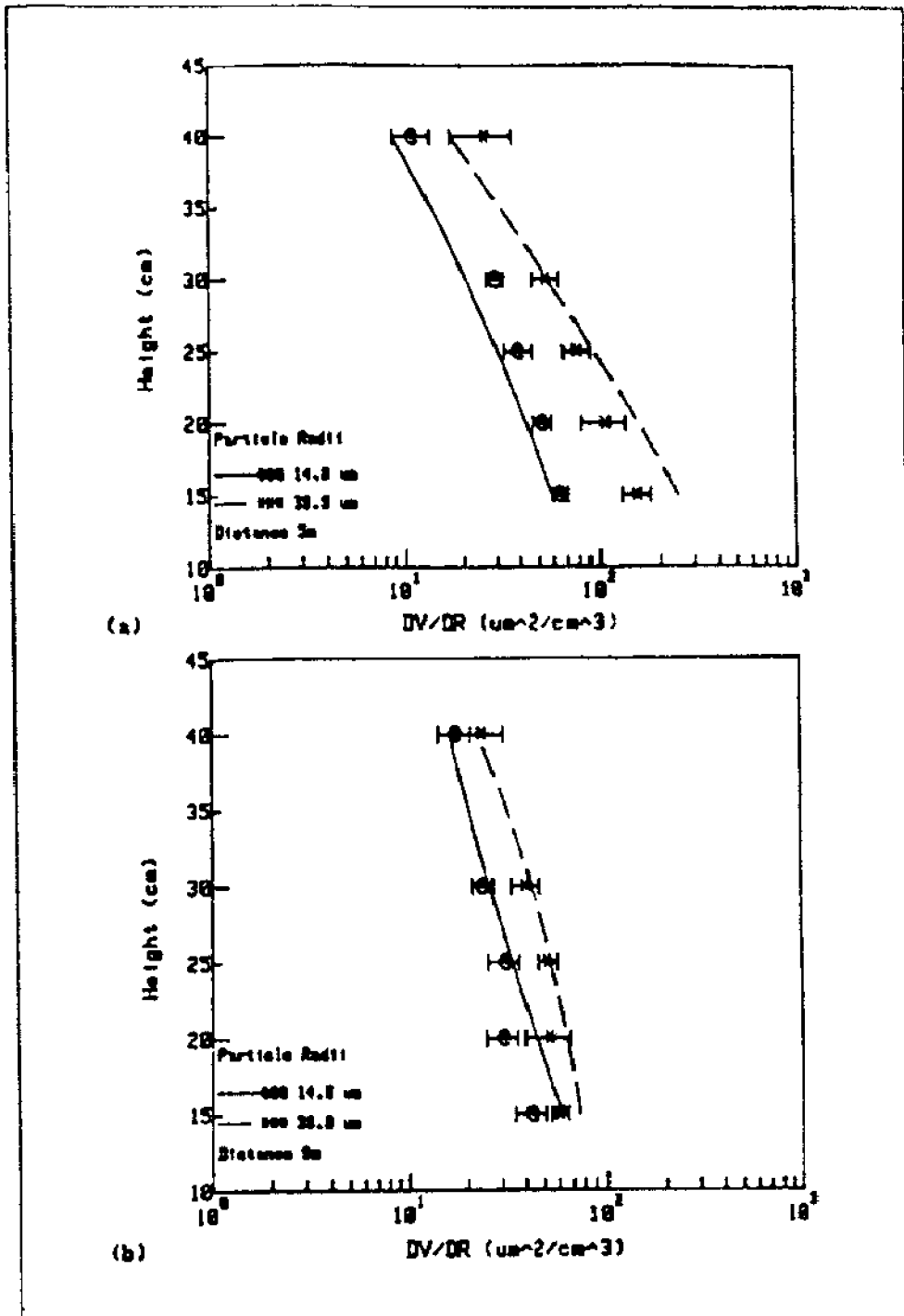


Figure 3. Droplet volume concentration spectra vs. height profiles for two selected size droplets from HEXIST. The lines denote smoothed fits to measured data, the symbols denote values simulated with the Lagrangian model averaged over five model runs. The bars indicate the standard deviations from the mean values. The conditions for this example are a relative humidity near 100%, nominal wind speed of 9 ms^{-1} and initial radius of 15 and $40 \mu\text{m}$ for the two droplet sizes.
 (a) downwind fetch of 5 m.
 (b) downwind fetch of 9 m.

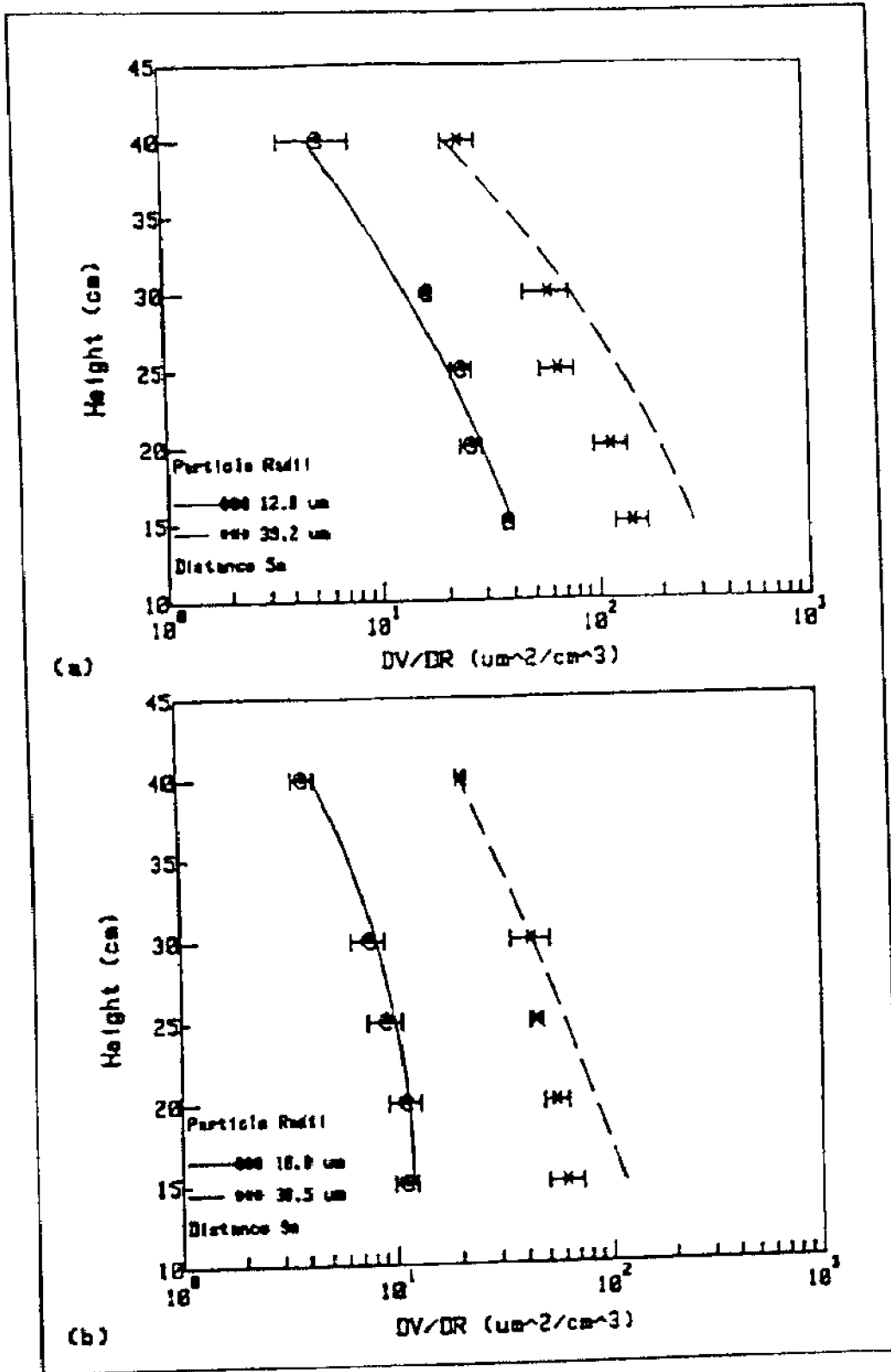


Figure 4. As in Figure 8 but for evaporating (nominal relative humidity near 50%) conditions. The initial radii at time of release are again 15 and 40 μm .

BUBBLE-MEDIATED SEA-AIR EXCHANGE

contribution to a total latent flux of 225 W/m^2 has been computed to be on the order of 1 W/m^2 . For the HEXIST situation the droplet liquid water mass was 10^{-4} of the vapor concentration, which is quite modest. In a subsequent experiment (named CLUSE), the entire surface of the water in the tunnel was turned into a whitecap. This yielded droplet concentrations and latent heat flux contributions more than two orders of magnitude greater.

The potential droplet contribution can be also crudely estimated by integrating the source function (Fig. 1b) over radius to obtain the total liquid water sea spray flux. This implies that the sea spray would contribute 785 W/m^2 to the total latent heat flux if the ocean were 100% whitecap covered and all droplets evaporated before impacting the sea surface. For the open ocean, this number must be considered to be uncertain by at least one half an order of magnitude. The HEXIST experiment (which had 1.5% 'whitecap' coverage and, hence, an 11 W/m^2 potential) suggests that about 10% of the spray liquid water was converted to vapor by

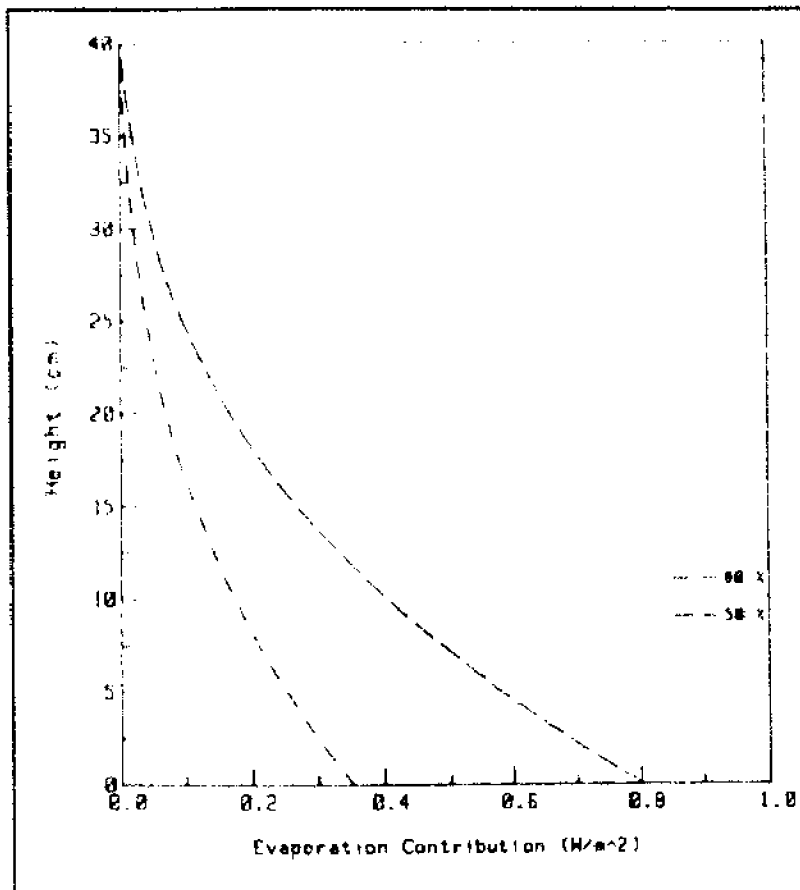


Figure 5. Estimate of the droplet contribution to the total water transfer 5m downwind of the whitecap for the 9 m/s HEXIST simulations using the second term from (32). The direct vapor transfer is estimated at 225 W/m^2 .

evaporation.

While the HEXIST and CLUSE measurements and model studies represent idealizations (fresh water evaporating in a wind tunnel), the implication is that droplets will make a significant contribution to the total evaporation when the wind speed exceeds approximately 15 ms^{-1} .

Acknowledgments

This work is supported by the Office of Naval Research (contract N00014-85-K-0250). The authors wish to acknowledge collaboration with Soren Larsen of RISØ National Laboratory in Roskilde, Denmark; Patrice Mestayer of IMST in Marseille, France; and Ken Davidson and Don Spiel of NPS in Monterey, California, USA.

References

- Anderson, R.J. and S.D. Smith, 1981: Evaporation coefficient for the sea surface from eddy-flux measurements. *J. Geophys. Res.*, **86**, 449-456.
- Blanc, T.V., 1985: Variation of bulk-derived surface flux, stability, and roughness results due to the use of different transfer coefficient schemes. *J. Phys. Ocean.*, **15**, 650-669.
- Blanchard, D.C. and A.H. Woodcock, 1957: Bubble formation and modification in the sea and its meteorological significance. *Tellus*, **9**, 145-158.
- Blanchard, D.C., 1971: Whitecaps at sea. *J. Atmos. Sci.* **28**, 645.
- Blanchard, D.C., 1975: Bubble scavenging and the water-to-air transfer of organic material in the sea. *Adv. in Chem.*, **145**, American Chemical Society, Washington, DC.
- Burk, S.D., 1984: The generation, turbulent transfer and deposition of the sea-salt aerosol. *J. Atmos. Sci.*, **41**, 3040-3051.
- Cipriano, R.J. and D.C. Blanchard, 1981: Bubble and aerosol spectra produced by a laboratory breaking wave. *J. Geophys. Res.*, **86**, 8085-8092.
- Cipriano, R.J., E.C. Monahan, P.A. Bowyer, and D.K. Woolf, 1987: Marine condensation nucleus generation inferred from whitecap simulation tank results. *J. Geophys. Res.*, to appear.
- de Leeuw, G. 1986: Vertical profiles of giant particles close above the sea surface. *Tellus*, **38B**, 51-61.
- Edson, J.B., 1987: Lagrangian model simulations of the turbulent transport and

BUBBLE-MEDIATED SEA-AIR EXCHANGE

- evaporation of spray droplets in a wind-water tunnel. M.S. thesis, Department of Meteorology, Pennsylvania State University, University Park, PA, 16802, USA.
- Edson, J.B., C.W. Fairall, S.E. Larsen, and P.G. Mestayer, 1988: A random walk simulation of the turbulent transport of evaporating jet drops in the air-sea simulation tunnel during HEXIST. *Proceed. 7th Conf. on Ocean-Atmosphere Interactions*, AMS, Anaheim, CA, 9-13.
- Fairall, C.W., K.L. Davidson, and G.E. Schacher, 1983: An analysis of the surface production of sea-salt aerosol. *Tellus*, 35B, 31-39.
- Fairall, C.W., J.B. Edson, and M.A. Miller, 1988: Heat fluxes, whitecaps, and seaspray. Technical report, Department of Meteorology, Pennsylvania State University, University Park, PA, 16802, 47 pp.
- Fitzgerald, J.W., 1975: Approximation formulas for the equilibrium size of an aerosol particle as a function of its dry size and composition and the ambient relative humidity. *J. Appl. Met.*, 14, 1044-1049.
- Francey, R.J. and J.R. Garratt, 1989: Is an observed windspeed dependence of AMTEX '75 heat transfer coefficients real? *Bound.-Layer Meteorol.*, 16, 249-260.
- Joffre, S.M., 1982: Momentum and heat transfers in the surface layer over a frozen sea. *Bound.-Layer Meteorol.*, 24, 211-229.
- Legg, B.J., and M.R. Raupach, 1982: Markov-chain simulation of particles in inhomogeneous flows: The mean drift velocity induced by a gradient in Eulerian velocity variance. *Bound.-Layer Meteorol.*, 24, 3-13.
- Ley, A.J., and D.J. Thomson, 1983: A random walk model of dispersion in the diabatic surface layer. *Quart. J. R. Meteorol. Soc.*, 109, 867-880.
- Ling, S.C. and T.W. Kao, 1976: Parameterization of the moisture and heat transfer process over the ocean under whitecap sea states. *J. Phys.Oceanogr.*, 6, 306-315.
- Ling, S.C., T.W. Kao, M. Asce and A. Saad, 1980: Microdroplets and transport of moisture from the ocean. *J. Eng. Mech. Div.*, 6, 1327-1339.
- Liu, W.T., K.B. Katsaros, and J.A. Businger, 1979: Bulk parameterization of air-sea exchanges of heat and water vapor including the molecular constraints at the interface. *J. Atmos. Sci.*, 36, 1722-1735.
- Meek, C.C., and B.G. Jones, 1973: Studies of the behavior of heavy particles in a turbulent fluid flow. *J. Atmos. Sci.*, 30, 239-244.
- Miller, M.A., 1987: Modeling the production and transport of sea-salt aerosols. M.S. thesis, Department of Meteorology, Pennsylvania State University, University Park, PA, 16802, USA.
- Miller, M.A. and C.W. Fairall, 1988: A new parameterization of spray droplet production by oceanic whitecaps. *Proceed. 7th Conf. on Ocean-Atmosphere Interactions*, AMS, Anaheim, CA, 174-177.
- Monahan, E.C., 1988: Whitecap Coverage as a Remotely Monitorable Indication of the Rate of Bubble Injection into the Oceanic Mixed Layer, in *Sea Surface Sound*, B.R. Kerman, Ed., Kluwer Academic Publishers, Dordrecht., 153, 85-96.

- Monahan, E.C., K.L. Davidson and D.E. Spiel, 1982: Whitecap aerosol productivity deduced from simulation tank measurements. *J. Geophys. Res.*, **87**, 8898-8904.
- Monahan, E.C., C.W. Fairall, K.L. Davidson, and P.J. Boyle, 1983: Observed inter-relations between 10 m winds, ocean whitecaps and marine aerosols. *Quart. J. R. Met. Soc.*, **109**, 379-392.
- Monahan, E.C., 1988: Whitecap Coverage as a Remotely Monitorable Indication of the Rate of Bubble Injection into the Oceanic Mixed Layer, in *Sea Surface Sound*, B.R. Kerman, Ed., Kluwer Academic Publishers, Dordrecht., **153**, 85-96.
- Nicholls, S. and C.J. Readings, 1979: Aircraft observations of the structure of the lower boundary layer over the sea. *Quart. J. R. Met. Soc.*, **105**, 785-802.
- Preobrazhenskii, L., 1973: Estimation of the content of spray drops in the near-water layer of the atmosphere. *Fluid Mech. Sov. Res.*, **2**, 95-100.
- Pruppacher, H.R. and J.D. Klett, 1978: *Microphysics of Clouds and Precipitation*, Reidel, Dordrecht, Holland.
- Reid, J. D., 1979: Markov chain simulations of vertical dispersion in the neutral layer for surface and elevated releases. *Bound.-Layer Meteorol.*, **16**, 3-22.
- Slinn, W.G.N., L. Hasse, B.B. Hicks, A.W. Hogan, D. Lai, P.S. Liss, K.O. Munnich, G.A. Sehmel, and O. Vittori, 1978: Some aspects of the transfer of atmospheric trace constituents past the air-sea interface. *Atmos. Environ.*, **12**, 2055-2087.
- Stramska, M., 1986: Vertical profiles of sea-salt aerosol in the atmosphere surface layer: a numerical model. *Acta Geophys. Pol.*, to appear.
- Woolf, D.K., E.C. Monahan, and D.E. Spiel, 1988: Quantification of the marine aerosol produced by whitecaps. *Proceed. 7th Conf. on Ocean-Atmosphere Interactions*, AMS, Anaheim, CA, 182-185.
- Wu, J., 1974: Evaporation due to spray. *J. Geophys. Res.*, **79**, 4107-4109.

..9..

Abstracts from Poster Presentations:**Time Constants for the Evolution
of Sea Spray Droplets**

Edgar L. Andreas
 U.S. Army Cold Regions Research and Engineering Laboratory
 72 Lyme Road
 Hanover, NH 03755-1290

At the instant sea spray droplets form, they begin exchanging heat and moisture with their environment. Because this exchange continues until the droplets reach thermal and moisture equilibrium or fall back into the sea, sea spray has the potential for enhancing the usual interfacial fluxes of sensible and latent heat (Figure 1). At high latitudes, especially, the heat and moisture available from sea spray may be an important energy source for the small, intense cyclones called polar lows (Kellogg and Twitchell, 1986) that form in the ice-edge region.

To understand the potential sea spray has for enhancing the air-sea fluxes, we must know how quickly a spray droplet can transfer its available heat and moisture. I have therefore adapted the micro-physical equations developed by Pruppacher and Klett (1978) for use in studying the thermal and moisture (size) evolution of sea spray droplets. I parameterize this evolution in terms of the time constants τ_T and τ_r . Given that a sea spray droplet starts at the sea surface temperature T_w , τ_T is the time required for its temperature T to come to within e^{-1} of its equilibrium temperature T_{eq} in air of temperature T_a . That is, τ_T is defined by $[T(\tau_T) - T_{eq}] / [T_w - T_{eq}] = e^{-1}$. Similarly, τ_r is defined by $[r(\tau_r) - r_{eq}] / [r_0 - r_{eq}] = e^{-1}$, where r is the instantaneous droplet radius, r_{eq} is the equilibrium radius for relative humidity RH and air temperature T_a , and r_0 is the droplet radius at

formation. Figure 2 shows model calculations of τ_T and τ_r for typical high latitude, polar low conditions. From this and similar figures not shown, we see that τ_T is always at least three orders of magnitude smaller than τ_r . Thus, for spray droplets, the sensible and latent heat transfers are essentially decoupled. In effect, the ambient relative humidity has negligible effect on the thermal evolution of spray droplets; and the air-sea temperature difference has negligible effect on their moisture (size) evolution.

In Figure 2 I have also plotted the time constant τ_f , the time required for a droplet of radius r_0 to fall 1 meter in still air. If τ_f is smaller than τ_T or τ_r , a spray droplet will likely fall back into the sea before transferring its available heat or moisture into the air.

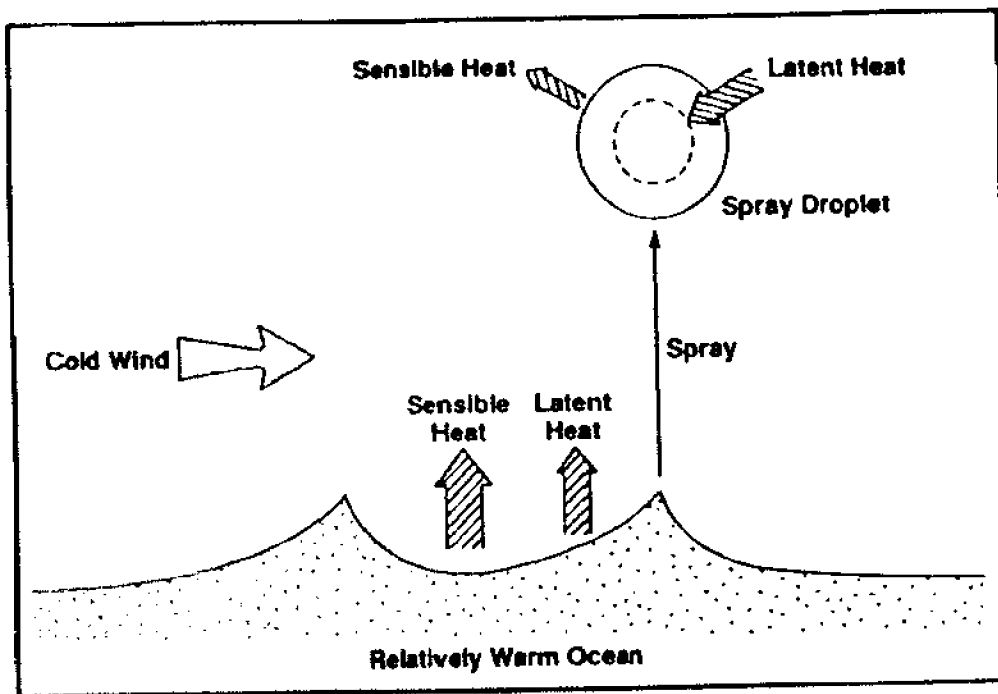


Figure 1. Conceptual model of heat and moisture transfer associated with sea spray at high latitude.

From the figure, we see that because of the rapidity of the thermal exchange, virtually all sea spray droplets reach thermal equilibrium with the air. Only droplets smaller than about 10-20 μm , however, effectively reach moisture equilibrium before falling back into the sea.

BUBBLE-MEDIATED SEA-AIR EXCHANGE

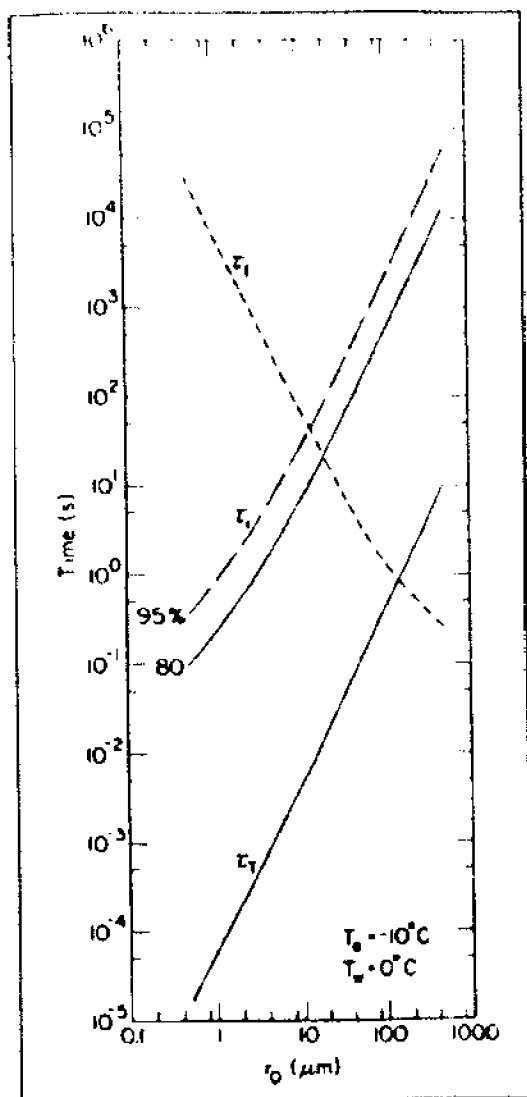


Figure 2. Time constants for the thermal exchange (τ_t) and for the moisture exchange (τ_m) at two relative humidities (RH=80, 95%) and the time required for a droplet to fall 1 meter in still air (τ_f). The air temperature T_a is -10°C , the sea water temperature T_s is 0°C , the sea surface salinity is 34 o/oo, and the atmospheric pressure is 1000 hPa.

Acknowledgments.

The office of Naval Research supported this work through contracts N0001986MP67847 and N0001488WM22012.

References

- Kellogg, W.W. and P.F. Twitchell, 1986: Summary of the Workshop on Arctic Lows, 9-10 May 1985, Boulder, Colorado. *Bulletin of the American Meteorological Society* 67, 186-193.
- Pruppacher, H.R. and J.D. Klett, 1978: *Microphysics of Clouds and Precipitation*. Dordrecht: D. Reidel.

Laboratory Whitecap Simulation Experiments: Temporal Variability and Irreproducibility of Aerosol Production

David K. Woolf*
University of Connecticut
Marine Sciences Institute

Aerosol measurements in laboratory whitecap simulation tanks at University College, Galway in Ireland and at the University of Connecticut suggest that large variations in aerosol production occur when laboratory simulations are run for a sufficiently long time despite a constant mechanical input. A fairly consistent result is found for the operation of a continuously flowing breaking wave simulation (primitive weirs). In these experiments, the large ($>5\mu\text{m}$ diameter at 80% relative humidity) drop production characteristically falls during a run, while the small drop production ($0.5\text{-}5\mu\text{m}$ diameter) is relatively steady. On the other hand, the results for repeated episodic events are very puzzling. In these experiments, variations in both large drop production and small drop production have been observed, in which no systematic behaviour is apparent. Redistribution of surface-active material is associated with the large amounts of bubbling during these experiments. This process may be principally responsible for the temporal variations in aerosol production. In particular, a build-up of material on the water surface as a result of bubble scavenging may progressively weaken jet-drop production during the operation of a weir. The potential influence of surfactants on aerosol production can be demonstrated by adding surfactants to the water surface during a series of breaking wave simulations.

In the figures, the calculated aerosol production ($>5\ \mu\text{m}$ di-

*present address: Dept. of Oceanography, The University, Southampton, U.K.

meter and 0.5-5 μm diameter) per event is shown for a series of thirty-five events during which deposits of oleic acid were added to the surface after events 7 and 27. There was a large fall in aerosol production as a result of each deposit, followed by a gradual recovery.

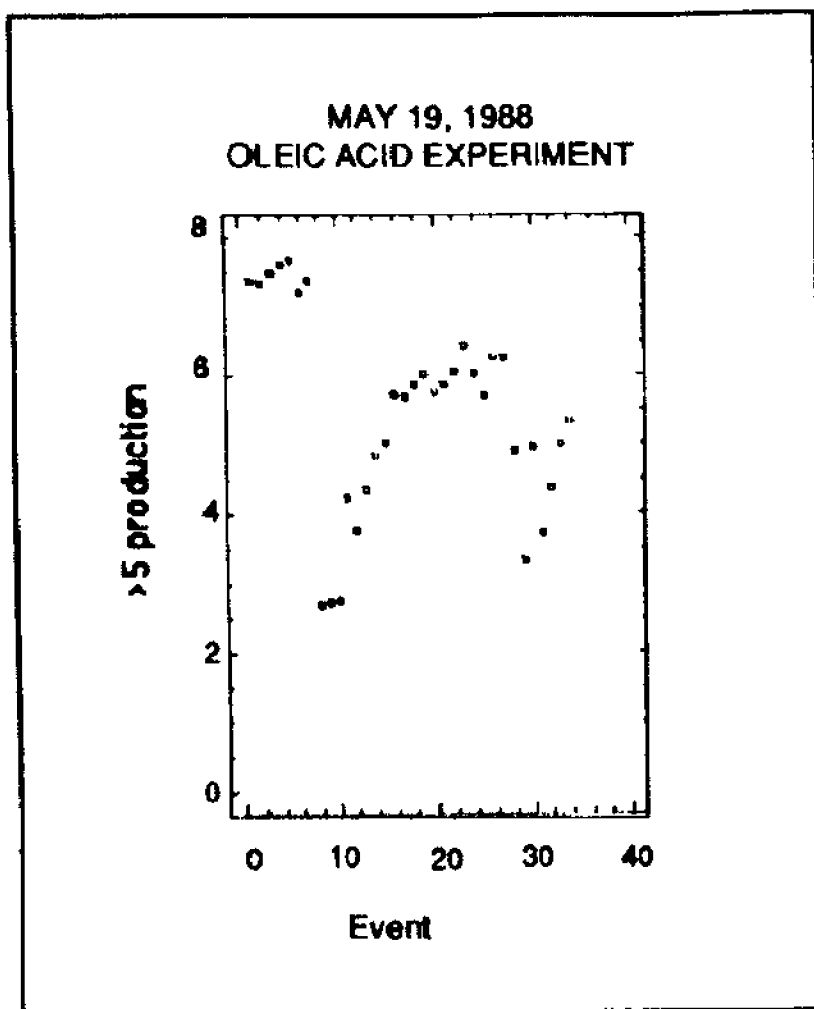


Figure 1. Production of aerosol particles whose diameters were greater than 5 μm , per breaking wave event, for a series of 35 such breaking wave events. Note that oleic acid was added to the water surface in the tank after events 7 and 27.

BUBBLE-MEDIATED SEA-AIR EXCHANGE

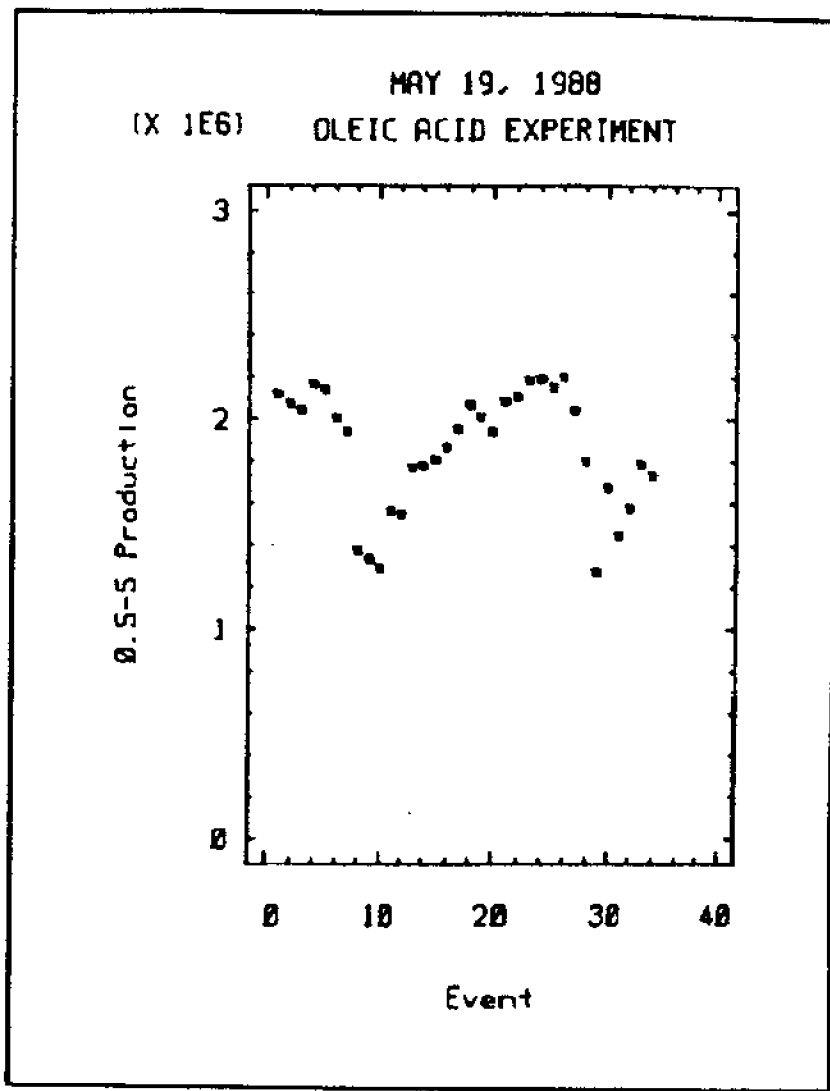


Figure 2. Production of aerosol particles whose diameters were between 0.5 and 5 μm , per breaking wave event, for a series of 35 such breaking wave events. Note that oleic acid was added to the water surface in the tank after events 7 and 27.

References

- Monahan, E. C., D.E. Spiel and K.L. Davidson, 1986: Model of marine aerosol generation via whitecaps and wave disruption. In: *Oceanic Whitecaps and Their Role in Air-Sea Exchange Processes*, E.C. Monahan and G. MacNiocaill, eds. D. Reidel Publishing Co., Dordrecht, Holland, 167-174.
- Woolf, D.K. 1988: The role of oceanic whitecaps in geochemical transport in the upper ocean and the marine environment. PhD Dissertation, National University of Ireland, Dublin, Ireland.

- Woolf, D. K. and E.C. Monahan, 1988: Laboratory investigations of the influence on marine aerosol production of the interaction of oceanic whitecaps and surface-active material. In: *Aerosols and Climate*, P.V. Hobbs, ed. A. Deepak Publishing, Hampton, Virginia (in press).
- Woolf, D.K., E.C. Monahan and D.E. Spiel, 1988: Quantifications of the marine aerosol production produced by whitecaps. Preprint Volume: *Seventh Conference on Ocean-Atmosphere Interaction*, 31 January-5 February 1988, Anaheim, CA, 182-185.

The Role Of Breaking Waves in the Control of the Gas Exchange Properties of the Sea Surface

T. Torgersen
R. Mason
D. Woolf
J. Benoit
M.P. Dowling
M. Wilson
E.C. Monahan

Introduction

The gas exchange properties of the surface ocean are a primary control on the response time of the atmosphere and the surface layer to natural and anthropogenic perturbation. If we are to successfully integrate ocean-atmosphere coupling into global- and local-scale models, a predictive parameterization of the gas exchange process must be established.

There have been numerous field and laboratory studies of the controlling parameters of gas exchange. The role of wind velocity has been clearly defined but the measured rates of gas exchange have little correlation with the instantaneous wind and the local wind velocity field. This is the result of the variability of the surface wind and the physical memory of the process of surface ocean mixing/gas exchange. The principal means of determining oceanic gas exchange rates, Rn-222 measurements, has an inherent radiochemical memory that integrates the process over several days. Finally, there is a nonlinear relation between the wind shear across the ocean surface and the boundary layer controlling gas exchange.

An initial series of experiments to determine the relationship between breaking waves and the gas exchange process was

recently completed. Breaking waves greatly increase the surface area available for gas exchange (in a highly nonlinear manner) and the relative area of breaking waves is related to both the surface roughness and the local wind field. Such an approach may provide a parameterization and/or a real time satellite predictive data base for the accurate determination of oceanic gas exchange rates which could be incorporated into a coupled ocean-atmosphere model.

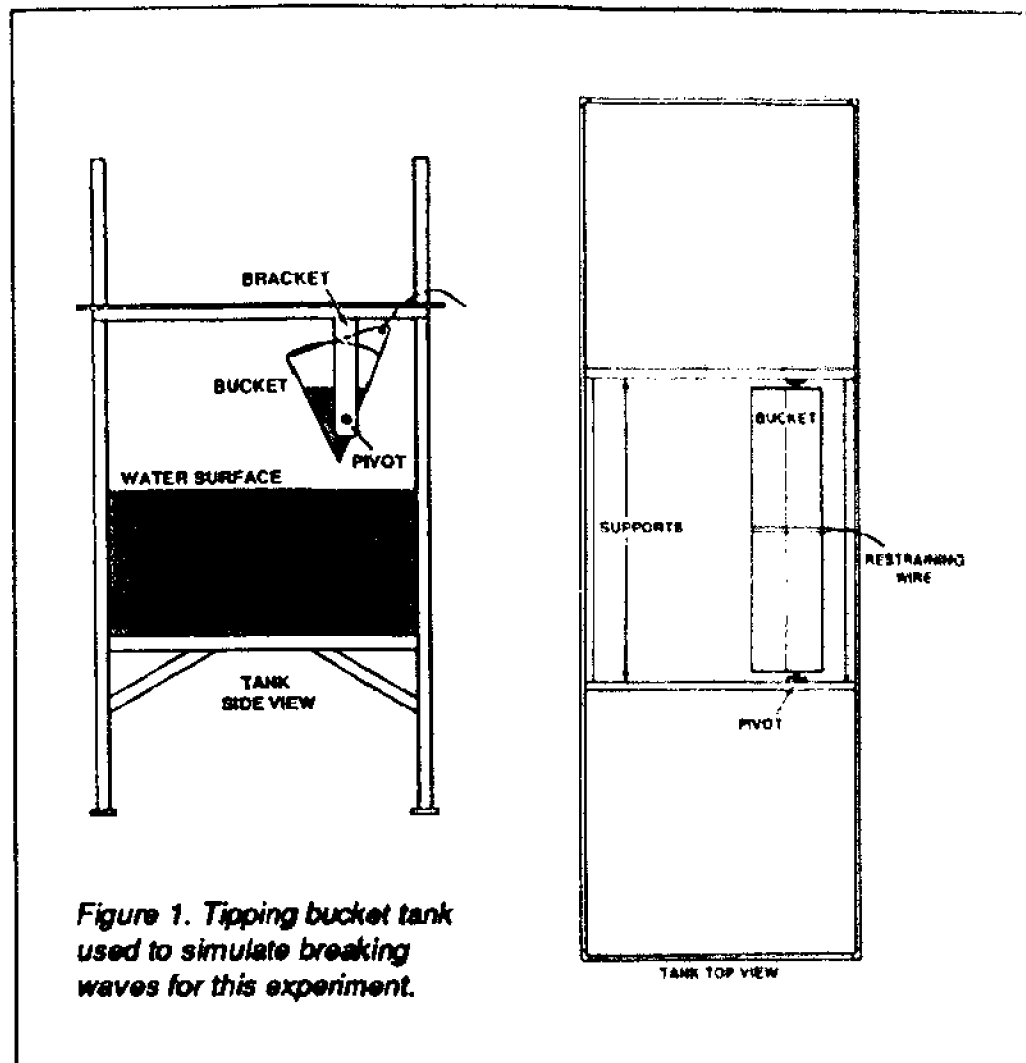
The gases used to study this process were Rn-222 and Hg⁰. These gases (with C-14) represent the methodology and data base for most oceanic gas exchange work. Furthermore, the developing technology in this Department allows for the collection of atmospheric Hg⁰ and thus the possibility of quantifying the role of the breaking event itself as distinct from the wave and turbulence processes which accompany breaking waves.

Experimental Set-Up

Sources for Rn-222 (Ra-226) and Hg⁰ (Hg metal) were established using gas permeable membranes which isolate the gas and liquid phase. These sources were placed in a quiescent tank for several days to initialize the concentrations at some reasonably high value. The spike sources were then removed and the experiment was begun under several different conditions; in both seawater and freshwater.

- (1) **BUCKET TIPPING AT A FIXED RATE:** a tipping bucket was employed to simulate the formation of oceanic whitecaps and the accompanying bubble formation (Fig. 1).
- (2) **STIRRING ONLY:** a submersible pump was used to horizontally homogenize the tank for the breaking wave experiments and it was necessary to conduct a control experiment.
- (3) **NULL EXPERIMENT:** a null experiment was conducted (no bucket tipping, no stirring) to determine any experimental artifacts.

BUBBLE-MEDIATED SEA-AIR EXCHANGE



The system was adjusted so that eight litres of water were spilled from the bucket each 210 seconds. A video system was used to monitor the bucket tipping events and a Homomatsu Area Analyser used to record and analyse the tipping events. A typical whitecap decay profile is shown in Figure 2. The effective time averaged whitecap coverage was calculated to be 0.014%.

Water samples were periodically collected and analyzed for radon and elemental mercury. Both techniques relied on degassing of the sample and trapping of the analyte on a suitable absorbent (gold-coated beads for Hg^0 , charcoal for Rn) prior to quantification. Analysis for mercury relied on cold vapor atomic fluorescence spectroscopy; radon was quantified by radiochemical techniques.

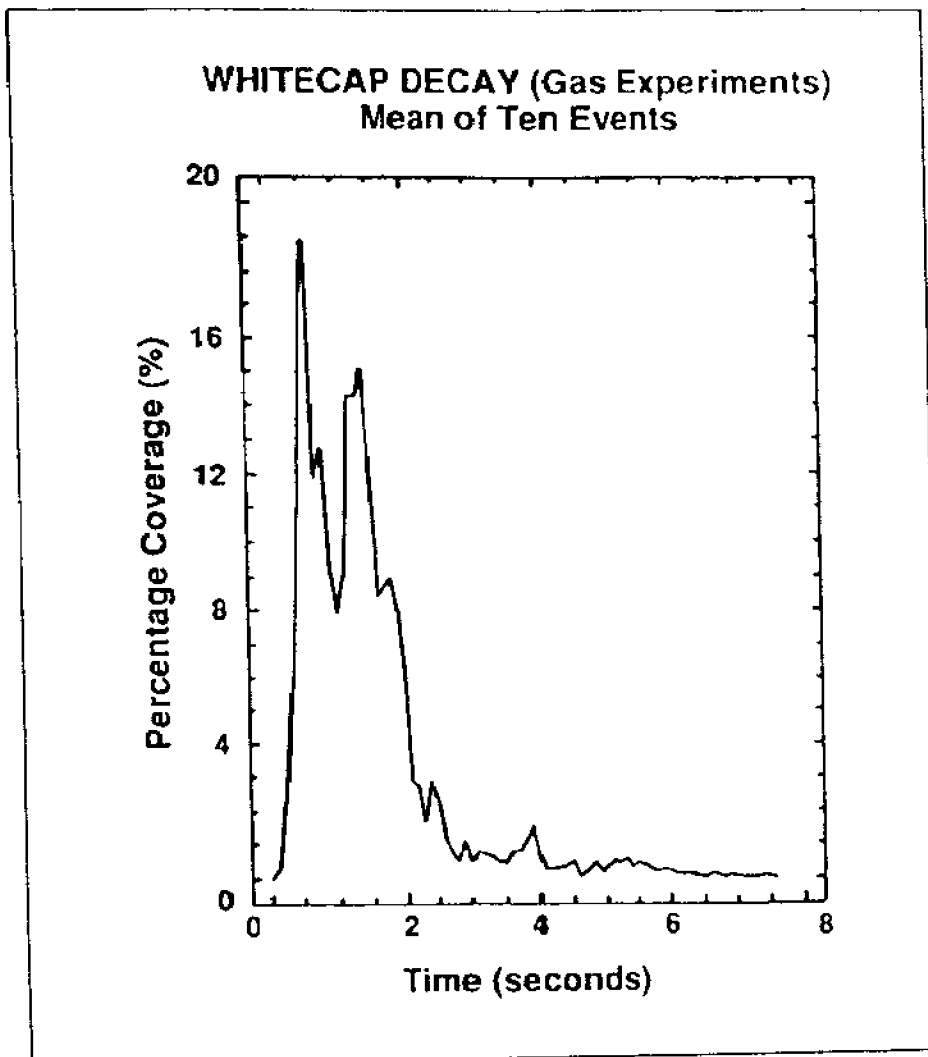


Figure 2. Whitecap coverage and decay from tipping bucket gas exchange experiments.

Under the experimental conditions, the descriptive equation governing the loss of gases is:

$$\partial R_n / \partial t = -\lambda_{222} R_n - \text{atmospheric loss}$$

$$\partial Hg^o / \partial t = \text{atmospheric loss}$$

which can be solved to yield:

$$\ln (R_n / R_{n_0}) = -(\lambda + k/h)t$$

BUBBLE-MEDIATED SEA-AIR EXCHANGE

$$\ln (Hg^{\circ}/Hg^{\circ}_0) = - (k/h)t$$

where k is the gas exchange coefficient (cm/min) and h is the mean tank depth.

For Hg° , the radiodecay constant is zero and for all practical purposes, the radiodecay of Rn-222 was a secondary correction in all experiments. Gas exchange coefficients, k , were determined by a least squares linear regression shown in Fig. 3. In all cases, significant correlations were found for both Hg° and Rn. The calculated values for k are listed in Table I.

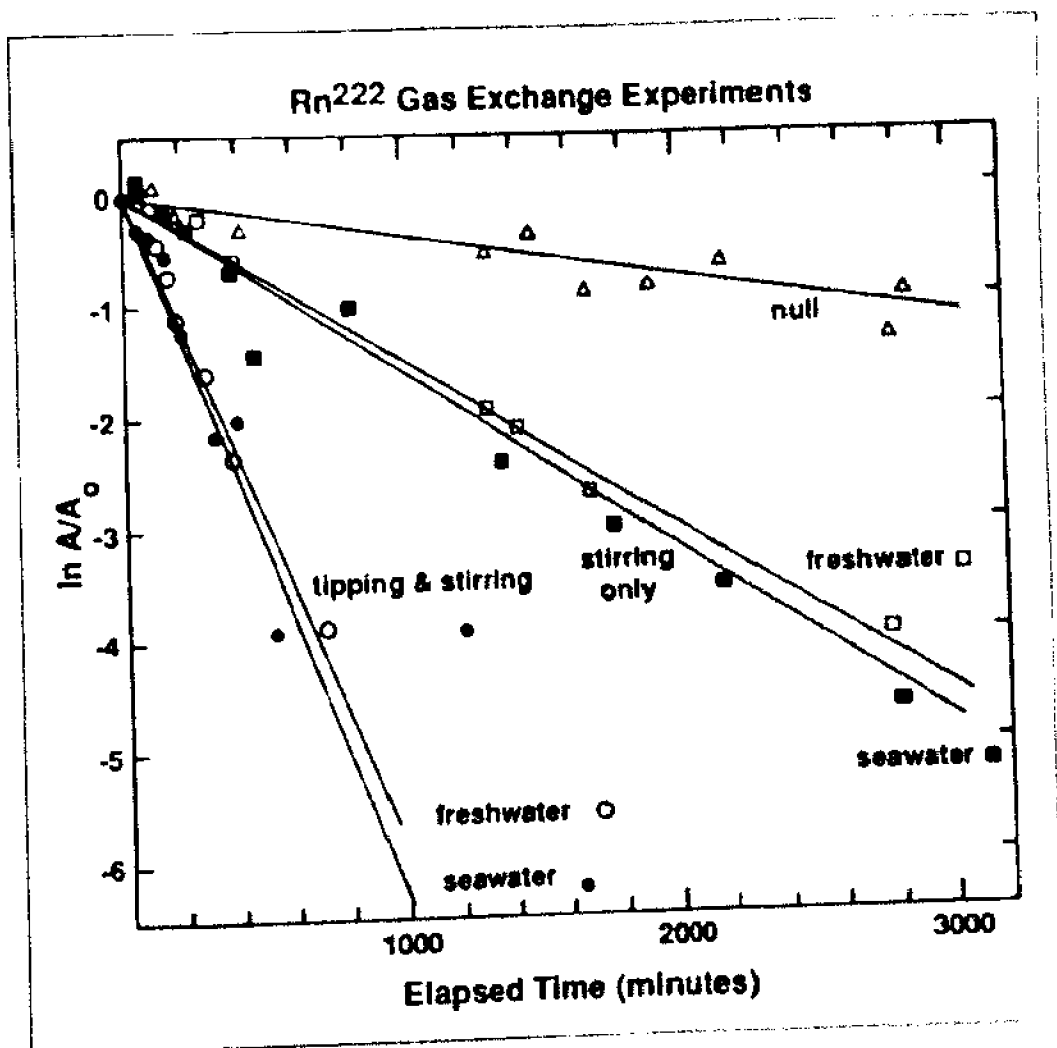


Figure 3. Fractional decay of Rn-222 activity as a function of time for gas exchange experiments. Different experiment conditions noted in the diagram.

Table 1. Gas transfer coefficients for Hg^0 and ^{222}Rn for various experiments. Hg was removed by gas exchange but the results indicate the influence of an additional unparameterized process.

Experiment	Slope, ^{222}Rn	Slope, Hg	K_{Rn} (cm^2/min)	K_{Hg} (cm^2/min)	$K_{\text{Rn}} / K_{\text{Hg}}$
1. Sea Water Bucket Tipping	-0.0066 ± 0.00016	-0.0042 ± 0.00026	-0.1749 ± 0.0043	-0.1092 ± 0.0068	1.602 ± 0.509
2. Sea Water Stirring Only	-0.0018 ± 0.000069	-0.0018 ± 0.00018	-0.0473 ± 0.0019	-0.0468 ± 0.0047	1.017 ± 0.937
4. Tap Water Stirring Only	-0.0015 ± 0.000036	-0.0010 ± 0.00025	-0.0421 ± 0.001	-0.0260 ± 0.0043	1.620 ± 1.25
5B. Tap Water Bucket Tipping	-0.0058 ± 0.00021	-0.0033 ± 0.0002	-0.1547 ± 0.0055	-0.0858 ± 0.003	1.803 ± 0.867

Results and Discussion

The results of gas exchange coefficient determinations for various experimental conditions are shown in Figure 3. Gas exchange rates were greatest for the bucket tipping experiment and slowest for the null experiment. The simulation of breaking waves by the tipping bucket increased the rate of gas exchange of Rn by almost four times in both the seawater and freshwater experiments. The increase in rate of loss of Hg^0 was somewhat less. A comparison of seawater and freshwater experiments indicates that the gas exchange rate of Rn was 12% faster in seawater.

The rate of gas exchange of Hg^0 was always slower than for Rn-222 which is counter to the relationship that would be predicted from gas exchange theory. In addition, the difference was more marked in freshwater than in seawater. These results indicate that a process other than gas exchange was affecting the Hg^0 exchange. Current experiments are designed to examine the experimental effects of kinetic reactions for competing Hg species and/or possible experimental artifacts such as adsorption/desorption phenomena.

Comparison of the data with the literature shows that the transfer velocity found during the stirring experiments is of the order of those found in the field under wind speeds of approximately 4 ms^{-1} .

Conclusions

The quantification of our breaking wave simulation indicates that an effective whitecap cover of 0.014% effectively increased the rate of gas exchange by a factor of 3.7. Although the overall rate of gas exchange in these experiments more closely approximate small lakes ($z=200\mu$) than the ocean ($z=30 \mu$), the results indicate that the processes inherent in the breaking of waves exert strong control on the gas exchange process. The relationships between wave height, wind speed and whitecap cover as well as the physical memory retained in these processes combined with the

ability to measure whitecap cover and surface roughness by satellite, potentially make this approach a more usefully predictive than the wind velocity parameterization.

The IMST Frit Bubble Spectra: Characteristics and Comparisons with Laboratory and Oceanic Breaking Wave Spectra

Ramon J. Cipriano and David K. Woolf
Marine Sciences Institute
University of Connecticut
Avery Point
Groton, Connecticut 06340

Abstract

For similar operating mechanisms, different IMST frits have fairly reproducible bubble spectra. The spectrum in the frit-produced bubble plume reaching the water surface is a sensitive function of position in it. For a given airflow rate, as distance from the plume axis increases, the spectrum narrows markedly, the maximum concentration decreases significantly, and the peak in the frequency distribution shifts to smaller bubbles. For a given position in the plume, increasing the airflow rate broadens the spectral shape, and simultaneously lowers the amplitude of the frequency peak while shifting it to larger bubble radii. The spectral width also broadens markedly as the orientation of the frit changes from horizontal to vertical. Both examples of spectral broadening are almost certainly due to enhanced bubble coalescence. For similar frit parameters, the seawater spectrum will have a much greater population of smaller bubbles, whereas both seawater and freshwater spectra tend to converge at larger bubble radii. As compared to bubble spectra obtained in several laboratory whitecap simulations, wherein the bubbles are formed the breakup of air entrained by wave breaking, the frit spectra are much

narrower, and have much steeper negative slopes at the large end. These experiments do suggest that realistic whitecap bubble spectra can be synthesized using an array of different frits, or a set of similar frits of suitable geometry.

..10 ..

Identification of Critical Research Topics

Panel Discussion Summary

Moderator: S.E. Larsen
Risø National Laboratory
DK-4000 Roskilde
Denmark

The symposium from which this report originates ended with a panel discussion. The purpose was to identify questions of importance for improvement of our insight into the oceanic bubble-droplet processes with respect to both the mechanisms driving these processes and their importance for air-sea exchange.

The outcome of this discussion may be of interest to a more general public than those present during the meeting. Therefore, the summary presented here has been included in the symposium proceedings.

Of the many unresolved questions, the discussion tended to revolve around a number of themes that will also be used to stratify the summary.

First, the discussion centered on the microdescription of individual bubbles and their droplet production. Here the general concern was that although much information is available from laboratory work, many uncertainties remain due to the multiparameter character of the problems. Notably the following items were raised:

- When bubbles burst at the water surface, both jet drops and film drops are ejected. Ejection characteristics including size relations between bubbles and drops need to be more thoroughly described, to facilitate the work on relating conditions just below the sea surface to those just above.
- The lack of systematic knowledge about ejection

characteristics becomes especially marked when we consider bursting bubbles in a foam pad or bubbles bursting through a surface film. In both cases our knowledge is essentially limited because the ejection characteristics are highly variable.

- It was emphasized that more experiments on enrichment factors are needed. The enrichment factors are defined as the ratio between the concentration of a contaminant (mostly bacteria have been considered) in a drop and the corresponding bulk concentration in the water from which the drop originates. The enrichment arises from a combination of bubble scavenging when it rises through the water, and the fact that most of the bubble film is included in the drop ejection when the bubble bursts. Quite thorough laboratory work has been done on the enrichment factors, but only for rather limited bubble and contaminant sizes and contaminant types.

- In recent years the experimental techniques have been complemented by detailed numerical models. This technique may be particularly useful in connection with many of the above-considered problems, e.g., the characteristics of bubble bursting, because these are associated with multitudes of governing parameters and their variation. Such problems might more easily be systematically studied by numerical models.

Next, the problems about assigning source functions to the marine aerosols were discussed. These questions were considered because in order to accurately predict the evolution of the aerosol spectrum, one needs to have a reliable parameterization of the aerosol source at the surface as function of the relevant parameters, such as wind speed, ocean surface characteristics and diameter. The following points were raised:

- There is a need to establish consensus for the source functions. This would involve description not only of the amount of droplets ejected from characteristic surfaces in different size bins, but also of the ejection characteristics such as speed, direction and height.

- Also, the turbulence transport close to the waves needs to be considered more closely. This turbulent diffusion is the only process that can take the ejected droplets further up than their

ejection height. Since many source functions are estimated backwards from measurements of spectra at greater height, a generally accepted method for describing the turbulence fluxes close to the surface becomes important, both when comparing different source function estimates and when using these estimates to determine aerosol spectra.

- Finally, it was emphasized that although aerosols from wave-generated bubbles were probably dominating, one should not completely neglect the other mechanisms. Here the chop and spume droplets especially are well-known for high wind speed. However, maybe it was worth considering other bubble sources such as rain and snow. Rain and snow would not only scavenge the already existing particles, but also could create new populations with different compositions, reflecting the composition of the precipitation.

In spite of the above considerations, the dominating importance of breaking waves for the oceanic bubble/droplet populations is well recognized. Therefore, the relations between whitecaps, foam structure and bubble production were considered essential. Several points were raised:

- The possibility for linking the whitecap coverage and thereby the bubble production to the wave spectrum seemed a promising approach. It would provide a rational way of describing the whitecap coverage and bubble and aerosol spectra for inhomogeneous (limited fetch) and non-stationary situations, by use of wave spectral models. It was realized that these models were far from perfect and also that a number of issues would have to be resolved concerning the detailed bubble and foam structure around a wave.

- The structure, size and distributions of different parts of the whitecap are situated relative to a breaking wave. There was general agreement about the necessity to distinguish at least between the foam situated directly on the actively spilling or plunging part of the waves and the foam situated where the bubbles re-emerge behind the wave front.

- The participants in the discussion emphasized the need for measurement of bubble spectra under the different parts of the waves to build up the systematic knowledge needed. It was pointed

out that relying on bubble trap data might be dangerous because the large bubbles rise so rapidly to the surface that they might easily be under-represented in the measured spectra. Some optimism was expressed with respect to the optical measurements.

- As different bubble populations might reside at different parts of the waves, the droplet source functions must equally be expected to vary with the wave phase. It was pointed out that the active spilling front of a wave was also the part where the jet drop production was very intense.

- Consensus was that one, for all the talk about waves, should not neglect the importance of other parameters for the bubble-droplet production, such as water temperature and surface films.

The final part of the discussion was centered around the general significance of bubbles and spray processes for the air-sea transfer. They are found to be of importance in two different ways: a) They are the only way for the ocean to eject non-gaseous substances into the atmosphere; b) Even when transfer does take place without necessarily involving the bubble processes, these processes might still provide such effective pathways that they dominate when present.

The following examples within the two categories were discussed:

- It was agreed that important aspects of processes of type a had been included in the discussion reported above, such as transfer of bacteria and other types of unpleasantries from the ocean to the atmosphere. Another example is the production of sea salt aerosols being one of the major sources of condensation nuclei in the atmosphere. Examples of the transfer processes of type b are legion. Especially the following two types were discussed:

- The transfer of water vapor from the ocean to the atmosphere is an exceedingly important meteorological process, since the latent energy thus transferred provides the main driving energy for atmospheric motions on many scales. The contribution to this flux from the spray droplets is presently being studied fairly

intensively, especially within the HEXOS research program. Many of the hereby raised questions about the interaction between droplet and temperature and humidity fields in the marine boundary layer are still unanswered. It is clear, for example, that while the droplets must add to the total water flux, they do influence the thermal properties of both the atmospheric and the oceanic layers close to the interface quite differently from the pure evaporative water transfer. Unfortunately, generally accepted quantitative descriptions are still lacking. However, some analyses show the transfer coefficients for both heat and water vapor to increase very fast for the wind speed larger than 15 ms^{-1} with the increase being due to spray droplets. If these results stand up to scrutiny, the spray droplet transfer will certainly be of interest for the dynamics of high wind phenomena such as gales and hurricanes, but might also from a climatic point of view provide for enhanced feedback between windiness and evaporation.

- The bubble process can also act to enhance the air-ocean transfer by simply destroying part of the microlayers on both sides of the air-water interface. These microlayers, where Brownian diffusion dominates the transfer processes, are not very well understood. They tend to be only a few millimeters in depth and very often are shown to constitute the controlling resistance for many types of heat and mass exchange between water and air-if they are indeed established. For calm water surfaces they are certainly present; for rough sea, however, they are likely to be at least partly disrupted by the bubble processes, the presence of which therefore might increase transfer velocities for high winds considerably. Two examples were discussed: For particles in the $0.01\text{-}1 \mu\text{m}$ diameter range the deposition velocity might or might not show a strong minimum (with deposition velocity about one order less than deduced from turbulent diffusion), dependent on the ability of the bubble process to circumvent the resistance in the microlayers. Another example relates to the transfer of gases of low solubility to the water. When entering the water the slow diffusion across the microlayer might result in layer concentrations so close to saturation that their transfer to the water is further reduced. As expected, data show that the onset of the

S.E. LARSEN

bubble processes enhance the transfer velocity for such gases. During the discussion there was agreement among the participants that although there was an ample supply of model descriptions of the phenomena, there still was too little hard experimental data to resolve the uncertainties about the oceanic and atmosphere microlayers and their partial disruption by bubbles and spray.

RA:

NOV 17 1989

RECEIVED
NATIONAL ARCHIVES DEPOSITORY
DATE: NOV 17 1989